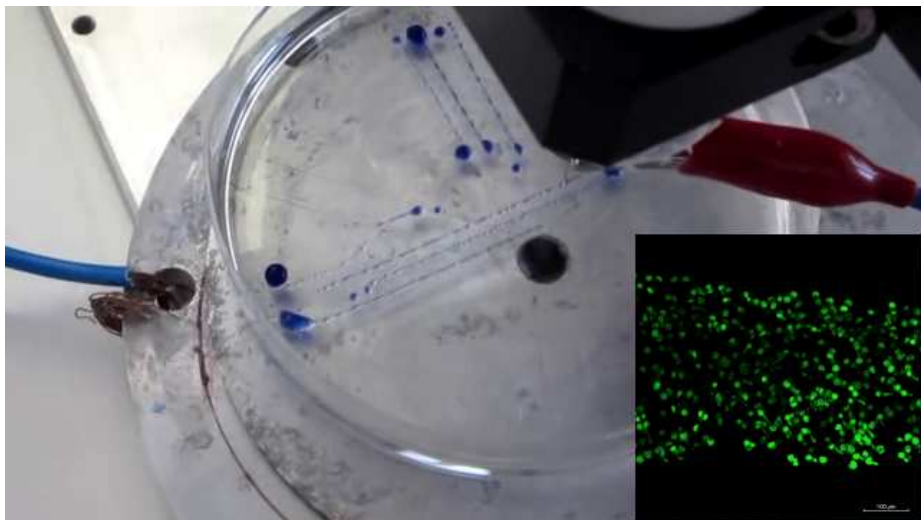


Strategies for cells encapsulation and deposition

Luca Gasperini



April 2013

Strategies for cells encapsulation and deposition

Luca Gasperini

E-mail: luca.gasperini@gmail.com

Advisors:

Prof. Claudio Migliaresi

Dr. Devid Maniglio

Ph.D. Commission:

Prof. Claudio Migliaresi

Dr. Pranesh Aswath

Prof. Orfeo Sbaizero

Dr. Arthur J Coury

University of Trento,

Department of Industrial Engineering

April 2013

University of Trento - Department of Industrial Engineering

Doctoral Thesis

Luca Gasperini - 2013

Published in Trento (Italy) - by University of Trento

ISBN: 978-88-8443-474-6

Contents

	Page
List of Figures	vii
List of Tables	xiii
Abstract	1
1. Introduction	3
1.1. Background information	5
1.1.1. Alginate	5
1.1.2. Electro hydro dynamic process	7
1.1.3. Gelatin	8
1.1.4. Commercially available bioprinters	8
2. Scaffold fabrication through injection in gelatin	11
2.1. Introduction	11
2.2. Materials	13
2.2.1. Description of printer	13
2.3. Methods	15
2.3.1. Preparation of alginate solution and gelatin hydrogel	15
2.3.2. Printing	15
2.3.3. Post processing	16

2.4. Results	17
2.4.1. Base building block, the alginate column	17
2.4.2. More extended structures	17
2.4.3. Post Processing	18
2.5. Discussion	18
2.6. Conclusions	22
3. Cells Encapsulation	27
3.1. Overview	27
3.2. Electro hydro dynamic encapsulation	29
3.2.1. Introduction	29
3.2.2. Materials	29
3.2.3. Methods	30
3.2.3.1. Preparation and sterilization of alginate and crosslinking solution	30
3.2.3.2. Preparation of alginate solutions contain- ing cells	30
3.2.3.3. Cell entrapment in alginate coating	31
3.2.3.4. Cell encapsulation and release	32
3.2.3.5. Geometry of beads	33
3.2.3.6. Scanning Electron Microscopy	35
3.2.3.7. Confocal microscopy	36
3.2.4. Results and Discussion	37
3.2.4.1. Confocal Microscopy of Entrapped Cells	37
3.2.4.2. Measurements of beads	38
3.2.4.3. Scanning electron microscopy	45
3.2.4.4. Confocal Microscopy of encapsulated cells	48
3.2.4.5. Cell Release	49
3.2.5. Conclusions	52

3.3. Electro hydro dynamic encapsulation: more biological evaluations	53
3.3.1. Introduction	53
3.3.1.1. Cell viability	55
3.3.1.2. DNA quantification	55
3.3.1.3. Western Blot	55
3.3.2. Materials	56
3.3.3. Methods	56
3.3.3.1. Cell viability	58
3.3.3.2. DNA quantification	58
3.3.3.3. Western Blot	58
3.3.3.4. Confocal images	59
3.3.4. Results and discussion	59
3.3.4.1. Cell viability	59
3.3.4.2. DNA quantification	65
3.3.4.3. Confocal Microscopy	67
3.3.4.4. Western Blot	68
3.3.4.5. Conclusions	73
3.4. Addendum: EHD Co-encapsulation of gelatin in alginate	74
3.4.1. Introduction	74
3.4.2. Materials	75
3.4.3. Methods	76
3.4.3.1. Preparation and sterilization of alginate, gelatin and oil.	76
3.4.3.2. Preparation of gelatin containing cells	76
3.4.3.3. Encapsulation with metallic sieve as mold	77
3.4.3.4. Gelatin in Oil Emulsion	77
3.4.3.5. EHD co-encapsulation and release	77

3.4.3.6.	Confocal Microscopy	78
3.4.3.7.	Cell release	78
3.4.4.	Results and discussion	78
3.4.4.1.	Encapsulation with metallic sieve as mold	78
3.4.4.2.	Gelatin in oil emulsion	81
3.4.4.3.	Gelatin and alginate with EHD encapsulation	83
3.4.4.4.	Confocal	84
3.4.4.5.	Cell release	85
3.4.5.	Conclusion	85
4.	Electro hydro dynamic printing	87
4.1.	Introduction	87
4.2.	Materials	89
4.3.	Methods	91
4.3.1.	Preparation and sterilization of alginate, agarose and gelatin	91
4.3.2.	Preparation of alginate containing cells	91
4.3.3.	Printing	92
4.3.4.	Agarose mold and alginate dissolution	93
4.3.5.	Confocal microscopy	94
4.4.	Results	94
4.4.1.	Description of printing process	94
4.4.2.	Process parameters	99
4.4.3.	Flux of solution vs speed	100
4.4.4.	Voltage vs speed	101
4.4.5.	Distance from target vs speed	103
4.4.6.	Printed samples with cells	104
4.5.	Discussion	105

4.6. Conclusions	109
4.7. Acknowledgment	110
5. Conclusions	111
Acknowledgments	113
A. Appendix	115
A.1. Technical data (from the manufacturers)	116
A.1.1. Eco-PEN300	116
A.1.2. Jenome JR2300N	117
A.1.3. nScript Bioassembly tool	118
A.1.4. Envisiontec 3D-Biplotter™	119
A.1.5. Syseng Bioscaffolder	120
A.1.6. Standard formulation (salts)	121
A.1.6.1. DMEM	121
A.1.6.2. Phosphate buffer saline w/o Ca and Mg	121

List of Figures

1.1. The desktop robot placed under a biological hood used as the positioning system for the bioprinter	5
1.2. Commercially available bioprinters. From left to right: Bioassembly tool (nScript, USA), 3D-Bioplotter (Envisiontec, Germany), Bioscaffolder (SysENG, Germany). On the bottom the samples obtained by those printers. . . .	8
1.3. Demonstration of our print at the “notte dei ricercatori” (researchers night), extruding a fluorescein loaded gel. A 3 dimensional grid was manufactured with 20 layers . . .	9
2.1. The deposition system of the printer, eco-PEN extrusion head (right) and controller (left)	14
2.2. Scheme of the printing process by injection in gelatin. First the gelatin coating is perforated then is filled with alginate. Subsequent depositions allow the formation of more complex structures.	16
2.3. Pictures of a single vertical injection of alginate in gelatin (hydrogel formed starting from a water solution), on the right picture taken with the optical microscope. Bar is 100 μm	18

2.4. 30 vertical injection in gelatin forming a continuous 3mm section in x-z. (hydrogel formed starting from a PBS solution)	19
2.5. Top: Parallelepiped constituted by 120 injection, base is 3 mm x 3mm. Bottom: parallelepiped constituted by 180 injections base is 3 mm x 4.5 mm. (hydrogel formed starting from a DMEM solution).	24
2.6. Alginate sample after postprocessing. Left: sample inside the warm PBS bath. The upper part marked as A is the parallelepiped injected while the lower part B is a residue of the injection process. Right: Sample removed from the bath.	25
3.1. Comparison between the Sobel (left) and Canny (right) methods for edge enhancing	34
3.2. Alginate beads, geometrical features.	35
3.3. 5 million B50 cells entrapped in 1 ml of 2% alginate hydrogel, live(green)/dead(red) confocal assay after 24 hours (left) and 72 hours (right) after entrapment. Living cells on the top, close to the nutrient solution. Bar is 200 μm	38
3.4. A) Beads diameter using different needles vs Applied voltage; G22S (Outer diameter: 0.718 mm, Inner Diameter: 0.168 mm), G26S (O.D.: 0.474 mm, I.D.:0.127 mm), G33 (O.D.: 0.210 mm, I.D.:0.108 mm); dripping zone (a), transition zone (b) and jetting zone (c) marked for the G33 needle B) picture of holder,	39

3.5. Beads manufactured with alginate 2% at 9KV containing (A) no cells, (B) 5 millions cells/ml of alginate and (C) 10 millions cells/ml; (D) Beads as measurable objects recognized by the software for Figure A	42
3.6. Beads diameter vs applied voltage for alginate 1% (left) and alginate 2% (right). Starting solution containing no cells (top), 5 millions cells/ml (middle) and 10 millions cells/ml (bottom).	43
3.7. SEM images of cryo fractured alginate coating	45
3.8. SEM images of the alginate capsules	46
3.9. SEM images of alginate morphology	47
3.10. Confocal Live/Dead assay (Green/Red) of encapsulated B50 cells , 5 millions cell per ml of alginate, using EHD at 9KV, 5 cm from target. A) Alginate 1% after 1 day, B) Alginate 2% after 1 day, C) Alginate 1% after 7 days, D) Alginate 2% after 7 days. Bar is 100 μm	48
3.11. Released cells from alginate 2% beads cultured on tissue culture dish, picture taken 3 (above) and 72 hours (bottom) after release, encapsulated for 1 (A,C) and 7 days (B,D). Bar is 250 μm	50
3.12. Confluence of cells encapsulated for 1 day on the left, cells encapsulated for 7 days unable to reach confluence on the right. Bar is 500 μm	51
3.13. Beads and released cells, beads were partially treated with PBS, some beads dissolved and released the entrapped cells	52
3.14. Cell viability, well plate control.	60
3.15. Cell viability for B50, comparison between alginate substrate and beads.	61

3.16. Cell viability for 3T3, comparison between alginate substrate and beads.	61
3.17. Cell viability for MRC5, comparison between alginate substrate and beads.	62
3.18. after 1 day of encapsulation on the left, after 7 days of encapsulation on the right. Significance only for values post reseeding	63
3.19. 3T3 Reseeded after 1 day of encapsulation on the left, after 7 days of encapsulation on the right. Significance only for values post reseeding	64
3.20. MRC5 Reseeded after 1 day of encapsulation on the left, after 7 days of encapsulation on the right. Significance only for values post reseeding	64
3.21. Number of cells inside the beads, normalized to the number of cells at D0.	66
3.22. Live/Dead assay: 3T3 Cells, top day 1, bottom day 7. On the left confocal image with green living cells, on the right optical image.	67
3.23. Live/Dead assay: MRC5 Cells, 1 and 7 days	68
3.24. Western blot of MRC5 cells, Gapdh marker	69
3.25. Western blot of MRC5 cells, Hsp70 marker	70
3.26. MRC5, nuclei (blue) and cytoskeleton (red) on the left, nuclei (blue) and hsp70 (green) on the right. MRC5 cells grown on alginate coating, day3.	71
3.27. MRC5, nuclei (blue) and cytoskeleton (red) on the left, nuclei (blue) and hsp70 (green) on the right. MRC5 cells grown on control well plate, day3.	72

3.28. MRC5, nuclei (blue) on the left, hsp70 (green) on the right. MRC5 entrapped in beads, day3.	73
3.29. Metallic sieve on the left still containing some capsules, on the right the capsule after the ejection from the sieve . . .	79
3.30. Sieves and solution spreading. On the left metallic sieves only, in the middle sieves with alginate after partial ejection of beads, on the right sieve with gelatin, the gelatin didn't fill only the pores as alginate.	80
3.31. Gelatin capsules formed by a metallic sieve, on the left a gelatin capsules on the right the detachment of the gelatin coating formed on the sieve	80
3.32. Gelatin capsules without cells: capsules collected from the bottom of the vial (left) and oil present on the top (right)	81
3.33. Gelatin capsules containing cells, bar is 250 μm	82
3.34. Gelatin capsules inside an alginate bead	83
3.35. EHD encapsulation confocal images, on the left laser only and on the right laser plus light to outline the borders of the beads.	84
4.1. EHDJ deposition system	90
4.2. Deposition of alginate A) the printer B) two different kinds of deposition by changing the speed of the needle C)thickness of the continuous line deposition D) beads that "fuse" together to create a continuous line	95
4.3. Beads closer together by decreasing the speed of the needle. Bar is 500 μm	96
4.4. Cross shaped alginate deposition with enough mechanical properties to be handled. Bar is 500 μm	97

4.5. Square shaped continuous deposition, border 5 cm. On the right magnifications that show the evolution of the deposition increasing the number of layers.	98
4.6. Printing a “small thick sample”, A) initial deposition design with sacrificial part B) sample with sacrificial part removed C and D) sample after few layers of deposition.	99
4.7. From left to right depositions at 0.005ml/min, 0.01ml/min, 0.02ml/min. Top row shows the geometrical feature of the depositions varying the needle speed from 1 to 6 mm/s. Middle row shows depositions obtained at 1 mm/s while last row shows depositions at 6 mm/s. Scale bar is 500 μm	101
4.8. Geometrical feature at different voltages of the depositions varying the speed of the needle from 1 to 6 mm/s, the magnifications show the depositions obtained at 6 mm/s. Bar is 500 μm	102
4.9. From left to right depositions at a distance of 4, 5, 6, 7 mm showing the geometrical feature of the depositions varying the needle speed from 1 to 6 mm/s (left ot right). Magnifications show the depositions obtained at 1 mm/s. Bar is 500 μm	103
4.10. Alginate deposition after 1 day (left) and 7 days of culture (right)	104
4.11. Alginate EHDJ deposition after 7 days: on the left picture at optical microscope, on the right a 3D image obtain with the confocal microscope	105
4.12. Alginate EHDJ deposition after treatment: on the left picture at optical microscope, on the right a 3D image obtain with the confocal microscope	106

List of Tables

- 3.1. Diameter , eccentricity and form factor for beads manufactured with a solution of alginate 1% and alginate 2% using a gauge 33 needle. In bold the best experimental setup: high circularity and low dispersion of values. . . . 44
- 3.2. Scheme of experimental procedure 57

- 4.1. Feature of the printer system reported (gray background) compared to other printers found in scientific literature (white background). * Tested but not reported[77] 108

Abstract

Tissue engineering aims at reconstructing living tissue by using scaffolds that are seeded with the patient's cells *in vitro*, then transplanted in the body where needed. We have investigated a bottom-up approach for scaffold production and cells seeding, combining in a single step cells encapsulation and deposition of the encapsulated cells in specific architectures. In this thesis two 3D deposition or bioprinting methods are presented. Both methods manufacture scaffolds with small volumes of material that could be the building blocks for more extended structures. The first system is based on the extrusion of alginate solutions while the second exploits the electro hydro dynamic process to create a jet of liquid alginate beads containing cells. The building blocks of the scaffold are placed at predefined position on a specific target substrate where they crosslink without the need of further postprocessing. Particular attention was given to the electro hydro dynamic process and to the investigation of the parameters influencing the encapsulation of cells, the deposition of the beads on the substrate, the compatibility of the printing process conditions with cells and their survival after printing.

1. Introduction

A substantial part of tissue engineering consists in the repair of damaged tissue and organs thanks to the combined use of scaffolds and cells. Typically a scaffold is designed and fabricated, cells are seeded *in vitro*, then the scaffold/cell combination products are transferred to the body site where new tissue is generated. The procedure requires the selection of proper materials, the design and the fabrication of a scaffold possibly mimicking architecture and mechanical properties of the damaged tissue extra cellular matrix (ECM), the seeding of cells taken from the patient's tissue and their cultivation *in vitro* in static or dynamic conditions, finally the implantation of the scaffold/cells combined product in the patient's body site.

Body tissues, however, are complex structures inhabited by different types of cells, with continuous nutrition that is mainly provided by a dense network of capillaries branching from the bodies main blood vessels.

While tissue engineering has been so far successful with thin tissues where the blood vessels of the host can provide nutrients via diffusion [43], the vascularization of complex extended three dimensional tissues is still an open issue [85] needing fast angiogenesis and vascularization of the implanted scaffold/cell system after having been transplanted from the culture vessel to the body.

An improvement could be offered by computer aided systems able to control the positioning of cells, placed at specific space coordinates to mimic the complexity of the natural tissue following a bottom-up approach [30, 45], in order to build a scaffold piece by piece already containing cells through a technique named bioprinting.

The success of this approach to rebuild functional living tissue is unlikely to be in the near future but nevertheless the ability to place cells at predefined positions can potentially be exploited for a wide range of applications that range from manufacturing devices for the release of therapeutic molecules [26] or constructs to improve biological and pharmaceutical in vitro testing [8].

In this work two different methods for cells deposition were investigated. In both cases an alginate solution in PBS is placed to a predefined position with a desktop robot that acts as the positioning system. Alginate, the bio-ink, was used since it undergoes a fast sol-gel transition compatible with cell survival and it's relatively permissive to nutrient diffusion and waste removal. A gelatin with gel-sol transition when heated at physiologically compatible temperatures was used as bio-paper, to support the bio-ink and act as a source of ions. The alginate solution crosslinks when placed in contact with a gelatin hydrogel enriched in calcium ions, forming a hydrogel while gelatin undergoes a gel-sol transition and is easily removed after moderate heating of the bio-scaffold.

Both methods use the same positioning system, a Janome JR2300N desktop robot (Japan lent by Biotools srl a spin off from the University of Trento, Italy), shown in Fig. 1.1, but with a different setup and in particular with different deposition systems. The first method that is called INJECTION IN GELATIN (chapter 2), uses an extrusion head as the deposition system and the depositions are performed by injecting the alginate

1.1 Background information

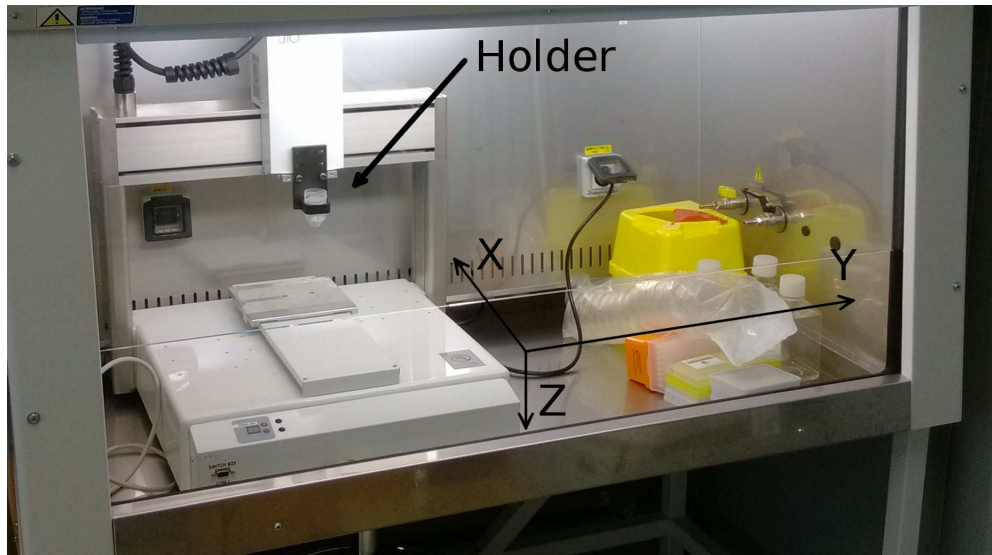


Figure 1.1.: The desktop robot placed under a biological hood used as the positioning system for the bioprinter

solution into a gelatin hydrogel along the z axis at specific x,y coordinates. The second method called ELECTRO HYDRO DYNAMIC PRINTING ([chapter 4](#)) is based on the EHD process and contactless printing is performed on the top of a gelatin coating.

1.1. Background information

1.1.1. Alginate

Alginate is a polyanionic polymer used in many different applications [5], it's commonly employed as stabilizer and thickener in the food industry and for the production of ethanol through the encapsulation of yeast cells. It's also an important polymer for health care, specifically for wound

treatment and has been used for many applications given its absorbent [10, 98], hemostatic [37, 83] and immunological properties [32, 68]. Since the first successful encapsulation of cells [53] in 1980 alginate has been widely used for cell cultures [58, 84].

Commercially available alginate is mainly derived from brown algae [90], dried, purified and processed to obtain a powder typically in salt form. The polymer consists of two blocks, (1,4)-linked β -d-mannuroic and α -l-guluronic [17].

Aqueous sodium alginate solutions can undergo a sol-gel transition in the presence of multivalent cations. The cations cooperatively bind the blocks of adjacent alginate chains, creating ionic interchain bridges which cause the gelification of the polymer solution [80]. The sol-gel transition can occur under mild conditions that are compatible with cell survival [107]. This gelation mechanism can be exploited by external gelation where alginate is delivered into a crosslinking solution or by internal gelation where an insoluble salt inside the alginate release ions after pH adjustments [15]. Divalent cations bind mainly to the guluronic blocks with larger ions producing stronger gels [25] that can be destabilized by phosphate buffer solutions, characterizing the sol-gel transition of alginate as reversible [88]. Alginate can be also crosslinked using solutions of polyelectrolytes as poly-l-lysine [66], poly-l-ornithine [91] and chitosan [39].

Alginate can easily form beads in the presence of a crosslinking solution given its fast sol-gel transition. Large beads are made by dripping the alginate in a crosslinking solution with a syringe or pipette [31, 3] while microbeads can be prepared by atomization and emulsification [35, 1].

1.1.2. Electro hydro dynamic process

The history of this process starts in 1882 when Lord Rayleigh estimated theoretically the amount of charge a drop of liquid could carry, hypothesizing the disruption of the droplet in small jets of liquids after this limit. Later in 1964 Sir Taylor modeled the shape of the cone formed by a droplet under the effect of an electric field creating the base for this technique.

The technique consists in spraying a polymer solution pumped through a needle connected to a high voltage generator. It's also called electrospray or, when is set up for the creation of fibers, electrospinning [4].

The solution that forms at the tip of the needle reacts to the presence of the charge by accumulating charges of opposite sign on its surface, the Coulombian repulsive forces produce tangential stresses, deforming the meniscus into a conical shape known as the Taylor cone [95]. If the voltage is high enough the electrostatic repulsion on the surface can overcome the surface tension at the apex of the liquid cone leading to its disintegration (Rayleigh limit) and creating a jet of drops[71].

The key parameters of this process are the chemical composition and physical properties of the solution, its flow rate, the magnitude of the potential difference and the diameter of the needle [99, 70]. These parameters influence the EHD mode [69] and, as a consequence, the geometrical features of the drop. For example at low voltages there is no or partial jetting determining an EHD mode called dripping, at higher voltages is possible to obtain the stable jetting mode or the ramified-jetting mode if the voltage is particularly high [21, 40].

1.1.3. Gelatin

1.1.4. Commercially available bioprinters

The majority of bioprinters are custom built but lately some systems have become commercially available. Most of these printers are constituted of a three axes positioning system, detailed information on the deposition process used are not always available.

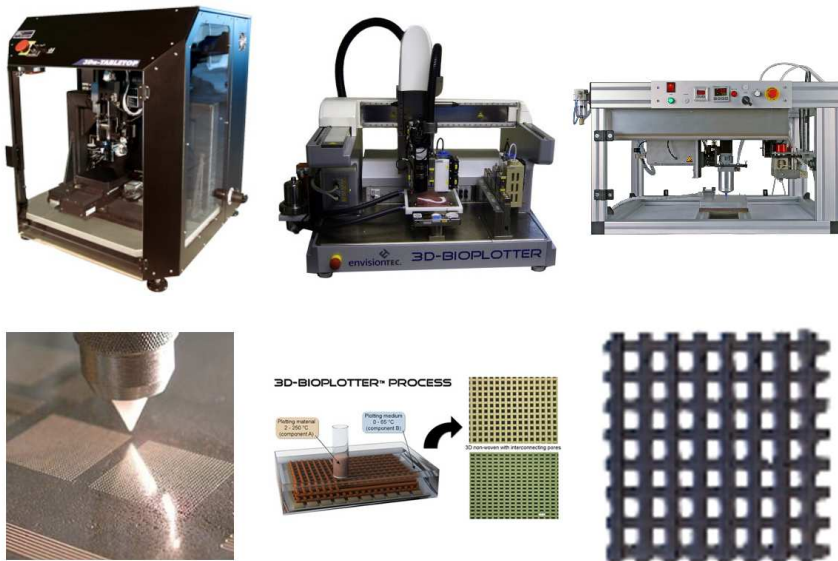


Figure 1.2.: Commercially available bioprinters. From left to right: Bioassembly tool (nScript, USA), 3D-Bioplotter (Envisiontec, Germany), Bioscaffolder (SysENG, Germany). On the bottom the samples obtained by those printers.

The BioAssembly Tool has a positive displacement pump [54] called SmartPump™, the 3D-Bioplotter uses a pneumatic pump [55, 62] while the Bioscaffolder seems to use a similar system. All three printers follow

1.1 Background information

a similar principle: Thanks to a pump an extrusion through an orifice is obtained which is placed very close to the substrate. By moving the orifice or the sample, and balancing its speed to the flux of solution extruded, the extrusion is evenly placed on the substrate. 3D structures are obtained by the deposition of more layers of material.

The technical data of the aforementioned printers is available in the Appendix.



Figure 1.3.: Demonstration of our print at the “notte dei ricercatori” (researchers night), extruding a fluorescein loaded gel. A 3 dimensional grid was manufactured with 20 layers

As a comparison [Fig. 1.3](#) shows our printer with a set up similar to the commercially available ones, extruding a fluorescein loaded gel on a generic substrate.

2. Scaffold fabrication through injection in gelatin

2.1. Introduction

Injection in gelatin was the first deposition method tested and it was initially developed for aiming at possible applications in neural regeneration. The neural tissue is primarily constituted by neurons and glial cells. Neurons are elongated cells (up to 1 m in humans) that electrochemically transfer signals between different parts of the body. The thin elongated section of the neurons is called axon. Each axon is insulated from the outside environment by a sheet of myelin produced by glial cells. If the axon is cut, the parts of the body that were connected to it cannot communicate anymore leading to drastic consequences, for example movement impairment. In the peripheral neural system the principal glial cells are called Schwann cells [19] and are responsible for the neural regenerative capabilities. In fact, if a lesion is not too extended, Schwann cells can rearrange in bands that connect the two stumps of the axons, creating the right chemotactic environment for axon regrowth. This environment is difficult to recreate artificially since it involves very precise gradients of different biological molecules whose role is still not clearly defined. In the central neural system Schwann cells are absent, and the glia con-

sists mainly of astrocytes and oligodendrocytes. In case of a lesion in the neural tissue they create an environment that opposes regeneration, the so called glial scar [18]. A possible strategy to help neural regeneration is to create a scaffold with a cylindrical hollow structure made with a hydrogel containing Schwann cells. So that Schwann cells can still have chemical contact with the outside environment to create the right chemotactic environment for axon regrow possibly counteracting the effect of the environment created by the glial scar [65] and physically constraining axon regrowth[33]. There is a rising interest in using olfactory ensheathing glial cells (OEG) for this specific application [28]. OEG are cells present in the olfactory section of the neural system (nose) and have promising peculiar characteristics for the regeneration of the central neural system. In fact they are the only cells belonging to the glia of the central system known to favor axon regrown in the presence of the glial scar. It's not clear which of the two paths (using Schwann cells or OEG) will be the most successful but in both cases the direct use of these cells, for example through injection, has led to poor results given the strong inflammatory response in the lesion site. In both cases a scaffold made by an hydrogel that can separate the loaded cells from the immune system of the patient without blocking the chemical communication with the environment shows potential for the regenerative process. In this section a method for printing this kind of scaffolds will be presented, by injecting an alginate solution into a gelatin hydrogel obtaining an elongated hollow structure.

2.2. Materials

Alginic acid sodium salt from brown algae (alginate), calcium chloride dihydrate and gelatin from porcine skin were purchased from Sigma-Aldrich (USA). Phosphate buffer saline without calcium and magnesium (PBS), Dulbecco's modified eagle medium (DMEM) were purchased from Invitrogen (USA). The positioning system of the printer is a Janome JR2300N desktop robot (Japan), the deposition system is a Viscotec eco-PEN300 (see [sec. A.1.1](#)) connected to a gauge 33 stainless steel needle (O.D. 0.210 mm, I.D. 0.108mm) (Germany) lent by BIOtools srl (Italy)

2.2.1. Description of printer

The printing system is composed by a 3 motorized stages (desktop robot) and a deposition head [Fig. 2.1](#) (right). This last one is constituted by a rotating sealed displacement unit, fed with a liquid or semi liquid solution by means of a syringe. The solution is sucked from the deposition head and forced out by a motorized rotating screw through a needle connected to the bottom part.

The electronic controller is connected to the desktop robot, it can manage the eco-PEN independently or by on/off impulses sent by the robot. The electronic controller has three operation modes:

1. Time mode: a flow rate and a time are set, the controller will start the deposition for the set amount of time at the set flow rate
2. Volume mode: a flow rate and a volume are set, the controller will start the deposition with the set flow rate for the time necessary to obtain a deposition of the set volume.
3. Impulse mode: the on/off signals are received through a I/O port

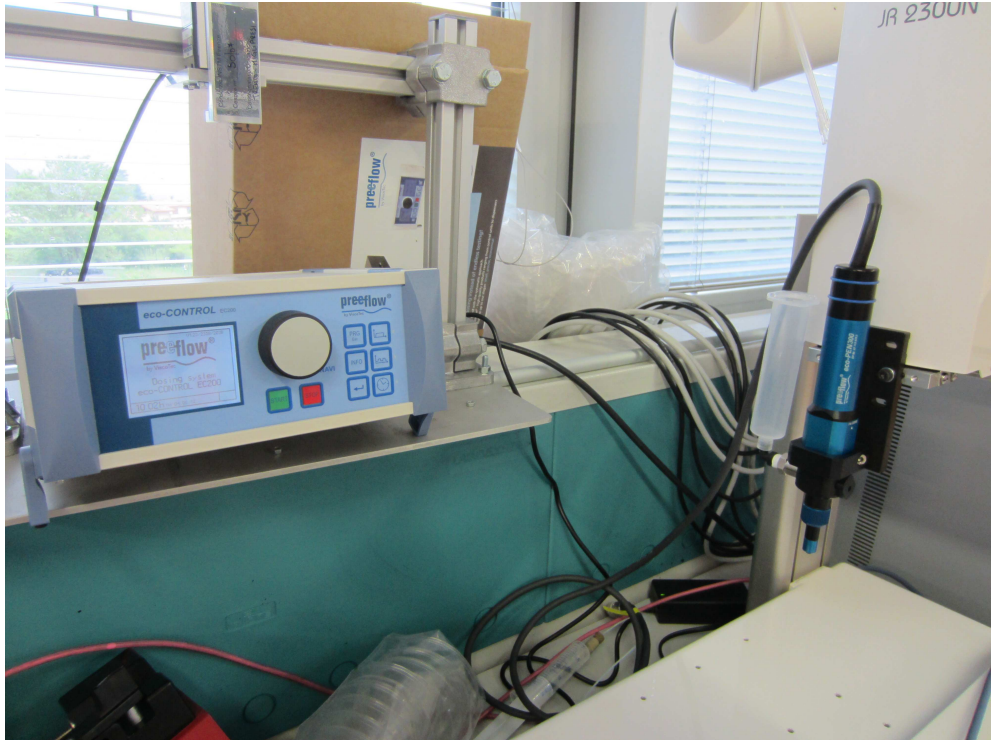


Figure 2.1.: The deposition system of the printer, eco-PEN extrusion head (right) and controller (left)

connected to the robot, a flow rate must be set.

All three modes have an option to set the amount of liquid to suck back at the end of the deposition to avoid post dripping.

In this experiment mode 3 was used, the start and the end of the deposition were controlled by the desktop robot. This way it is possible to couple the deposition and the positioning system to start and stop the deposition at specific coordinates.

2.3. Methods

2.3.1. Preparation of alginate solution and gelatin hydrogel

Alginate powder was dissolved in PBS for 8 hours at room temperature under mild stirring to obtain a 2 % alginate solution (2g/100ml). Two drops of Trypan Blue 0,4% (Invitrogen) per milliliter of alginate were added as contrast agent. Gelatin powder was added into three different solutions and dissolved under mild stirring condition at 40°C for 3 hours to obtain a 10% gelatin solution. The three different solutions used were PBS, DMEM and a 400 mM calcium chloride obtained by dissolving the salt in distilled water. The solutions obtained were poured inside a 48 well plate to fill it completely and left at room temperature for at least three hours for the sol-gel transition to complete.

2.3.2. Printing

The printer was calibrated for the gelatin coating, in particular z was set at zero where the tip of the needle was at the the bottom of the Petri dish and the z coordinate of the point where the tip of the needle was on the top surface of the gelatin hydrogel was recorded.

For the actual printing process the needle was first moved on top of the gelatin and then it was moved to $z=0$, perforating the coating (Fig. 2.2 A). The positioning system was set to send the start signal for deposition and, at the same time, to start moving along negative z (towards the top of the gelatin hydrogel). The end of the deposition was set at the top of the gelatin Fig. 2.2 B. This created an alginate column entrapped in a gelatin hydrogel and was used as the base building block of other samples

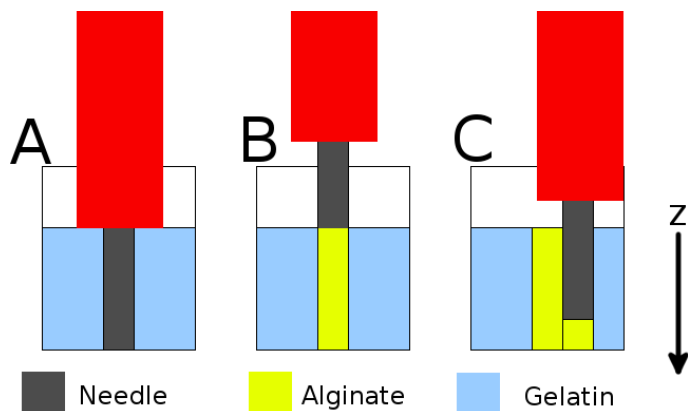


Figure 2.2.: Scheme of the printing process by injection in gelatin. First the gelatin coating is perforated then is filled with alginate. Subsequent depositions allow the formation of more complex structures.

obtained by repeating this deposition at different positions. More precisely the needle was moved outside the gelatin, the x (or y) coordinate was changed and the deposition procedure was performed again (Fig. 2.2 C) to obtain a series of vertical deposition that together formed the final structure.

The controller was set for a flow rate of $50 \mu\text{l}/\text{min}$ and the z speed of the positioning system at $5 \text{ mm}/\text{s}$.

2.3.3. Post processing

The gelatin was removed from the well plate with a pair of tweezers and different post processing steps were performed based on the solution where gelatin was initially dissolved. With gelatin dissolved in PBS a piece containing the alginate depositions was cut and placed in a calcium chloride bath for 10 minutes to crosslink the alginate. In the other two cases the calcium chloride bath was not needed since DMEM and the

calcium chloride solution already contain calcium ions and the alginate crosslinks after being extruded from the needle during the injection in gelatin.

All samples were place in warm PBS for 30 minutes to remove the gelatin.

2.4. Results

2.4.1. Base building block, the alginate column

The vertical alginate deposition shown in [Fig. 2.3](#) is about 100 μm in diameter, for this reason all the structures printed using this base building block were produced by a sequence of depositions at a distance of 100 μm .

2.4.2. More extended structures

By repeating the base building block along a line it was possible to obtain a wall like structure, constituted by tight vertical columns.

From [Fig. 2.4](#) it's possible to observe that after 30 depositions there is a layer of alginate (stained in blue) on top of the gelatin. This layer is partially formed when the needle exits from the gelatin because the flux of alginate doesn't stop immediately at the end of the injection.

By further increasing the number of depositions it was possible to obtain more complex structures such as an hollow parallelepiped and a more complex parallelepiped with 4 subdivisions. From [Fig. 2.5](#) it's possible to observe the points of perforation before the injection into gelatin (top left) and that the section constituting the deposition is characterized by a uniform thickness (right part of figures).

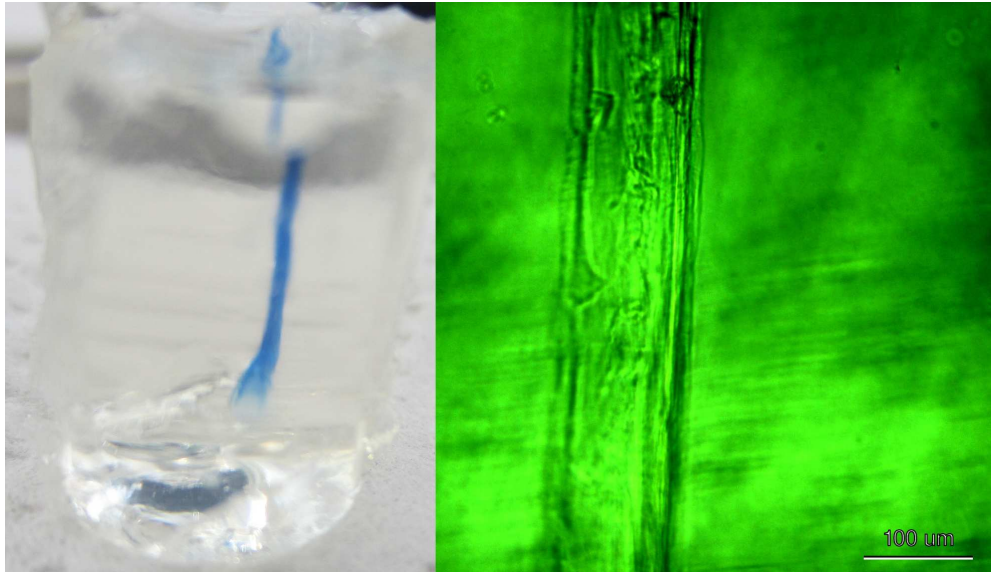


Figure 2.3.: Pictures of a single vertical injection of alginate in gelatin (hydrogel formed starting from a water solution), on the right picture taken with the optical microscope. Bar is 100 μm

2.4.3. Post Processing

After the warm bath in PBS to remove the gelatin only the alginate hydrogel is left.

As seen from [Fig. 2.6](#) the sample partially keeps its shape after the removal of gelatin and it maintains enough mechanical properties to be lifted from the warm bath.

2.5. Discussion

It was not possible to inject the alginate into the gelatin dissolved in the calcium chloride solution in a clean manner, the sol-gel transition was too



Figure 2.4.: 30 vertical injection in gelatin forming a continuous 3mm section in x-z. (hydrogel formed starting from a PBS solution)

fast and a block of alginate hydrogel solution formed and stuck at the tip of the needle after the initial depositions. As already said with this printing system the gelatin hydrogel was perforated by the metal needle and the hydrogel stuck at the tip ruined the sample after some depositions. The same happened for other concentrations of solution until the calcium chloride solution was substituted with DMEM (see salt formulation on page 121). Given the presence of divalent cations in DMEM (much less than in the calcium chloride solutions tested) the process was slightly inclined to clog and a pause was needed after some depositions

to clean the needle. Without considering the need for crosslinking in postprocessing, there were no other substantial differences compared to gelatin dissolved in water.

The pictures taken from the camera didn't show the thickness of the deposition correctly due to the blue stain diffusing out from the alginate, giving the idea of a thicker structure than it actually was. The pictures taken with the microscope gave a better idea of the real dimensions, in that case the stainer was not used and the sample was obtained after dissolving the gelatin containing a single injection of alginate. It's worth pointing out that the needle used for the deposition was a gauge 33 with a O.D. 0.210 mm, that is much bigger than the diameter of the alginate column (Fig. 2.3). We think that this is due to the fact that while the needle is removed from the gelatin, the hydrogel tries to regain its original shape squeezing the alginate that is not completely gelly yet, coming out from the top of the gelatin and contributing to the formation of the alginate coating on top of the gelatin.

The deposition started inside the gelatin then the needle was moved towards negative z (up) and the deposition was stopped when it reached the top of the gelatin template. The flux of solution didn't stop immediately and a liquid drop was formed at the tip of the needle. With the following depositions that drop was placed on the top of the gelatin coating just before the perforation and underwent a sol-gel transition coating the gelatin (Fig. 2.5). The electronic controller of the injection head has a suck back option that allows setting a volumetric amount but this option wasn't useful in this case. The quantity of liquid that drips from the needle slightly changed every injection and the suck back couldn't be set precisely. For example setting the suck back too high led to an alginate column with a void at the base in the subsequent injection.

After postprocessing the sample partially kept its shape, it wasn't rigid enough to avoid collapsing on itself after being removed from the PBS but enough to don't get destroyed in the process of moving it with a pair of tweezers. It should be noted that the gelatin was removed just to be able to observe the alginate without the matrix where it was injected, eventually the sample could be used with the gelatin directly since gelatin becomes a liquid at physiological conditions. If the external matrix is needed for the final application this injection system gives the possibility of using also other hydrogels, for example agarose.

While using this injection system it was possible to observe some shortcoming, some of which could be easily fixed while others were much more difficult to solve. As already said after each injection a small drop formed at the tip of the needle that coated the gelatin with the subsequent depositions. Increasing the number of injections the coating that formed got thicker. The coating on the gelatin should be removed from the sample after the process, a procedure that was difficult to perform without cutting a portion of the actual sample and decreasing its height. This was problematic since the possible height of the sample is limited by the availability of needles with a small diameter on the market. It's very difficult to find needles with that diameter, or similar, longer than the one we used ($1/2'' = 1,27\text{cm}$). This means that in order to manufacture a sample bigger than half an inch, more deposition runs are needed, the depositions must be placed on top of each other and some way must be found to join them together. It should be pointed out that when the needle was perforating the gelatin, sometimes, rather than creating a new hole, it followed the previous one. A longer needle with the same dimensions as ours will bend even more and this phenomenon would be likely more marked.

This printer was set up for a “vertical” (along z) deposition at fixed x - y positions that can be repeated to create more complex structures. With this approach it is feasible to produce structures that are composed only by vertical lines (a spheroid can't) while it can be used to form components of cylindrical structures such as nerve grafts and synthetic blood vessels.

Another intrinsic limit of this approach is the fact that this is a contact printing system: the deposition system is in contact by design with the substrate where the sample is printed. Some issues of the printer like the possibility of clogging when DMEM is used and the formation of the unwanted alginate coating on the gelatin matrix are strongly related to this aspect.

2.6. Conclusions

This simple printing system was a smart approach to cells deposition since it gave the possibility to entrap cells in a hydrogel and precisely deposit them using a sacrificial gelatin matrix. The gelatin acts as a support and, at the same time, can contain the calcium ions needed to crosslink the alginate. The samples obtained can be moved directly to physiological conditions without the need of further postprocessing. The setup of the printer allows the formation of vertical hollow structures. However the aforementioned shortcomings pushed us to move towards another direction, to a contactless more versatile printer, but keeping some feature of this injection system.

The injection into gelatin was abandoned after observing its shortcomings in favor of electro hydro dynamic printing. For this reason the injection in gelatin method was not deeply characterized. Furthermore

2.6 Conclusions

the injection in gelatin was developed for a specific application while the electro dynamic printing has wide potential applications when a precise deposition of a cell laden hydrogel is needed.

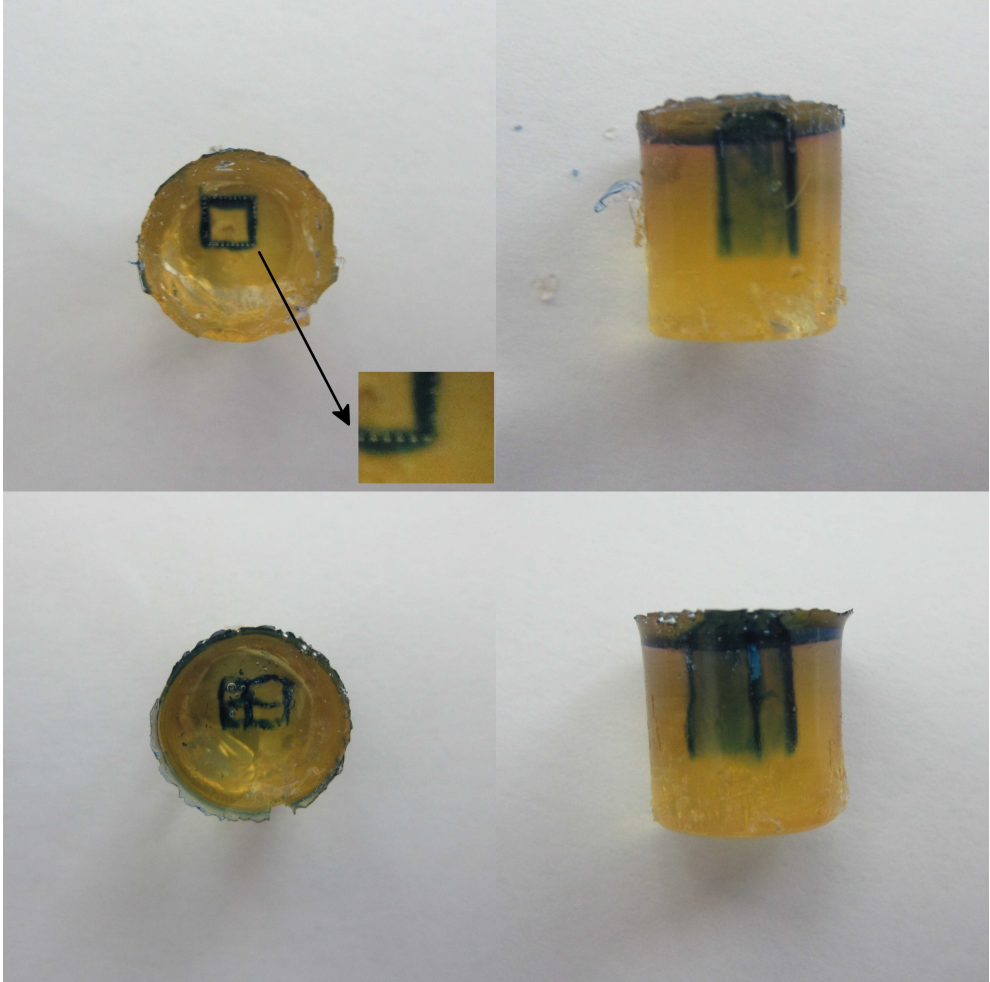


Figure 2.5.: Top: Parallelepiped constituted by 120 injection, base is 3 mm x 3mm. Bottom: parallelepiped constituted by 180 injections base is 3 mm x 4.5 mm. (hydrogel formed starting from a DMEM solution).



Figure 2.6.: Alginate sample after postprocessing. Left: sample inside the warm PBS bath. The upper part marked as A is the parallelepiped injected while the lower part B is a residue of the injection process. Right: Sample removed from the bath.

3. Cells Encapsulation

This chapter covers the encapsulation process of cells, the printer presented in the next chapter is based on this process.

3.1. Overview

Cell encapsulation aims at entrapping living cells within a semi permeable matrix, it's an attractive procedure for a variety of applications in biotechnology. Encapsulation partially isolates cells from the outside environment by means of a semipermeable matrix which physically blocks objects or molecules larger than a critical size while allowing the transit of small sized molecules.[96]. This characteristic is interesting since it's possible for example to transplant non autologous cells needed for a specific therapy and physically blocking the host immune system in order to avoid the use of immunosuppressants drugs and, as a consequence, their unwanted effects [94, 12]. Encapsulation techniques have been investigated to treat a wide variety of endocrine diseases such as diabetes [24], anemia [63] and dwarfism [16], but the potential of the technique has been tested also in different applications such as the creation of micro environments for cells to mimic a tumor [46], to maintain undifferentiated embryonic stem cells for long periods of time [87], or as a source of growth factors [42].

One effective method to produce capsules containing cells is the Electro Hydro Dynamic process (EHD). If an aqueous polymer solution containing cells is pumped, these will be entrapped in the solution drops that are ejected from the needle against a target of opposite voltage [38]. Moreover, if the target is a liquid that reacts with the polymer solution and induces its sol-gel transition, the drops become gelled beads with entrapped cells. This technique has been exploited to entrap several molecules inside different materials, such as chitosan, polylactic acid and polycaprolactone. For instance, Xu and Hanna [103] prepared spherical bovine serum albumin loaded chitosan capsules showing that the final capsule size was strongly influenced by the flow rate, and Xu et al. [104] entrapped bovine serum albumin in polylactic acid analyzing the effect of polymer concentration on the geometrical features of the beads while Ding et al. [27] studied Taxol-loaded polycaprolactone beads showing the ability to manufacture highly loaded monodispersed beads.

This technique can be applied to manufacture complement compatible cell-laden microcapsules using alginate [78], a polymer commonly used for microencapsulation of therapeutic agents [34, 41, 92] and by far the most studied material for encapsulation of living cells [64, 93, 81, 44, 9]. Alginate is both a biopolymer and a polyelectrolyte. It's considered to induce a low immunogenic response, it's degradable with degradation kinetics that can be chemically tuned [106, 48].

3.2. Electro hydro dynamic encapsulation

3.2.1. Introduction

In this study we encapsulated B50 neuroblastoma rat cells in a thick alginate coating to determine the bead size compatible with cells survival considering the limited transport of nutrients with depth. Based on these results we encapsulated cells in beads using the EHD process and evaluated the effect on the geometrical parameters of the beads not only of the inner diameter of the needle, the concentration of the polymer and the voltage applied but also the density of cells in the alginate solution. By using a software for automated biological image processing that relies on solid algorithms for image analysis we were able to measure the diameter, eccentricity and form factor of the beads. We assessed the viability of cells inside the beads, and their behavior when reseeded on a tissue culture plate after being released from the capsules with a technique that only involves washes in a phosphate buffer solution, without the need of citrate [56] or chelating agents

3.2.2. Materials

Alginic acid sodium salt from brown algae (alginate) and calcium chloride dihydrate were purchased from Sigma-Aldrich (USA). Calcein-AM, Propidium Iodide (PI), Phosphate buffered saline without calcium and magnesium (PBS) and Dulbecco's modified eagle medium (DMEM) were purchased from Invitrogen (USA). Needles of the electrospraying apparatus were made of type 304 stainless steel and were purchased from Hamilton (Bonaduz/Switzerland), three kinds of needles were used : gauge 22S (Outer Diameter: 0.718 mm, Inner Diameter: 0.168 mm),

gauge26S (O.D.: 0.474 mm, I.D.:0.127 mm), gauge 33 (O.D.: 0.210 mm, I.D.:0.108 mm). Neuroblastoma B50 cell line was purchased from the Istituto Profilattico Sperimentale, Brescia, Italy.

3.2.3. Methods

3.2.3.1. Preparation and sterilization of alginate and crosslinking solution

Alginate powder was dissolved under mild stirring in PBS for 8 hours at room temperature to obtain alginate solutions at the desired concentration (1% wt/vol, 1g/100ml; 2% wt/vol, 2g/100ml). A syringe filled with the solution was connected to a pump to be filtered through a 0.22 μm filter under sterile conditions overnight and immediately used after filtration. The crosslinking solution consisted in calcium chloride dihydrate dissolved into distilled water at a concentration of 400 mM, filtered through a 0.22 μm filter under sterile conditions.

3.2.3.2. Preparation of alginate solutions containing cells

About one million of B50 rat neuronal cells were defrozen and expanded by using standard protocols. In particular, cells were seeded for 24 h in a 25cm² flask using DMEM containing 2mM L-Glutamine and 10% Fetal Bovine Serum (Gibco) as culture medium. Then cells were washed in PBS to remove residues of dimethyl sulfoxide left from the freezing solution. At sub confluence (80%) cells were detached from the flask with 0,05 % Trypsin/EDTA (Euroclone) and reseeded in a bigger flask (175 cm²) till confluence, subsequently cells were detached and moved to a 15 ml vial. Cells inside the vial were centrifuged at 1000 rounds/min

3.2 Electro hydro dynamic encapsulation

for 10 minutes, the supernatant was removed, and cells were accurately washed with PBS to remove any residues of culture medium since it contains some cations (ex. Ca^{2+}) that could crosslink the alginate in a non-controlled way and centrifuged again. Cells on the bottom of the vial were dispersed in the PBS by vibration and an aliquot of the solution was taken to count the number of cells using a Cellometer Auto T4 and Trypan Blue 0,4% (Invitrogen) as contrast agent. Cells were centrifuged again, the supernatant was removed and the right amount of alginate solution was added to obtain an alginate solution containing cells with the desired cell concentration (5 and 10 millions cells per milliliter of solution). DMEM, PBS , Trypsin/EDTA and the alginate solution used had been warmed at 37°C before use.

3.2.3.3. Cell entrapment in alginate coating

Under a biologic hood about 6 ml of alginate solution containing 30 millions cells was poured on the bottom of 6 wells of a 24 well plate (1 ml of alginate with 5 millions cells per well), the well was filled with the crosslinking agent and left at room temperature for 20 minutes. The crosslinker was removed with a pipette and the hydrogel obtained was washed three times in culture medium. Due to shrinking the hydrogel samples were not perfectly round and their diameter was between 12 and 16 mm. Finally they were moved to an incubator (37°C , 5% CO_2) inside a 6 well plate containing culture medium. A 6 well plate was chosen to allow a bigger volume of nutrient solution compared to the 24 one. The medium was changed every day up to 7 days.

3.2.3.4. Cell encapsulation and release

A custom electrically insulated holder was made and placed under a biological hood (Fig Fig. 3.4 B). A 3 ml syringe was loaded with alginate solution (or alginate solution containing cells) connected to a polytetrafluoroethylene tube and placed on the pump set to a fixed flux of 0.05 ml/min, the other side of the tube was connected to a stainless steel needle and placed in the holder under the hood. The positive electrode of a generator (ES30, Gamma High Voltage Research Inc, USA) was connected to the needle while the ground was connected to a metallic plate placed under a Petri dish containing the sterile calcium chloride solution and placed below the needle at a distance of 5 cm. The pump was switched on ejecting droplets of cells containing alginate solution from the needle, that immediately formed gel beads in the calcium chloride solution. After 10 minutes the calcium chloride solution containing the gel beads was poured into a 15 ml vial. The vial was mildly centrifuged to pellet the beads (500 rpm, 30 seconds), the supernatant was removed, DMEM at 37°C was added and the beads concentrated at the bottom were dispersed by vibration. The procedure was repeated three times to ensure the complete removal of calcium chloride. Finally DMEM was added and the solution containing the beads was moved to an incubator inside a small flask with a filter cap.

At fixed times, cells entrapped within the gel were released by dissolving the gel. The gel was dissolved by first removing the DMEM containing cations with a quick wash in PBS at room temperature and then by placing it in an incubator with PBS at 37°C, centrifuged and finally suspended in medium until seeding.

3.2.3.5. Geometry of beads

The solution containing the beads was shaken, different aliquots were taken, put on a glass and images of the beads were taken with an optical microscope (Carl Zeiss Axiotech 100). All images were acquired in wet state. At least 20 images were taken to have 30 measurements per experimental point for a total of 2700 measurements (see Fig [Fig. 3.5A](#) and [Fig. 3.6](#)).

CellProfiler [\[52\]](#)(Broad Institute, USA), an open source software, was used to process the images and measure the geometrical parameters of the beads. The software was configured after a series of trial and error tests aimed at minimizing all errors that could arise using an automatic procedure. Loaded images were first converted to gray scale by combining together the red blue green components in order to enhance the outline of the beads using the Sobel method [\[89\]](#)(computational time of 2.5 s on a 2.4 GHz processor). This method was able to render higher contrast white edges on a black background compared to other algorithms as Prewitt [\[74\]](#)(2.5s), much less noisy images compared to Roberts [\[79\]](#)(3.1 s) and continuous borders compared to Canny [\[14\]](#)(7.8 sec).

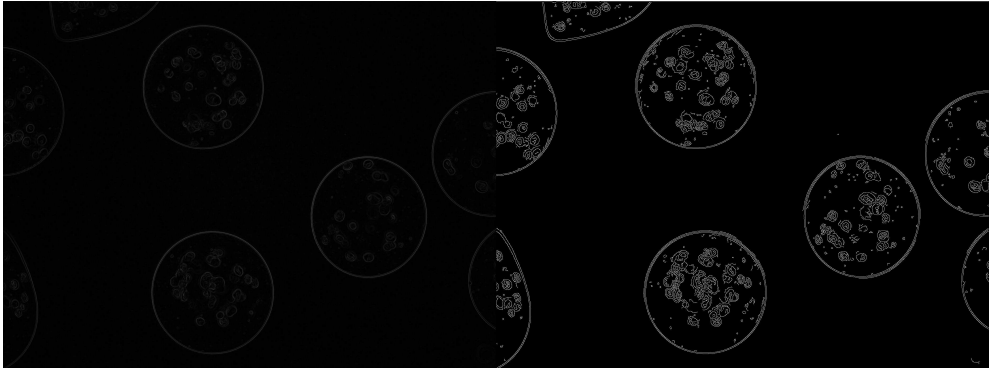


Figure 3.1.: Comparison between the Sobel (left) and Canny (right) methods for edge enhancing

The output images were processed using the Kapur [44](25s) thresholding method in order to identify the beads (objects) and separate them from the background. This method was chosen since it gives the most consistent results among all the other methods tested as Otsu [67] and Ridler-Calvard [75]. It was applied using an adaptive thresholding since the illumination was not constant on the picture, clumped objects were separated by their round shape. Cells were not considered as an object since the software was setup to ignore smaller entities contained already in a larger object. The resulting objects of this process (the alginate beads) were processed further by measuring the biggest and smallest axes, eccentricity (e) and form factor (ff) which are 0 and 1 respectively for a perfect circular shape.

This part of the experiment was aimed at finding the best set up to obtain spherical monosized beads. Fig. 3.2 shows the typical beads obtain by the EHD process.

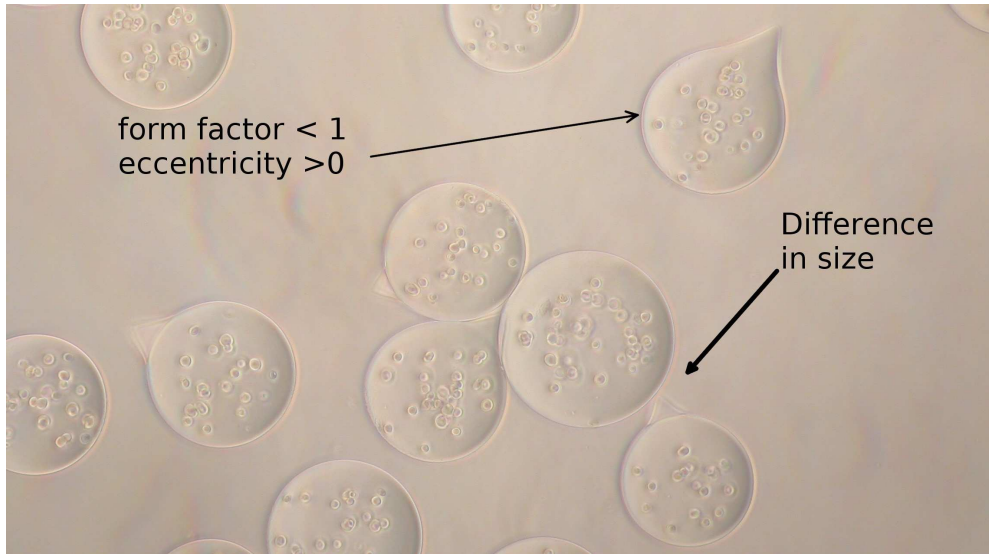


Figure 3.2.: Alginate beads, geometrical features.

The results of some samples were checked with ImageJ to assess the validity of the method. In some cases the software failed to recognize the beads correctly (mostly with clusters of beads together with uneven illumination) therefore some ad hoc modifications to CellProfiler were done, adjusting the threshold of the Kapur method.

3.2.3.6. Scanning Electron Microscopy

A standard scanning electron microscope (SEM) was used since the cryo SEM is not available in our laboratory. The preparation of the sample in absence of a cryo chamber involves the removal of water. The fixation of cells was problematic given the nature of the samples [2] so we performed the observations on the hydrogel coating and the beads without cells since the preparation of the sample would had destroyed the cells. SEM observations were performed in order to have an idea of the morphology of

the material the cells would be eventually in contact with. A small piece of coating was cut for the preparation of the sample while the beads were used as they were. In order to avoid the formation of big water crystals, samples were frozen with liquid nitrogen. Some samples were frozen by placing them on a copper plate in contact with a liquid nitrogen bath to increase the heat transfer at the interface between the sample and the liquid nitrogen. During freezing most of samples fractured while in the other cases they were fractured manually. Samples were placed on a stub to be coated with gold and observed with a SEM Supra (Zeiss - Germany).

3.2.3.7. Confocal microscopy

A live/dead assay using Calcein-AM and Propidium Iodide was performed on the hydrogel coating and on the beads. The supernatant was removed from the samples with a pipette and new medium with 10% v/v Calcein-AM was added, then the samples were moved to an incubator and left there for 30 minutes. At the end of the incubation time the supernatant was removed and the samples were cleaned three times with calcium chloride before adding a PBS solution with 2% v/v Propidium Iodide. The samples were left for 3 minutes at room temperature and the washing procedure was performed again. All solutions used were at 37°C. In the case of beads the above procedure was slightly different since it was necessary to pelletize the beads using a 15 ml vial (500 rpm, 30 seconds) in order to remove the supernatant. Observations with the confocal microscope (Nikon A1, Japan) were performed in wet state, a separate image was taken for each setup, for Calcein-AM a 488 wavelength laser and a 500 to 550 nm detector were used while a 560 nm wavelength laser and a 570 to 620 nm detector were used for Propidium

Iodide.

3.2.4. Results and Discussion

3.2.4.1. Confocal Microscopy of Entrapped Cells

Fig. 3.3 was taken by observing the middle part of the hydrogel coating scanned in depth and then merging all single stacks. Already after 24 hours from encapsulation two distinct regions can be distinguished: one closer to the surface of the sample that was in contact with the nutrients solution where most cells are alive (colored in green) and a deeper one where most cells are dead (colored in red). At 72h the situation is even more marked, with a dense layer of living cells being confined to the top 250 μm . Starting from these results, we decided to produce beads with a diameter lower than 400 μm , in order to guarantee the survival of cells in all the volume of the beads. It's worth pointing that beads smaller than 400 μm would be likely needed as cell loading increases since higher densities of cells could impede diffusion of nutrient from the surface to cells in inner positions. Also, capsules smaller than 300 μm lead to a less marked immune response from the host compare to conventional size capsules (300 -1000 μm)[82]

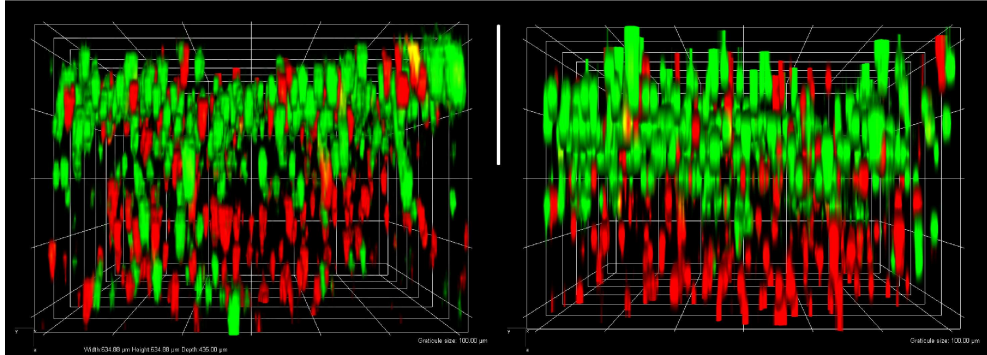


Figure 3.3.: 5 million B50 cells entrapped in 1 ml of 2% alginate hydrogel, live(green)/dead(red) confocal assay after 24 hours (left) and 72 hours (right) after entrapment. Living cells on the top, close to the nutrient solution. Bar is 200 μm

3.2.4.2. Measurements of beads

The effect of the diameter of the needle on bead geometrical features was evaluated keeping the flux of material constant. This means that the total volume of alginate beads per minute was constant as well as the average amount of encapsulated cells.

3.2 Electro hydro dynamic encapsulation

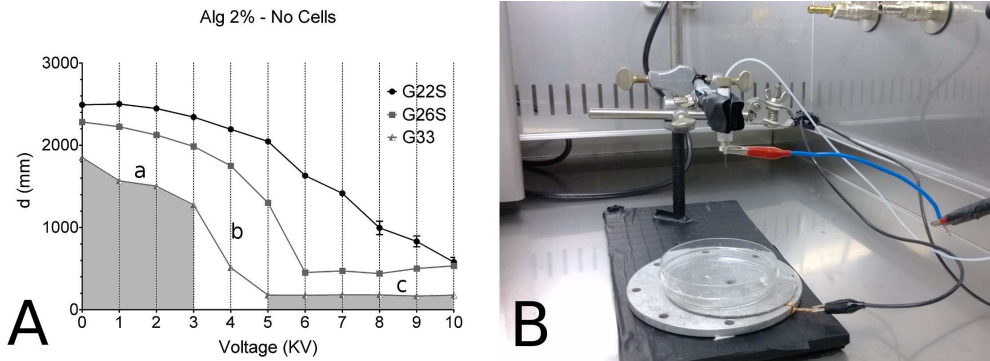


Figure 3.4.: A) Beads diameter using different needles vs Applied voltage; G22S (Outer diameter: 0.718 mm, Inner Diameter: 0.168 mm), G26S (O.D.: 0.474 mm, I.D.:0.127 mm), G33 (O.D.: 0.210 mm, I.D.:0.108 mm); dripping zone (a), transition zone (b) and jetting zone (c) marked for the G33 needle B) picture of holder,

In Fig. 3.4 we reported a typical correlation between voltage and diameter of the bead. As suggested by Moghadam et al. [60] it is possible to evidence three main regions: dripping zone (a), transition zone (b) and jetting zone (c), with the transition zone being characterized by a relevant increase in the data spreading and standard deviation. It is worth noting that an increase of the inner diameter of the needle determines an upper right shift of the graph, which means that a higher voltage is needed to reach a stable jetting zone because of the presence of a wider dripping and transition zone and that bigger beads are obtained at a given voltage. As an example, using the G33 needle (I.D.:0.108 mm), beads with a diameter consistently smaller than $400 \mu\text{m}$ could be obtained. With the G26s needle (I.D.:0.127 mm) the beads formed in the jetting zone had a diameter very close to $400 \mu\text{m}$ while with the G22S (I.D.:0.168 mm) the dripping and transition zone were too wide to observe a stable jetting zone within the investigated voltages (0 - 10 kV) .

On the base of these observations it was decided to focus the cell entrapping experiments using the needle with the highest gauge (higher gauges correspond to lower inner diameters) to easily obtain beads with a diameter consistently smaller than $400\ \mu\text{m}$. It can be generally noted that, from applications in vivo for injections and also to bead deposition with bioprinters, smaller beads are usually preferred to obtain a high surface to volume ratio, so to enhance any mass transport phenomena through the hydrogel or to allow easier injections of a solution containing beads. It's also important to note that smaller needles induce high shear stresses on cells, that could affect cell viability and also their ability to spread and proliferate in cell culture plates after being released from the alginate capsule.

From [Fig. 3.5](#) it can be generally observed that by increasing cell density, higher voltage are required to obtain a transition to the jetting zone.

Both for alginate 1% and alginate 2% by increasing the cell density the transition zone becomes wider and the jetting zone shifts to the right. As an example in the case of alginate 1% without cells the transition zone occurs between 4 and 6 kV with a peak in standard deviation at 5KV while with cells in solution range becomes wider. Zones where the data scattering start to increase significantly fall in the range of 5 and 6KV in the case of $5 \cdot 10^6$ cells/ml and 4, 5 to 6 kV in the case of $10 \cdot 10^6$ cells/ml with a wider range of observed diameters. The stable jetting zone was observed at higher voltages than in the case without cells (6 kV vs 5 kV). Once the jetting zone is reached, by increasing the voltage the process becomes less stable, there is an increase in standard deviation and the presence of very small beads with a diameter far from average can be observed from the appreciable deviation of the bottom line (minimum values) and the central line (average) in the plots regarding Alginate 1%

in [Fig. 3.6](#). With a solution of 10 millions cells per milliliter of alginate and low potentials it was not possible to obtain regular beads ([Fig. 3.5D](#) and [Fig. 3.6](#))

A similar behavior was obtained for alginate 2%: without cells the high standard deviation was found at 4KV (transition zone) and the stable jetting zone is reached at 5 kV. By adding cells the high standard deviation range falls between 4 and 5 kV for alginate with $5 \cdot 10^6$ cells/ml at 3, 4 and 5 kV for $10 \cdot 10^6$ cells/ml. Also in this case with the increase of the cell concentration the voltage required to reach the stable jetting zone increases. Once the jetting zone was reached a slight increase in average diameter of the beads was observed when cells were present. It was possible to obtain beads with constant diameters from 6KV up regardless of the cell density. By analyzing the beads shape in terms of eccentricity and form factor, it is possible to notice that the presence of cells induces the generation of a more regular and spherical geometry [Fig. 3.5 A, B and C](#).

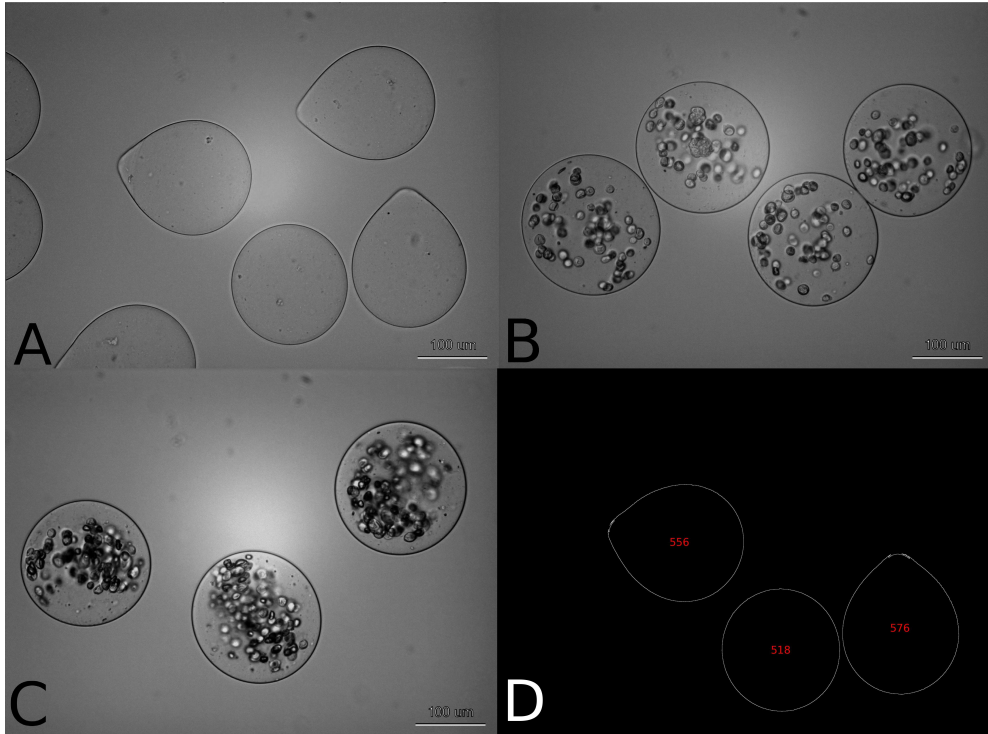


Figure 3.5.: Beads manufactured with alginate 2% at 9KV containing (A) no cells, (B) 5 millions cells/ml of alginate and (C) 10 millions cells/ml; (D) Beads as measurable objects recognized by the software for Figure A

3.2 Electro hydro dynamic encapsulation

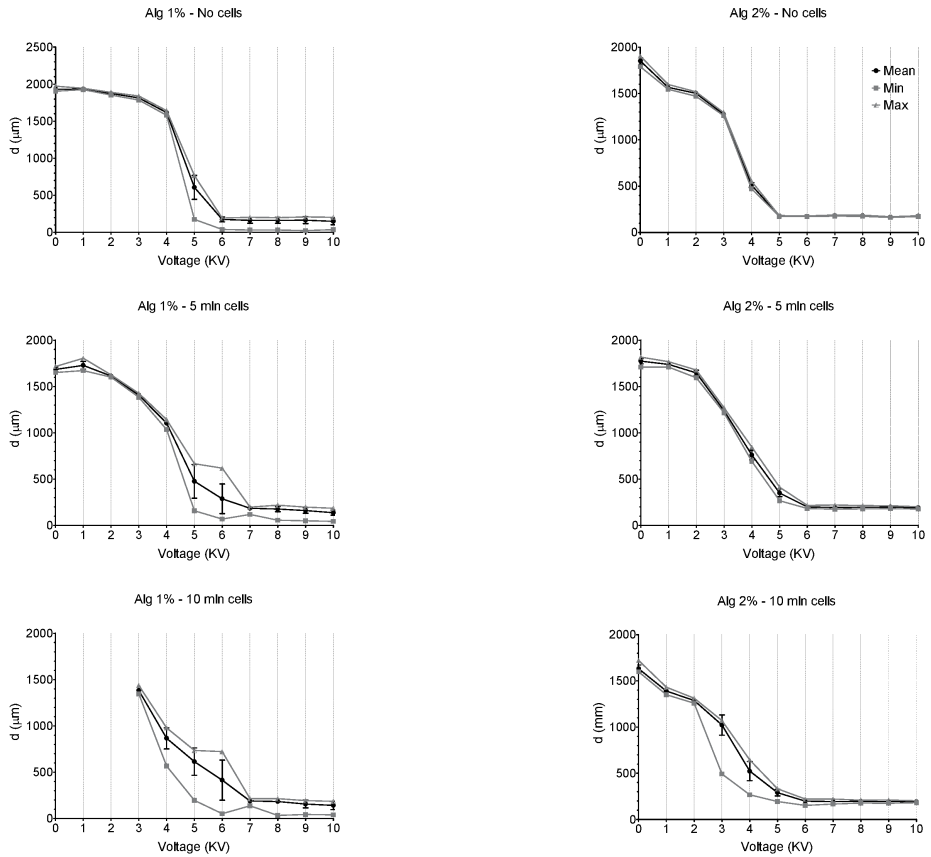


Figure 3.6.: Beads diameter vs applied voltage for alginate 1% (left) and alginate 2% (right). Starting solution containing no cells (top), 5 millions cells/ml (middle) and 10 millions cells/ml (bottom).

<i>Diameters (μm)</i>						
	<i>Alginate 1%</i>			<i>Alginate 2%</i>		
ΔV (kV)	<i>No Cells</i>	<i>5 millions</i>	<i>10 millions</i>	<i>No Cells</i>	<i>5 millions</i>	<i>10 millions</i>
0	1931 \pm 18	1685 \pm 22		1851 \pm 35	1744 \pm 29	1631 \pm 41
1	1935 \pm 17	1728 \pm 42		1567 \pm 14	1739 \pm 16	1389 \pm 20
2	1873 \pm 13	1613 \pm 9		1502 \pm 16	1647 \pm 29	1288 \pm 17
3	1813 \pm 14	1408 \pm 13	1383 \pm 24	1275 \pm 9	1240 \pm 12	1022 \pm 109
4	1617 \pm 20	1104 \pm 23	866 \pm 113	512 \pm 26	760 \pm 51	523 \pm 103
5	607 \pm 161	477 \pm 182	615 \pm 148	178 \pm 2	352 \pm 41	290 \pm 35
6	175 \pm 33	288 \pm 160	171 \pm 274	175 \pm 4	200 \pm 9	198 \pm 13
7	163 \pm 41	187 \pm 14	191 \pm 8	181 \pm 4	195 \pm 11	195 \pm 9
8	163 \pm 41	178 \pm 28	185 \pm 24	180 \pm 4	197 \pm 10	197 \pm 8
9	165 \pm 48	162 \pm 30	158 \pm 42	166 \pm 13	198 \pm 9	194 \pm 6
10	149 \pm 46	138 \pm 27	142 \pm 45	177 \pm 4	192 \pm 6	192 \pm 5
<i>Eccentricity and Form Factor</i>						
	<i>Alginate 1%</i>					
ΔV (kV)	<i>No Cells</i>		<i>5 millions</i>		<i>10 millions</i>	
	<i>Eccentricity</i>	<i>Form Factor</i>	<i>Eccentricity</i>	<i>Form Factor</i>	<i>Eccentricity</i>	<i>Form Factor</i>
7	0.21 \pm 0.07	0.70 \pm 0.23	0.22 \pm 0.06	0.81 \pm 0.06	0.24 \pm 0.08	0.78 \pm 0.10
8	0.21 \pm 0.08	0.74 \pm 0.20	0.21 \pm 0.09	0.80 \pm 0.14	0.22 \pm 0.06	0.79 \pm 0.12
9	0.20 \pm 0.07	0.77 \pm 0.21	0.23 \pm 0.06	0.73 \pm 0.17	0.21 \pm 0.08	0.79 \pm 0.17
10	0.23 \pm 0.09	0.72 \pm 0.21	0.27 \pm 0.12	0.74 \pm 0.21	0.25 \pm 0.08	0.75 \pm 0.16
	<i>Alginate 2%</i>					
ΔV (kV)	<i>No Cells</i>		<i>5 millions</i>		<i>10 millions</i>	
	<i>Eccentricity</i>	<i>Form Factor</i>	<i>Eccentricity</i>	<i>Form Factor</i>	<i>Eccentricity</i>	<i>Form Factor</i>
7	0.41 \pm 0.11	0.81 \pm 0.07	0.18 \pm 0.06	0.84 \pm 0.06	0.23 \pm 0.07	0.85 \pm 0.03
8	0.40 \pm 0.13	0.79 \pm 0.14	0.24 \pm 0.09	0.84 \pm 0.06	0.24 \pm 0.09	0.77 \pm 0.15
9	0.39 \pm 0.12	0.85 \pm 0.04	0.22 \pm 0.06	0.85 \pm 0.03	0.22 \pm 0.06	0.79 \pm 0.13
10	0.40 \pm 0.13	0.76 \pm 0.17	0.27 \pm 0.07	0.84 \pm 0.04	0.27 \pm 0.07	0.83 \pm 0.07

Table 3.1.: Diameter , eccentricity and form factor for beads manufactured with a solution of alginate 1% and alginate 2% using a gauge 33 needle. In bold the best experimental setup: high circularity and low dispersion of values.

3.2.4.3. Scanning electron microscopy

A preferential direction of pores can be clearly seen from [Fig. 3.7](#) and we believe that it's likely to be the effect of the preparation of the sample due to its high initial water content. In fact it's possible to observe pores in the same direction of the temperature gradient established during freezing: from the inner part of the sample to the external surface. The sublimation of the water crystals leaves a porous directional structure.

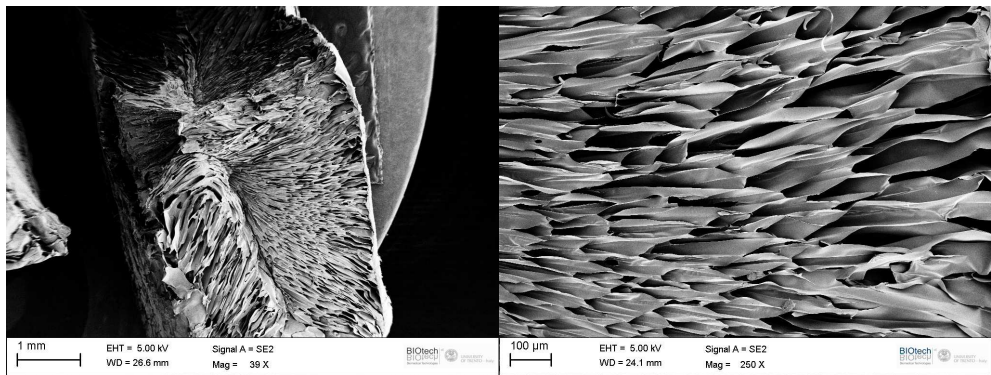


Figure 3.7.: SEM images of cryo fractured alginate coating

The same situation is also present using capsules. In this case, as shown in [Fig. 3.8](#), some capsules didn't fracture during their preparation. Due to preparation, capsules partially lose their spherical features presenting a corrugated and irregular surface. An external skin is formed that sometimes detaches from the bulk. We believe that it could be due to how alginate crosslinks, starting from the external surface being the first in contact with the divalent cations when the solution is placed in the calcium chloride bath. In fact, if the drops of alginate are removed soon after being placed in the bath, a hydrogel skin forms but their bulk remains liquid. If the beads are kept for longer time in the bath also the bulk un-

dergoes a sol-gel transition. We think that as soon as the liquid drops are submerged in the bath a quick crosslinking reactions occurs that forms the hydrogel skin and after that cations diffuse inside the bead, slowed down by the external hydrogel that acts as a diffusional barrier. It's reasonable to think that this forms a strongly bound external skin that binds more weakly to the bulk leading to an easy detachment after the preparation of the sample.

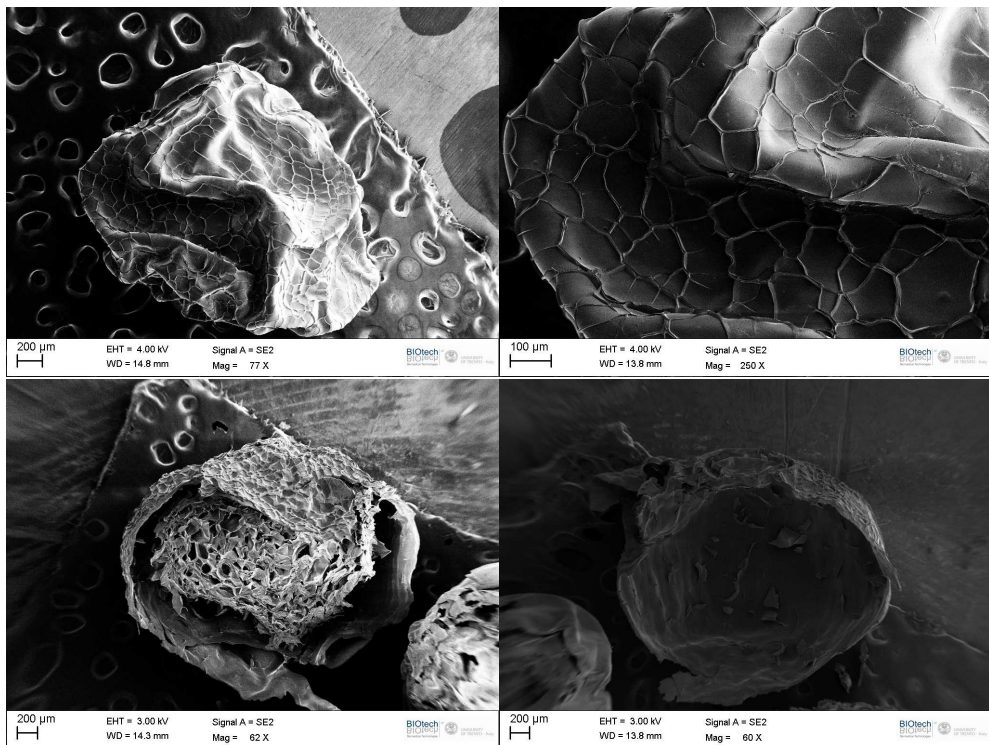


Figure 3.8.: SEM images of the alginate capsules

In few cases pores didn't completely fill the surface of the fracture and as shown in [Fig. 3.9](#), it was possible to observe what seems the actual morphology that characterizes the hydrogel: a three dimensional network

3.2 Electro hydro dynamic encapsulation

with submicron pores. It's worth noting that, based on their phenotype, cells can have a wide range of dimensions but typically they are bigger than 5-10 μm in their inactive state.

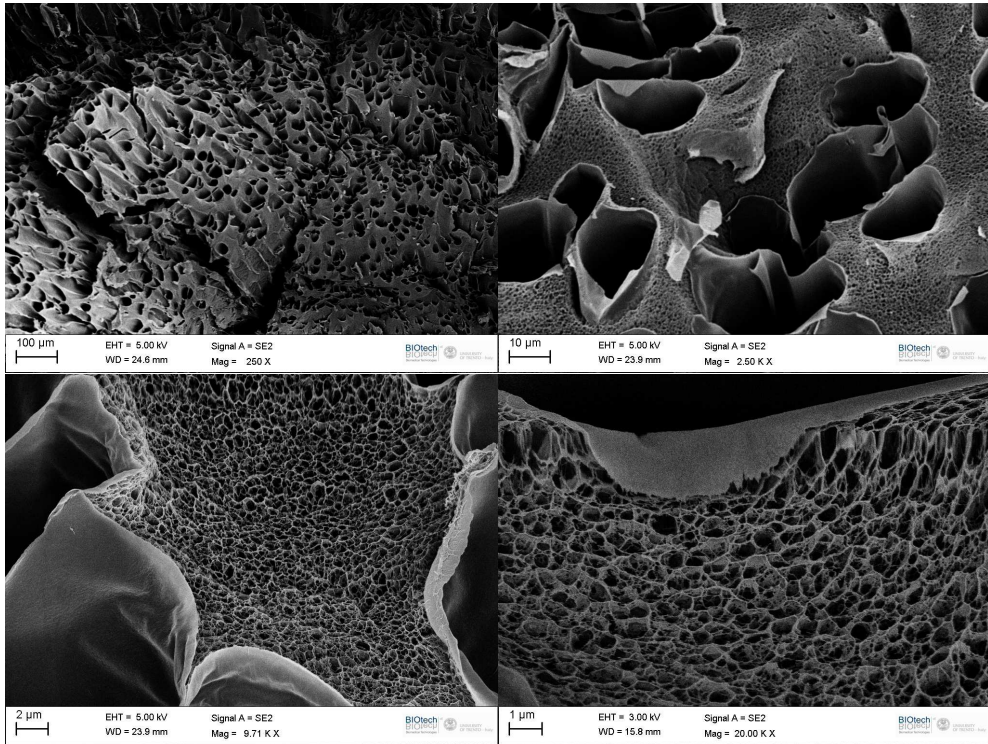


Figure 3.9.: SEM images of alginate morphology

The scanning electron microscopy for hydrogel was performed since it's quite common to find this procedure in literature applied to hydrogels. However in our case it was problematic since it's difficult to state firmly that a particular morphology is not due to the preparation of the sample and in particular to the ice crystals formed given the initial high water content.

3.2.4.4. Confocal Microscopy of encapsulated cells

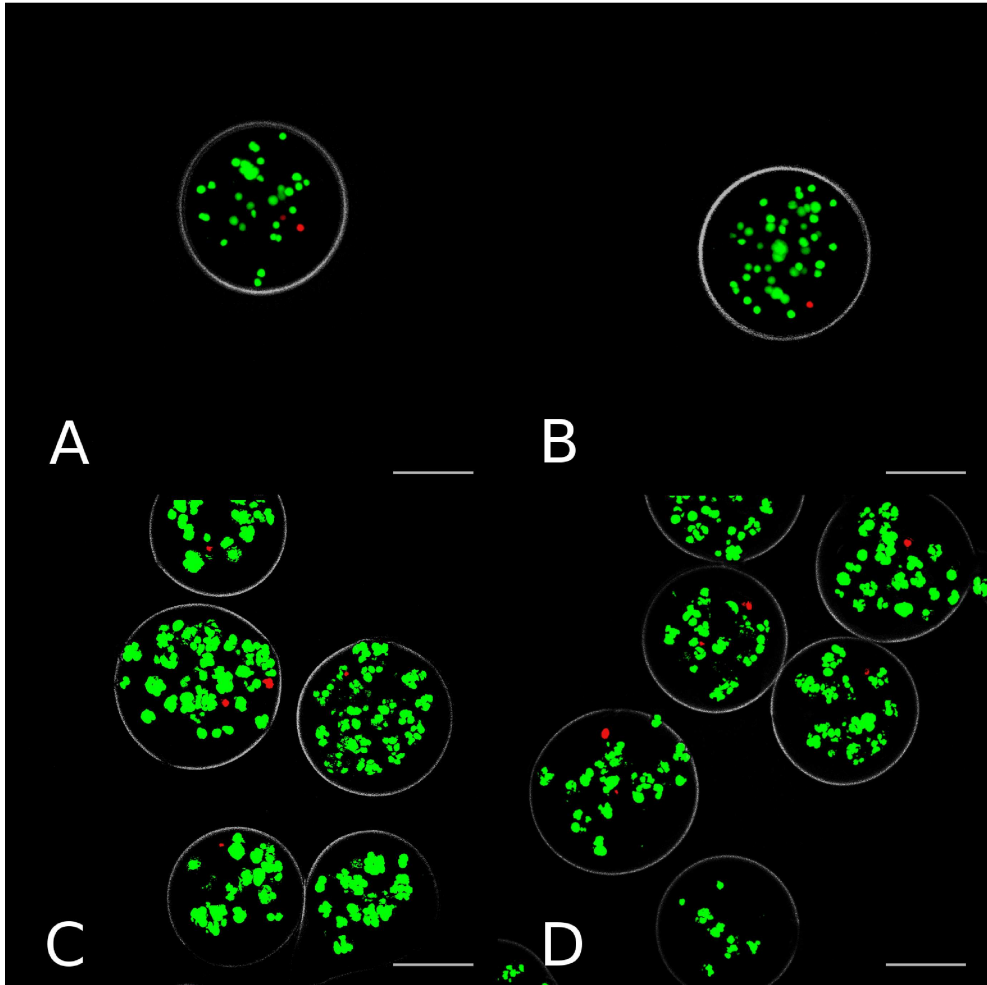


Figure 3.10.: Confocal Live/Dead assay (Green/Red) of encapsulated B50 cells , 5 millions cell per ml of alginate, using EHD at 9KV, 5 cm from target. A) Alginate 1% after 1 day, B) Alginate 2% after 1 day, C) Alginate 1% after 7 days, D) Alginate 2% after 7 days. Bar is 100 μm

For the confocal observation we chose to observe the cells inside beads smaller than $400\ \mu\text{m}$, as close as possible to be mono sized and as similar as possible to a sphere (low standard deviation, minimum difference between the maximum and minimum diameters observed, low eccentricity and high form factor). The best candidates were beads manufactured at 9KV using alginate 2% with 5 millions cells per milliliter and they were compared to beads manufactured using alginate 1% and the same setup to evaluate if different polymer densities have a role in cell viability inside the beads.

Different from the previous case, [Fig. 3.10](#) shows alginate beads containing mostly living cells with few dead cells. Cells were evenly distributed inside the beads with a small tendency to aggregate in the middle. We also observed an increase in the signal after 7 days. It must be noted that when cells are mixed with the alginate solution some bubbles are formed so it's not possible to speculate if cells are able to proliferate inside the actual hydrogel or if they proliferate by filling the air bubbles formed during the mixing procedure.

3.2.4.5. Cell Release

Cells were cultured inside the beads for 1 and 7 days, about 1 million cells were released and reseeded in a culture flask, images were taken after 3 hours from release and, when possible, every 12 hours after that. Cells were able to re-attach and proliferate on the tissue culture flask. In both cases after 3 hours cells attached randomly on the surface however after 72 hours cells confined in the beads for 7 days showed a different behavior than those confined inside the beads for only 1 day. Cells encapsulated for one day spread evenly on the surface showing a behavior similar to a standard defrost as shown in [Fig. 3.11 A](#), while cells encapsulated for

7 days showed a much stronger tendency to form clusters as shown in Fig. 3.11 B.

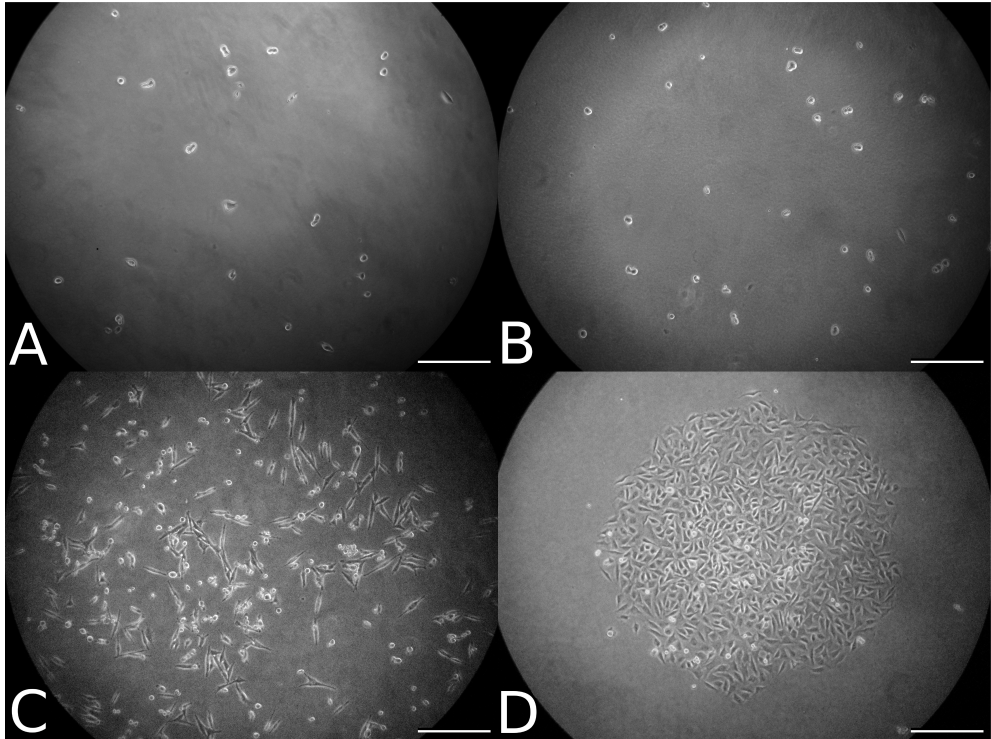


Figure 3.11.: Released cells from alginate 2% beads cultured on tissue culture dish, picture taken 3 (above) and 72 hours (bottom) after release, encapsulated for 1 (A,C) and 7 days (B,D). Bar is 250 μm

In this case, after seeding, cells migrate to form clusters leaving large portions of completely cell free tissue culture plate. In contrast to cells encapsulated for 1 day, cells encapsulated for 7 days couldn't reach confluence, with the progression of the cell culture small clusters grew and coalesced together however bigger cluster did not and a complete confluence could not be observed. Moreover there is the presence of some

sediments that look like acellular constructs.

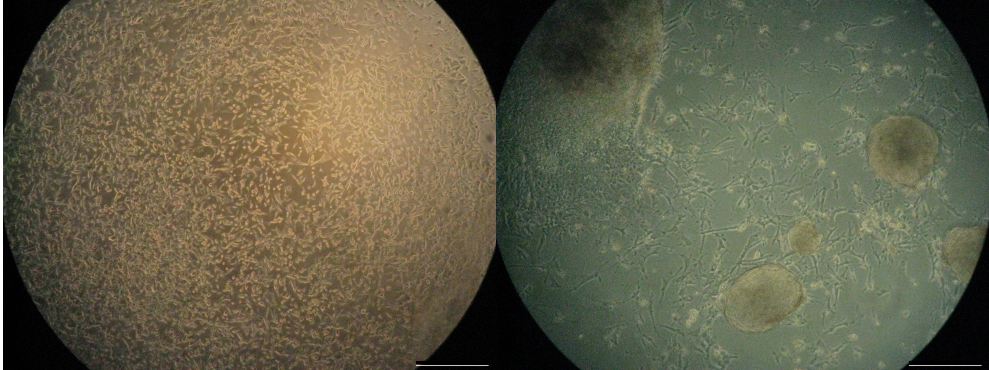


Figure 3.12.: Confluence of cells encapsulated for 1 day on the left, cells encapsulated for 7 days unable to reach confluence on the right. Bar is $500 \mu m$

Other experiments made later on with a different batch of cells, different cell lines (human MRC5 and mouse 3T3 not tumoral) and with different needles of higher inner diameter confirmed this behavior (data not reported), it seems that longer encapsulation times trigger some different cell behavior once they are released even if they maintain their ability to attach and proliferate on the tissue culture dish. It's worth noting that the same amount of cells was initially released from the beads and re-seeded in the same conditions. This kind of behavior was not previously reported in any experiment concerning cell encapsulation and we believe that it is important to understand since it could lead to unwanted cell behavior. We are currently investigating to fully understand its possible long term implications.



Figure 3.13.: Beads and released cells, beads were partially treated with PBS, some beads dissolved and released the entrapped cells

3.2.5. Conclusions

The electro hydro dynamic system has been proved to be a versatile and effective way to encapsulate living mammalian cells in alginate. It is versatile since the geometrical characteristics of the obtained beads can be tuned by easily changing some parameters such as cell density in solution, applied voltage and diameter of the needle. It is possible to obtain capsules very close to monosized and with a spherical shape. Cells inside the capsules remain alive after the encapsulation process and

maintain the ability to reattach and proliferate on a tissue culture dish after being released. Cells encapsulated for a few days demonstrated a different behavior than control cells.

3.3. Electro hydro dynamic encapsulation: more biological evaluations

3.3.1. Introduction

In the previous experiments we characterized a process that leads to the formation of capsules containing living cells. Thanks to that characterization we found the best parameters of the process to obtain mono dispersed spherical beads. We found that cells were alive and could reattach to the tissue culture plate once released. In this section a deeper biological evaluation is presented.

We used B50 which is a tumor cell line with a quick metabolism and a high proliferation rate, this allowed us to obtain a high number of cells needed for the experiments in a short time. It should be noted that a full 175 cm^2 flask contains about 20 millions cells which are used with 4 and 2 ml of alginate to obtain the concentrations of cells needed. Cells are detached with 3ml of Trypsin/EDTA and after 3 minutes, as standard protocols suggest, 12 ml of DMEM are added to deactivate the Trypsin, leading to 15 ml of solution that is poured inside a vial of equivalent volume. After stirring, alginate is added and the solution is moved to a Petri dish for an easier filling of the 3 ml syringe. All these passages must be performed quickly in order to minimize the total time needed for encapsulation because of the presence of living cells that need specific environmental conditions. Alginate is a viscous solution that needs some

time to flow (when poured from a vial for example) so, given the time constraints and the many steps needed to prepare the syringe for the EHD encapsulation, about 1 - 1.5 ml of alginate are lost in the process. For this reason a cell line with high proliferation rate was initially preferred.

Tumor cells are usually much more resilient than non tumor cells furthermore their behavior after stress could be different due to their different gene profile. So we did some biological evaluation on other cell lines to have a more complete understanding of the effect of the encapsulation through the EHD process. In these experiments we also used non tumor 3T3 mouse fibroblasts, and MRC5 human fibroblasts.

The evaluations in this section were performed on beads manufactured with the EHD process at 9KV with gauge 33 needle, starting from a 2% alginate solution containing 5 millions cell per milliliter. The results of the characterizations were compared to a standard cell culture as control and on a cell culture on an alginate coating to rule out the effect of the material. We also performed tests on cells inside the beads and on cells released from the beads. This way it was possible to obtain specific information on the effect of the encapsulation process on cells, the response of cells induced by their entrapment inside the capsule and once released from it.

We evaluated cell viability with AlamarBlue®, DNA content with PicoGreen® and the productions of two proteins (GAPDH, HSP70) with western blot using specific protein markers (antibodies).

In the next sections a brief explanation of the biological evaluation methods used will be presented.

3.3.1.1. Cell viability

AlamarBlue® (Resazurin) is a quantitative assay aimed at evaluating cells viability, that is their ability to live and develop. Resazurin, a non fluorescent indicator dye, is reduced by cells to resorufin, making it useful to asses cell mitochondrial activity. Resorufin is red–fluorescent and its presence can be assessed with a spectrophotometer. Viable cells continuously reduce resazurin to resorufin while damaged and nonviable cells have lower metabolic activity generating a proportionally lower signal. AlamarBlue® is a non destructive test, resazurin isn't toxic and thus it's possible to perform more assays on the same sample.

3.3.1.2. DNA quantification

PicoGreen® is an assay aimed at quantifying the amount of DNA present in a sample, a synthetic dye binds specifically to DNA forming a fluorescent complex. Using a standard solution of DNA with known concentration it's possible to obtain a calibration curve to compare the fluorescent emissions and quantify the amount of DNA present.

3.3.1.3. Western Blot

It's an analytic technique used to detect and visualize proteins contained in a cellular lysate. Proteins are first separated by their molecular weight with electrophoresis. Proteins are then transferred onto a membrane where they are stained using specific antibodies. Typically, a primary antibody is used to bind to the specific protein, then a secondary antibody bound with a dye targets the primary antibody forming a complex that can be visualized.

GAPDH is a protein responsible for many functions in the cellular metabolism [86], Phadke et al. [73] state that *it acts at the interface between stress factors and the cellular apoptotic machinery*, it's overproduced in tumor cells [97]. It's a housekeeping protein, as is β -actin, and is commonly employed as a standard with the assumption that its production level remains relatively constant in different experimental conditions. However in hypoxia condition its production is increased up to 70% [108, 6].

HSP70 (Heat Shock Protein) is a housekeeping protein overproduced by cells under stresses [22, 101]. The upregulation of this protein is part of the heat shock response. Its overproduction is triggered by environmental stress conditions such as hypoxia, starvation and exposure to toxins.

3.3.2. Materials

Alginic acid sodium salt from brown algae (alginate) and calcium chloride dihydrate were purchased from Sigma-Aldrich (USA). Phosphate buffer saline without calcium and magnesium (PBS), Dulbecco's modified eagle medium (DMEM), Quant-iT™ PicoGreen® dsDNA Assay Kit, AlamarBlue®, Triton-X 100 0,05% were purchased from Invitrogen (USA). Proteinase K was purchased from Qiagen. Gauge 33 needle of the electrospraying apparatus was made of type 304 stainless steel and was purchased from Hamilton (Bonaduz/Switzerland). Neuroblastoma B50, 3T3 mouse fibroblasts and MRC5 human fibroblasts cells line were purchased from the Istituto Profilattico Sperimentale, Brescia, Italy.

3.3.3. Methods

Some assay must be performed directly on cells that must be separated from the substrate. From both the control plate and the alginate coat-

3.3 Electro hydro dynamic encapsulation: more biological evaluations

ing the medium was collected then the samples were washed, before detaching the cells with Trypsin/EDTA. All the solutions were stirred to pelletize the cells on the bottom of the vial. For the alginate beads a previously described protocol was used, in brief beads were washed in PBS at room temperature and then placed in an incubator with PBS at 37 °C. Finally the cells were collected after stirring.

The set up of the experiments was optimized to take into account a lot of variables that could affect cell behavior and this led to a rather complicated scheme that is shown in simplified form in [Tab. 3.2](#).

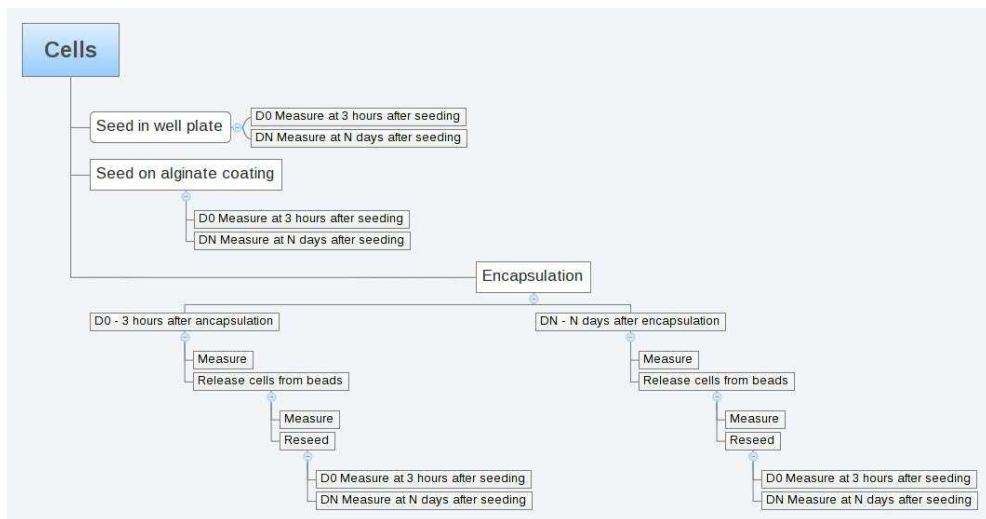


Table 3.2.: Scheme of experimental procedure

In brief two controls were used, cells seeded in a well plate (referred simply as control in the next paragraphs) and cells seeded on the alginate coating. To assess the effect of the encapsulation process some assays were performed with the cells inside the capsule then some of the capsules of the same batch were dissolved and the cells obtained were reseeded. The

exact procedure followed was a consequence of the assay performed, for example in AlamarBlue® it's possible to assess the vitality of the cells inside the beads while for the western blot cells must be released to obtain their lysates.

3.3.3.1. Cell viability

Samples were incubated in a 48 well plate protected from light for one and a half hours with a 15% solution of AlamarBlue® in DMEM. The incubation time was decided after a preliminary experiment. After the incubation, 100 μ l of supernatant were placed in a 96 well plate, 3 well plates were filled for each sample. Finally the samples were placed in a spectrophotometer and scanned. The effect of the alginate on the measured values was tested by performing the assay on an alginate coating and the empty beads comparing the results with a blank.

3.3.3.2. DNA quantification

Tryton-X was added to the cells, the solution was transferred to an Eppendorf where it was sonicated. The solution was diluted 1:10 with TE buffer and measured with the spectrophotometer.

3.3.3.3. Western Blot

About 1 million of B50 cells were collected and washed from each sample before being resuspended in a standard lysis buffer and centrifuged at 4°C (16000 rpm/20 minutes). The final concentration of the proteins was measured with a NanoDrop. NuPage® buffer and reducing agents were added and the samples were kept at 70°C for 10 minutes. The solutions were then placed on the channels of a hydrogel for electrophoresis

3.3 Electro hydro dynamic encapsulation: more biological evaluations

together with a protein standard (pure GAPDH and HSP70 respectively) and the electrophoresis was started. The proteins were then transferred on a membrane where they were incubated at 4°C overnight with the primary antibody following standard protocols, cleaned and incubated for two hours with the secondary antibody.

3.3.3.4. Confocal images

The pictures were taken on beads loaded with 5 millions cell per milliliter of alginate following standard protocols (already described)

Note on significance

In order to avoid an excessive number of symbols, on some graphs only the non significant values are marked

3.3.4. Results and discussion

3.3.4.1. Cell viability

As expected, the metabolic activity of B50 cancer cells on control well plate was overall higher compared to the other two cell lines evaluated, as shown in [Fig. 3.14](#). At day 2 confluence was already reached and this could explain the lower metabolic activity at day 3 due to contact inhibition. Like B50, 3T3 had a spike of metabolic activity at day 2 that significantly increases at day 3. On the other hand MRC5 had a constant metabolic activity that increased significantly only at day 3, 1 day later than the other two cell lines observed.

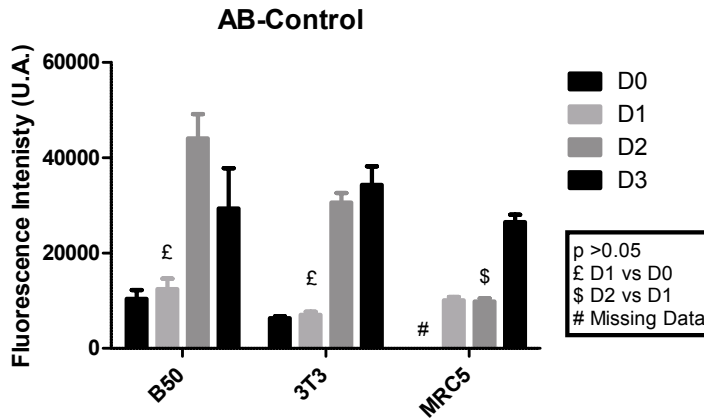


Figure 3.14.: Cell viability, well plate control.

The following three graphs compare the metabolic activity of the different cell lines seeded on the alginate coating and encapsulated inside the beads. All cell lines were influenced by the presence of alginate having a lower metabolic activity compared to control. Furthermore in all cases there is a lower metabolic activity inside the beads compared to the alginate coating that decrease with time indicating a possible quiescent state of cells when entrapped.

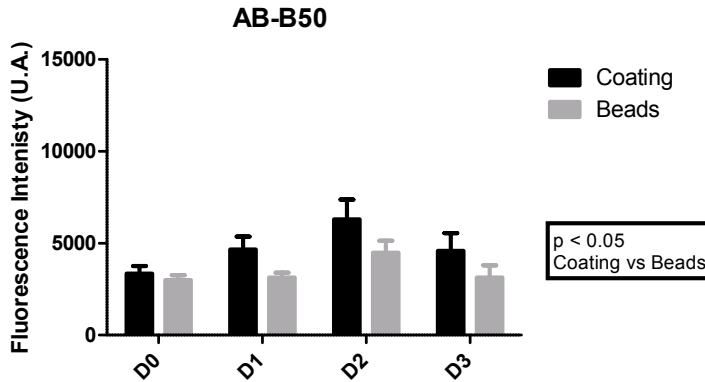


Figure 3.15.: Cell viability for B50, comparison between alginate substrate and beads.

As shown in [Fig. 3.15](#) for B50 the difference in viability between cells on the alginate coating and inside the beads is significant but not so marked as with other cell lines, especially at day 0 there is a relatively small difference that grows with time.

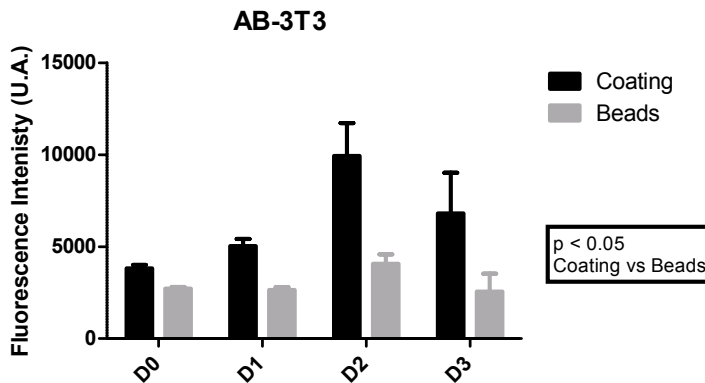


Figure 3.16.: Cell viability for 3T3, comparison between alginate substrate and beads.

As shown in Fig. 3.16 3T3 have a similar trend compared to B50, in this case the difference between the viability of cells on the coating and inside the beads is more marked

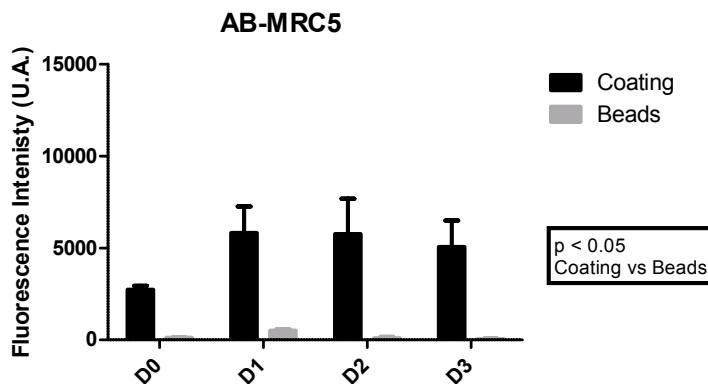


Figure 3.17.: Cell viability for MRC5, comparison between alginate substrate and beads.

Differing from the other two cases, MRC5 (Fig. 3.17) cells entrapped in the beads have a very weak signal. In this case the maximum values are not at day 2 like in the other two cases, after day one the metabolic activity decreases.

It should be noted that it's possible that the alginate bead acts as a diffusional barrier for resorufin slowing its supply in the limited time window of the incubation and, as a consequence, its metabolization by cells. However, as clearly proven by the B50 and 3T3 graph, resorufin can be metabolized if cells are inside the beads and if this limiting effect is actually present there is likely to be the same effect for all three cases. In fact, if we compare B50 and MRC5 cell lines, MRC5 show a much more limited viability when entrapped that when seeded on the alginate coating. This means that inside the beads, MRC5 cells seem to be in

3.3 Electro hydro dynamic encapsulation: more biological evaluations

a state characterized by a lower viability also due to their entrapment state and not only because of the presence of the material.

The following graphs show the trend in metabolic activity after releasing cells that were encapsulated for 1 (first value post reseeding is D3) and 7 days (first value post reseeding is D8). Cells were counted before seeding and for this reason this test take also into the account the effect on the overall metabolic decrease due to the cells that didn't reattach.

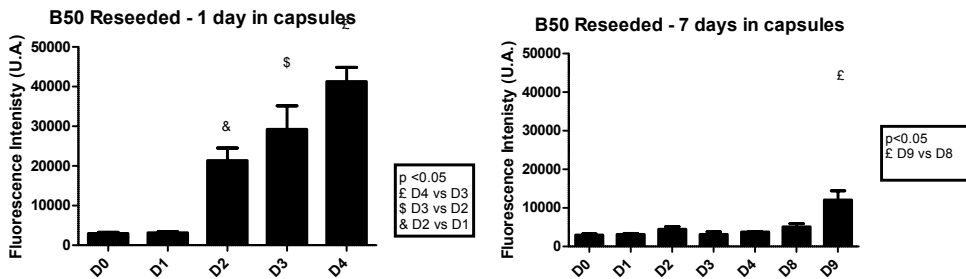


Figure 3.18.: after 1 day of encapsulation on the left, after 7 days of encapsulation on the right. Significance only for values post reseeding

B50 encapsulated for 1 day were able to regain the initial metabolic activity of control immediately after reseeding, in fact as shown in [Fig. 3.18](#) already at D2 the signal is higher than the signal for control cells at D0. When encapsulated for 7 days the recovery is slower and one more day is needed to regain the initial viability

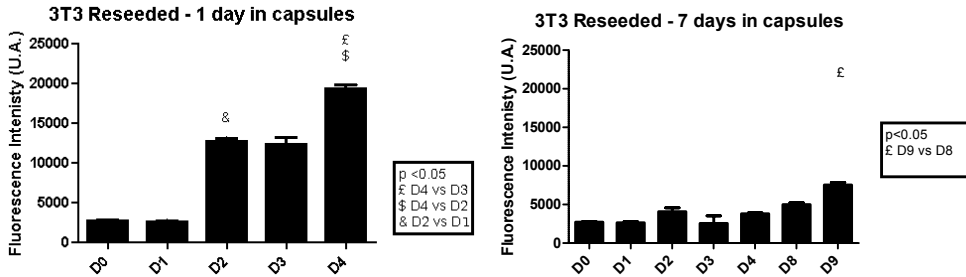


Figure 3.19.: 3T3 Reseeded after 1 day of encapsulation on the left, after 7 days of encapsulation on the right. Significance only for values post reseeding

3T3 have a similar trend to B50, as show in [Fig. 3.19](#) with an immediate recover if encapsulated for one day and a recovery delay of one day if encapsulated for seven.

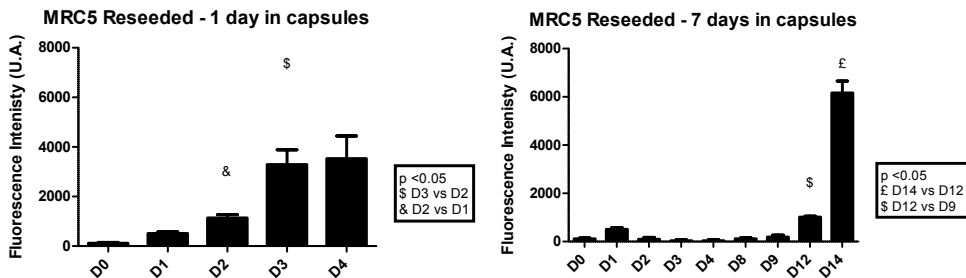


Figure 3.20.: MRC5 Reseeded after 1 day of encapsulation on the left, after 7 days of encapsulation on the right. Significance only for values post reseeding

MRC5, in contrast to the other two cell lines needed more time to recover their viability. In fact cells encapsulated for 1 day couldn't recover the initial metabolic activity completely after 3 days since release. Cells encapsulated for 7 days needed another week to regain a metabolic activity

comparable to control.

It's clear that all cell lines were affected by the encapsulation process, in particular human fibroblasts MRC5. Longer encapsulation times have a more marked impact on the sample to recover their initial metabolic ability. However this ability can be recovered and can become comparable to control even if longer times are needed.

3.3.4.2. DNA quantification

Fig. 3.21 shows the normalized number of cells inside the beads up to day 3. It's possible to observe a marked increase of cells in the case of B50, at day 3 the number of cells is more than double compared to D0. This confirms the previous observations on B50 with the confocal microscope where an increase of number could be observed (**Fig. 3.10**). 3T3 follow a similar trend but their number at day 3 only increases of a fraction of the initial number of encapsulated cells. The number of MRC5 remain constant, slightly but significantly decreasing at day 3. There is a relation with the viability assay, showing that a high metabolism of cells allows proliferation inside the beads (B50) while a lower metabolism doesn't. (MRC5)

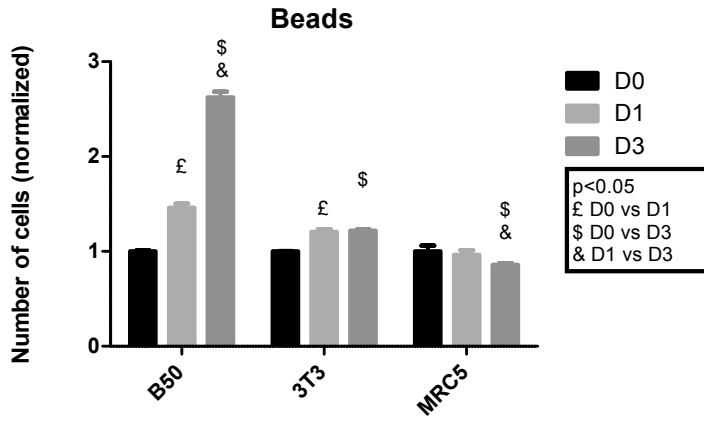


Figure 3.21.: Number of cells inside the beads, normalized to the number of cells at D0.

3.3.4.3. Confocal Microscopy

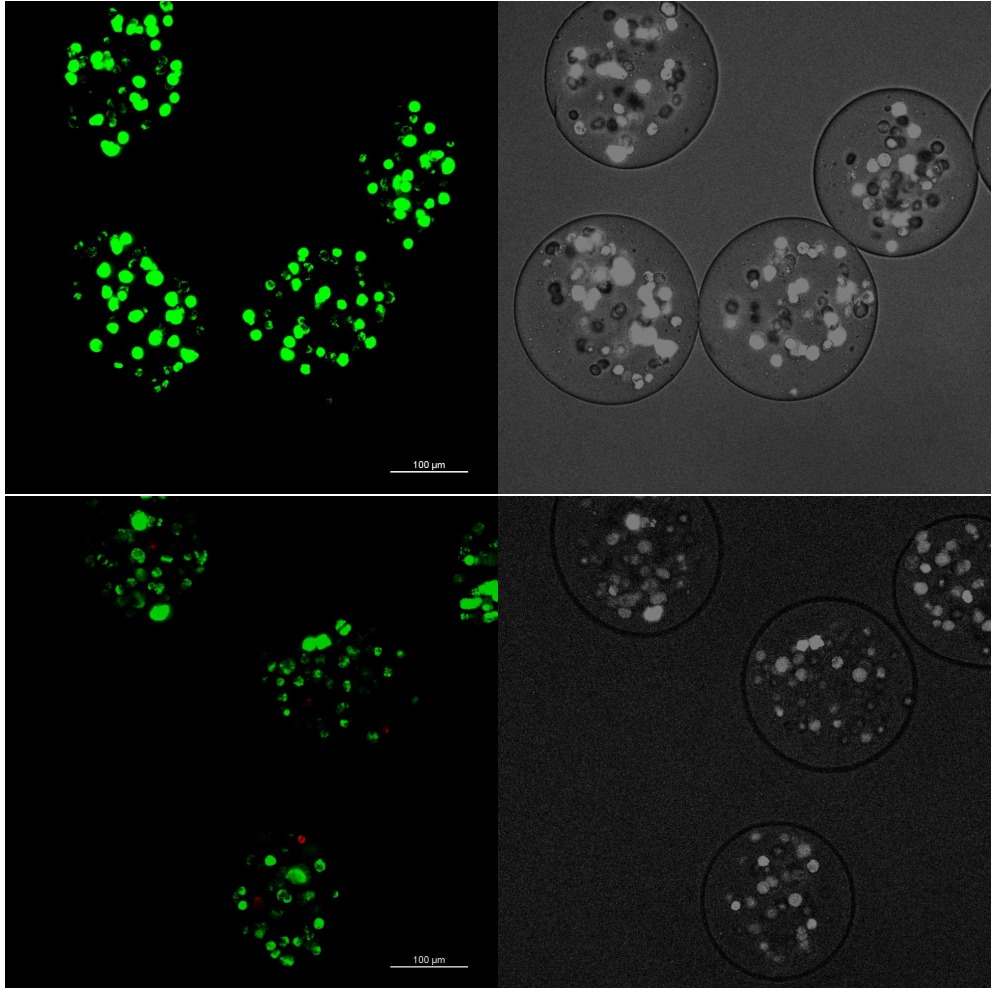


Figure 3.22.: Live/Dead assay: 3T3 Cells, top day 1, bottom day 7. On the left confocal image with green living cells, on the right optical image.

The confocal observations of 3T3 and MRC5 cells confirmed the viability of cells as was previously shown for B50. The signal seems weaker than

that from B50 in the case of cells encapsulated for 7 days and since the green dye must be metabolized by cells this could be a clue that longer encapsulation times put cells into a lower metabolic state. However cells remain viable.

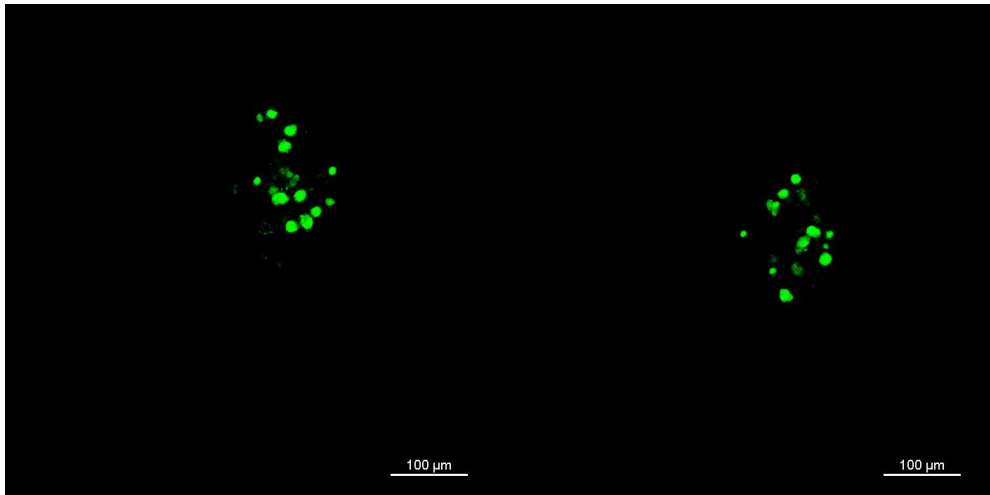


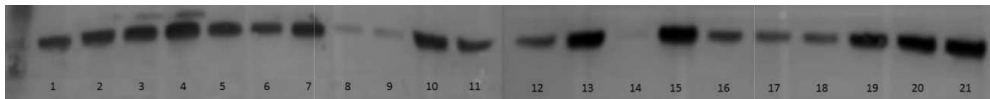
Figure 3.23.: Live/Dead assay: MRC5 Cells, 1 and 7 days

3.3.4.4. Western Blot

The results of the western blot were unexpected and are presented just as reference and for discussion. Gapdh is a house keeping protein used as a standard since in non hypoxia conditions its concentration is constant in cellular lysates. We initially tested the production of gapdh to set up a protocol for the western blot given the complication arising from working with encapsulated cells and obtaining lysates from them. A constant or increased level of gapdh when cells were in hypoxia conditions, was expected. However in the presence of alginate, the production of gapdh appeared lower.

3.3 Electro hydro dynamic encapsulation: more biological evaluations

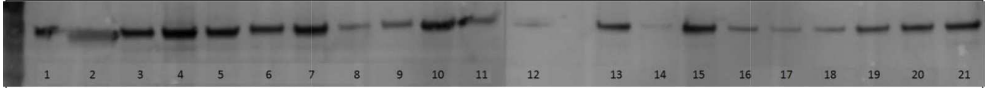
A lower production of gapdh is expected at D0 since cells still have to activate its production but wasn't expected at the following experimental times for example in the case of alginate coating and beads at day 1 (column 8 and 9)



- | | |
|----------------|--|
| 1. control | 12. D3 beads |
| 2. control | 13. D5 control |
| 3. control | 14. D7 beads |
| 4. D0 control | 15. cells release at D0 and re-seeded for 5 days |
| 5. D0 coating | 16. cells release at D1 and re-seeded for 5 days |
| 6. D0 beads | 17. cells release at D3 and re-seeded for 5 days |
| 7. D1 control | 18. cells release at D7 and re-seeded for 5 days |
| 8. D1 coating | 19. control |
| 9. D1 beads | 20. control |
| 10. D3 control | 21. control |
| 11. D3 coating | |

Figure 3.24.: Western blot of MRC5 cells, Gapdh marker

The same effect occurred for hsp70, with a marked decrease in production in the aforementioned columns.



- | | |
|----------------|---|
| 1. control | 12. D3 beads |
| 2. control | 13. D5 control |
| 3. control | 14. D7 beads |
| 4. D0 control | 15. cells release at D0 and reseeded for 5 days |
| 5. D0 coating | 16. cells release at D1 and reseeded for 5 days |
| 6. D0 beads | 17. cells release at D3 and reseeded for 5 days |
| 7. D1 control | 18. cells release at D7 and reseeded for 5 days |
| 8. D1 coating | 19. control |
| 9. D1 beads | 20. control |
| 10. D3 control | 21. control |
| 11. D3 coating | |

Figure 3.25.: Western blot of MRC5 cells, Hsp70 marker

It should be noted that cells are extracted from the beads by dissolving the alginate using PBS and stirring the solution to pellet the cells. The supernatant is removed, cells are washed and then a lysate is made or they are reseeded. We believe it's possible that alginate is not completely removed during this procedure interfering with the movement of the proteins in the electrophoresis run and leading to unexpected results in some columns. A similar situation could also justify the results referred for the alginate coating.

For example comparing control at column 10 and alginate coating at

3.3 Electro hydro dynamic encapsulation: more biological evaluations

column 11 it seems that the production of hsp70 on top of the alginate is much lower. The production seems even lower for cells encapsulated in the beads for three days in column 12 having a line barely recognizable on the membrane.

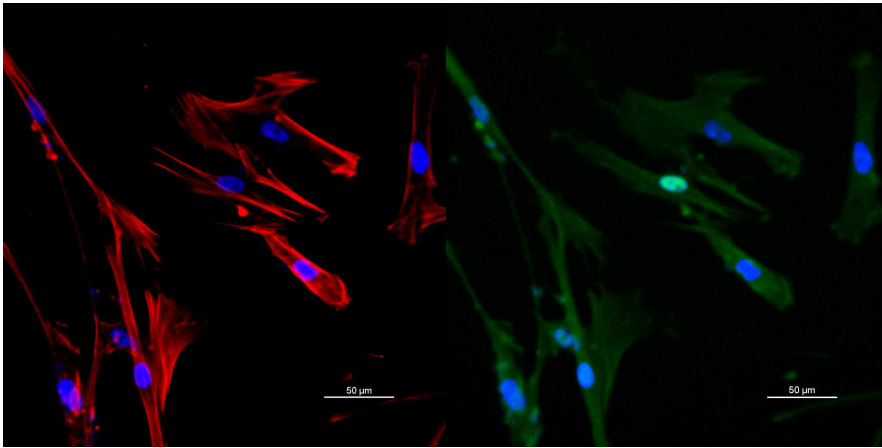


Figure 3.26.: MRC5, nuclei (blue) and cytoskeleton (red) on the left, nuclei (blue) and hsp70 (green) on the right. MRC5 cells grown on alginate coating, day3.

The confocal picture ([Fig. 3.26](#)) taken at the same experimental time of column 11 after immunostaining shows that the protein is indeed present in the cells when cultured on the alginate coating. While [Fig. 3.27](#) shows the situation corresponding to column 10, the control, where more cells are present, as expected.

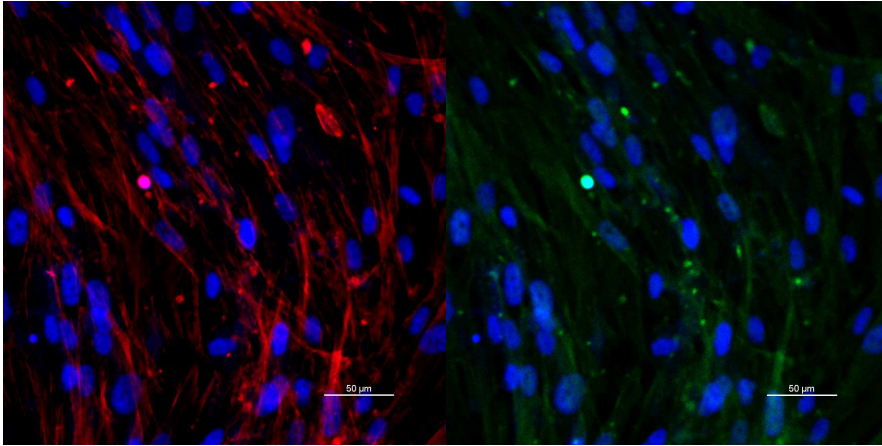


Figure 3.27.: MRC5, nuclei (blue) and cytoskeleton (red) on the left, nuclei (blue) and hsp70 (green) on the right. MRC5 cells grown on control well plate, day3.

Comparing the two pictures, even if confocal microscopy is not a quantitative observation, it's difficult to explain the barely visible line in the western blot for column 11. This is a clue that the results of the western blot could be misleading.

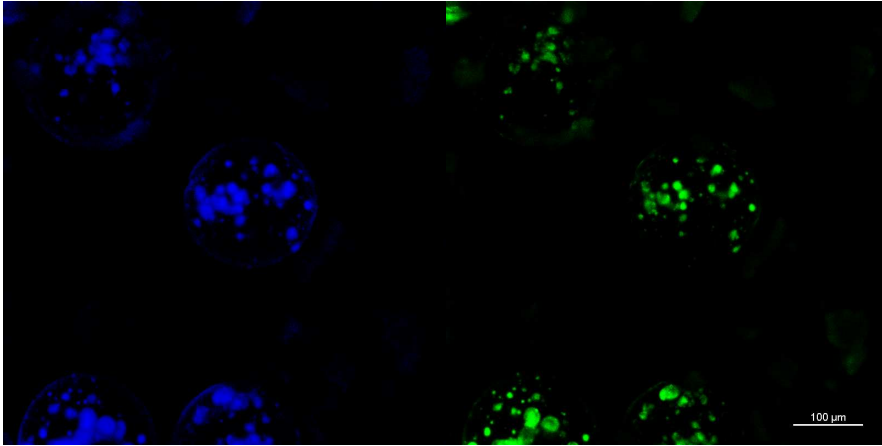


Figure 3.28.: MRC5, nuclei (blue) on the left, hsp70 (green) on the right. MRC5 entrapped in beads, day3.

3.3.4.5. Conclusions

These observations proved that cells were alive inside the beads even if their metabolism is slowed down, however it can be regained after reseeding. There was a difference in how cells respond to the encapsulation treatment, cells with a higher natural metabolism had, as expected, a less marked decrease in activity inside the beads and a faster recovery once released. Cells with a slower natural metabolism took more time to recover from encapsulation but their activity was not adversely affected.

3.4. Addendum: EHD Co-encapsulation of gelatin in alginate

3.4.1. Introduction

Once the cells are encapsulated in alginate they are uniformly distributed inside the hydrogel. This could limit the natural cell-cell interaction, the production of extra cellular matrix (ECM) and the interaction between cells and ECM which are fundamental for the reconstruction of a functional tissue in vitro [13, 105]. Alginate was chosen as the basic material for this thesis because there is a consistent amount of scientific literature dealing with its chemical modification and the tuning of its degradation kinetics without modifying drastically its ability to form gels.[50, 51, 36]. The tunable degradation of alginate could leave room for cells to build their own extracellular matrix until the alginate support is completely gone.

This section represents an attempt to set up an encapsulation process that leads to capsules containing small clusters of tissue [59] without relying on the degradation of alginate. The idea behind this attempt was to use gelatin as the encapsulation matrix of cells and then encapsulate the gelatin beads in alginate. This way the gelatin would become a liquid at physiological conditions and cells would be entrapped in the empty volume left by the gelatin beads inside the alginate leading to an alginate capsule containing small clusters of cells or maybe small clusters of functionalized tissue.

Gelatin is a complicated material to work with especially if the goal, like in this case, is to develop a protocol for cell encapsulation. Gelatin undergoes a sol-gel transition during cooling at about 35°C while cells

shouldn't be at temperature above 39-40°C to avoid damage leaving a relatively small window of 5°C degrees to work in. In fact the first attempt to create gelatin capsules was by using a metallic sieve as a mold to shape the hydrogel and then remove the capsules formed with a jet of nitrogen gas. Initially this method was developed for alginate with the idea of moving to gelatin once a protocol could be established. This method failed and tests with living cells were not performed. Subsequently another methods involving a water in oil emulsion was tested and gelatin capsules containing cells could be produced. Capsules created this way were encapsulated through the electro hydro dynamic process and observed with the confocal microscope. Overall the co-encapsulation using these two materials and methods here described had a lot of shortcomings and led to unexpected results.

This section describes a procedure that had potential but finally failed and it was abandoned after some months of work. For this reason it's only briefly described in following sections.

3.4.2. Materials

Alginic acid sodium salt from brown algae (alginate), calcium chloride dihydrate, low gelling agarose and gelatin from porcine skin, soy bean oil were purchased from Sigma-Aldrich (USA). Calcein AM, Propidium Iodide (PI), Phosphate buffer saline without calcium and magnesium (PBS), Dulbecco's modified eagle medium (DMEM) were purchased from Invitrogen (USA). Metallic meshes of different sizes (125 -200 μm) (for separation of powders) were purchased by Retsch (Germany). The needle of the electro hydro dynamic apparatus was a gauge 22S (Outer Diameter: 0.718 mm, Inner Diameter: 0.168 mm) was made of type 304

stainless steel and was purchased from Hamilton (Bonaduz/Switzerland). Neuroblastoma B50 cells line were purchased from the Istituto Profilattico Sperimentale, Brescia, Italy.

3.4.3. Methods

3.4.3.1. Preparation and sterilization of alginate, gelatin and oil.

Alginate powder was dissolved in PBS for 8 hours at room temperature under mild stirring to obtain a 2 % alginate solution (2g/100ml). Under a biological sterile hood the solution was loaded in a syringe and capped with a 0.22 μm Luer lock filter, at the other end of the filter a vial was attached and sealed with parafilm. The syringe was placed on an electrical pump set at 0.01 ml/min and filtered overnight. The sterile solution obtained in the vial was immediately used after filtration. The gelatin powder was dissolved under mild stirring in PBS for 3 hours at 45°C to obtain a gelatin solution (10g/100ml=10% , 20g=100ml=20%). The gelatin solution was filtered in a oven set at 45°C.

3.4.3.2. Preparation of gelatin containing cells

The cell culture was performed using standard protocols, exactly as described in a previous section of this chapter ([sec. 3.2.3.2](#)) using gelatin instead of alginate. In brief starting from a frosted vial of B50 cells a standard protocol was followed to obtain a culture of cells at confluence inside a 175 cm^2 flask. Cells were detached, counted and the right amount of warm gelatin solution was added to get 5 millions cell per ml of gelatin.

3.4.3.3. Encapsulation with metallic sieve as mold

The solution was poured on the sieve and carefully spread on the metallic net. The metallic sieve was left in a vertical position for five minutes to remove all the solution that didn't fill the voids of the sieve. Afterward the entire sieve was put in calcium chloride for crosslinking. With gelatin the protocol was similar but instead it was performed in an oven at 39°C on a preheated sieve. The sieve filled with gelatin solution was moved at room temperature to crosslink. A flux of nitrogen was used to remove the capsules from the metallic sieve in order to remove the hydrogel capsules. Underneath the sieve a water bath was placed to collect the capsules ejected from the sieve.

3.4.3.4. Gelatin in Oil Emulsion

A 50/50 blend of Span80 and Tween80 were used to stabilize the gelatin in the emulsion, 0,5 ml of the blend was added to 12,5 ml of sterile soybean oil, stirred and warmed up to 39 °C. About 2 ml of gelatin containing cells were added to the emulsion under stirring at room temperature, after 3 minutes the solution was moved inside a fridge for 5 minutes. A 50 ml vial was filled with the solution containing the beads and water was added to fill it completely. The vial was stirred for 10 minutes at 1000 rpm. The supernatant was removed leaving the gelatin beads in the bottom. The procedure was repeated two times to remove most of the oil.

3.4.3.5. EHD co-encapsulation and release

The alginate solution was added to the capsules produced with the water in oil emulsion, to obtain a 25% vol/vol of capsules in alginate. The

same procedure preciously described (sec. 3.2.3.4) was performed. In brief the alginate solution containing gelatin capsules was forced through the positively charged needle thanks to a pump set to a fixed flux. The beads ejected from the needle were collected in a calcium chloride bath and washed several times in PBS at room temperature before moving them inside a flask to an incubator.

3.4.3.6. Confocal Microscopy

The same method for alginate capsules without gelatin described in sec. 3.2.3.7 was performed, in brief it consists of two passages aimed at staining the cells with two different molecules. First an incubation in Calcein AM is performed followed by an incubation with Propidium Iodide.

3.4.3.7. Cell release

Cell were release from the beads following the method previously described (sec. 3.2.3.4). In brief beads were stirred and the nutrient solution was removed, some washes with PBS were performed to remove any residual divalent cation that could make the dissolution slower. Beads were placed in an incubator with PBS at 37 °C. Finally cells could be collected after stirring.

3.4.4. Results and discussion

3.4.4.1. Encapsulation with metallic sieve as mold

The initial tests with alginate gave decent results, the capsules were formed and successfully ejected from the metallic sieve keeping their

shape. The solution had to be spread on the metallic sieve very carefully so that only the voids were filled to favor the following detachment. The flux of gas actually teared the capsules from the metallic sieve as shown in [Fig. 3.29](#) where it was possible to see the unclean cuts on the edges of the capsules.

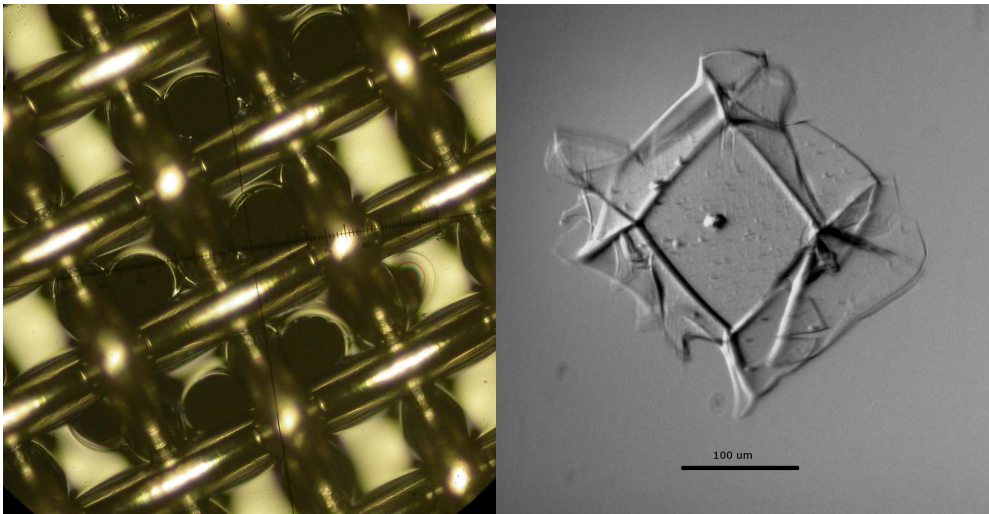


Figure 3.29.: Metallic sieve on the left still containing some capsules, on the right the capsule after the ejection from the sieve

This technique applied to gelatin didn't led to similar results, it was much more difficult to spread the gelatin solutions (10%, 20%) on the sieve. As shown in [Fig. 3.30](#) rather than filling only the voids a thin coating was formed leading to a much more difficult detachment of the capsule.

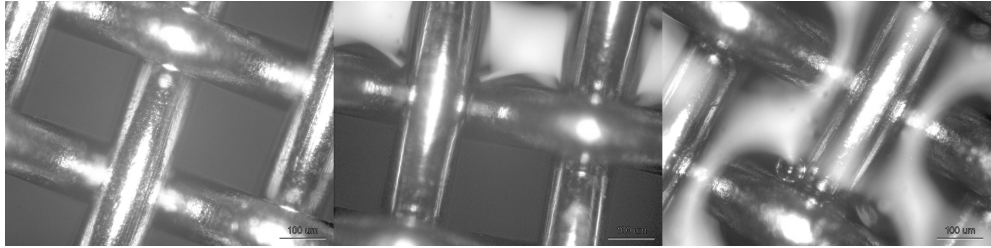


Figure 3.30.: Sieves and solution spreading. On the left metallic sieves only, in the middle sieves with alginate after partial ejection of beads, on the right sieve with gelatin, the gelatin didn't fill only the pores as alginate.

As seen from [Fig. 3.31](#) some capsules could be ejected but in most cases there was a complete detachment of the coating leading to the detachment of cluster of capsules. With high fluxes of gas the gelatin capsules were destroyed rather than ejected. Different concentration of solution were tested as different intensity of gas flux but a good balance that could lead to the ejection of single capsules without destroying them could not be found.

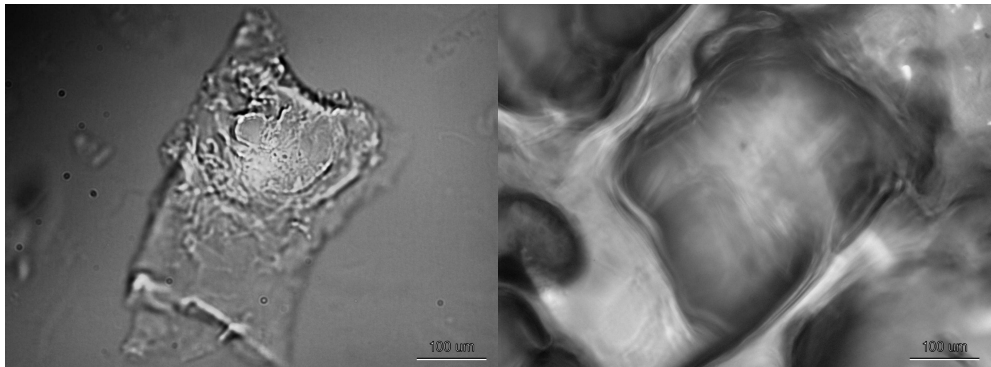


Figure 3.31.: Gelatin capsules formed by a metallic sieve, on the left a gelatin capsules on the right the detachment of the gelatin coating formed on the sieve

3.4.4.2. Gelatin in oil emulsion

An aliquot of the solution containing the gelatin beads was taken from the middle of a vial with a pipette after the washing procedure and a drop was placed on a microscope slide. A picture was taken and as it's shown from **Fig. 3.32 B** oil is still present on the top of the drop regardless of the washing performed after the preparation of the capsules. As show in **Fig. 3.32 A** the diameter of the capsules ranged from 10 to 70 μm

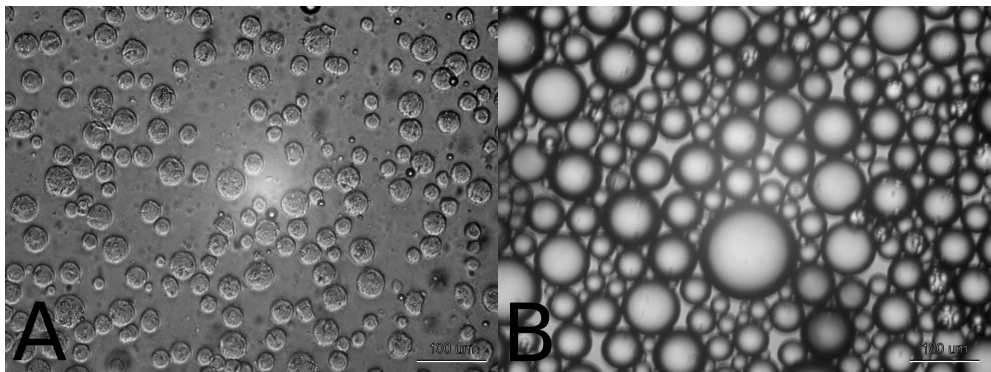


Figure 3.32.: Gelatin capsules without cells: capsules collected from the bottom of the vial (left) and oil present on the top (right)

This technique allowed the fabrication of smaller capsules if compared to the EHD process. In fact with the EHD process set up in the jetting mode it was possible to obtain capsules with a mean diameter between 150 and 200 μm but with a much lower dispersion of results.

The addition of cells led to capsules with a diameter that was even more dispersed but given the goal of these experiments the dispersion of the diameters observed was not considered an issue. The presence of the capsules with a diameter higher than 100 μm didn't allow to use a gauge 33 needle (I.D. 108 μm) as in the previous experiments. For this reason

a gauge 22S (I.D. $168 \mu\text{m}$) needle was chosen for the coencapsulation in alginate with the EHD process.

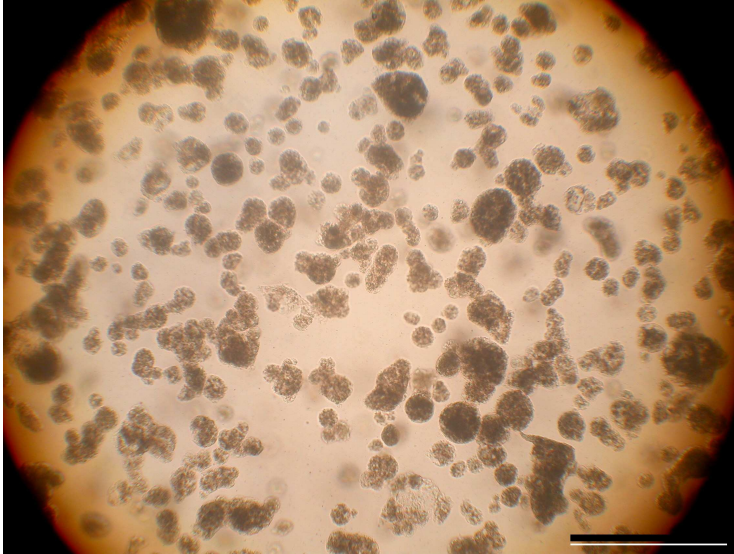


Figure 3.33.: Gelatin capsules containing cells, bar is $250 \mu\text{m}$

It should be noted that there are many factor related to temperature control that should be taken into consideration. After placing the gelatin solution in oil some time is necessary for the gelatin to become an hydrogel. The sol-gel transition also depends from the materials gelatin is in contact with, for example higher temperature are needed if the gelatin is placed in a metallic sieve, like the one we used in our previous experiment, compared to a polypropylene plate. Typically a reasonable amount of time is needed to allow the sol-gel transition but in the presence of cells there are time issues that must be respected since cells are not in their physiological environment. So the solution was placed in a refrigerator to increase the cooling rate and favor the sol-gel transition but excessive low temperature could affect cell behavior. For these reason the duration

of the solution inside the refrigerator was hard to establish and was set to 5 minutes after a trail and error approach.

3.4.4.3. Gelatin and alginate with EHD encapsulation

The EHD process using an alginate solution containing gelatin beads was inclined to clogging, the needle was changed and cleaned very often. However gelatin laden beads could be manufactured, as shown in [Fig. 3.34](#).

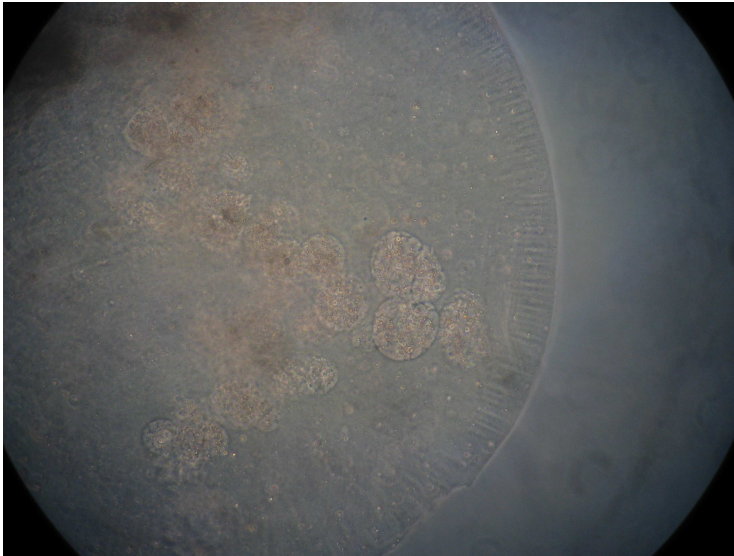


Figure 3.34.: Gelatin capsules inside an alginate bead

Since the needle system was clogging often a constant supervision was necessary and a long time was needed for the encapsulation process due to the many interruption of the process . Needles with bigger inner diameter exists but with those needles a much higher voltage is needed to reach the jetting condition obtaining beads bigger than 1 mm. It should be

noted that the process took place at room temperature to avoid the sol-gel transition of the entrapped gelatin. It took more than one hour from the end of the cell culture to the end of the encapsulation when the beads were placed back in the incubator.

3.4.4.4. Confocal

The pictures taken with the confocal microscope show portion of the beads with a high density of living cells while other parts have some green spots corresponding to living cells.

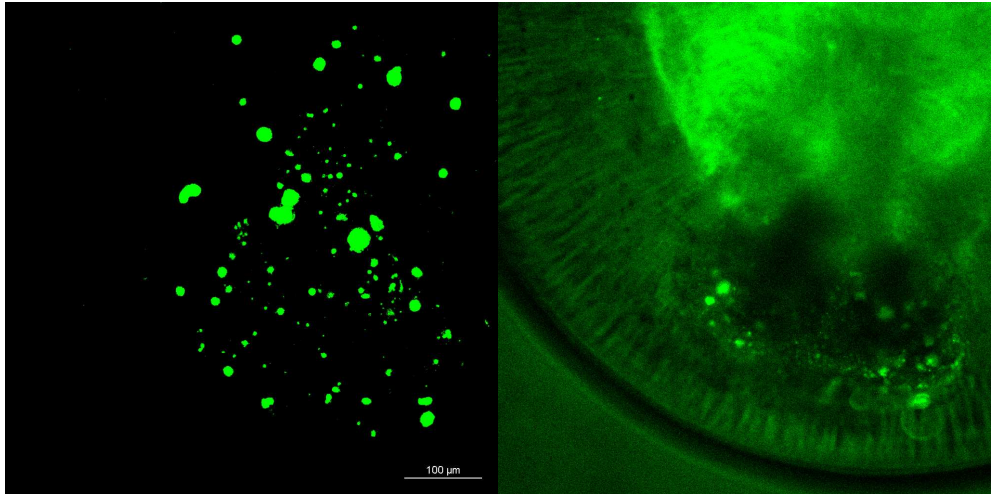


Figure 3.35.: EHD encapsulation confocal images, on the left laser only and on the right laser plus light to outline the borders of the beads.

In other occasions this subdivision could not be observed and living cells were present in extend portions of the picture. We believe that the shear stresses of the flow of solution and the ones present at the tip of the needle of the EHD encapsulation system destroyed part of the gelatin beads, partially spreading the cells inside the alginate.

3.4.4.5. Cell release

Cells didn't reattach after being release from the beads. This was unexpected since the confocal observation show very few dead cells in the beads.

3.4.5. Conclusion

Gelatin is an interesting material given its thermo responsiveness at temperatures close to physiological ones but its use in a coencapsulation system leads to problems difficult to overcome. Starting from the encapsulation of cells inside the gelatin there were aspects related to temperature control difficult to overcome because the process must be quick to avoid thermal stress on cells. In order to have a stable gelatin in oil solution surfactants were added and as consequence the removal of oil with water based solution was difficult, more washes were needed that makes the encapsulation process even longer. Furthermore the use of surfactants like Tween and Span in close contact with living cells it's debated for the their potential toxicity. Overall the process was abandoned given its shortcomings, in particular because of the clogging of the machine. In order to avoid it a bigger needle should be used that leads to bigger beads which find limited application, especially if this encapsulation system is used for a printing apparatus where small spot sizes are needed.

4. Electro hydro dynamic printing

4.1. Introduction

A bioprinter is made of a positioning and a deposition system, a bioink that feeds the deposition system which can contain cells, a biopaper that is the substrate where the cells and/or the scaffold lies after being printed. For example Xu et al. [102] reported the possibility to adapt commercial ink jet printers with a thermal head to print viable cells while Cui and Boland [23] with a similar printer were able to print human microvascular endothelial using a bioink made of cells and fibrin. Also laser printer have been studied, for example Barron et al. [7] used a forward transfer technique in which a laser transfers cells from a biological medium to a receiving substrate while Ringeisen et al. [76] printed pluripotent embryonal carcinoma cells with minimal single-strand DNA damage. These system have been proved valid in specific situations but a system able to print samples in 3D with high throughput good spot resolution and high load volume at the same time is still missing [77].

A valid deposition system is generally a system that allows a controlled ejection of undamaged cells that travel for a relative short distance before reaching the target deposition substrate. The electro hydro dynamic

jetting (EHDJ) system potentially fulfill this requirement. Moreover is a high throughput system that needs relatively low cost equipment commonly found in research laboratories is able to create micron size beads and the feeding solution is supplied through a syringe driven by a programmable pump giving a wide range of loading options [11].

In the EHDJ a solution (bioink) is fed through a positively charged metallic needle, the solution reacts to the presence of the charge generating repulsive forces and creating a jet. The EHDJ is a jetting system governed by process parameters that can be easily changed, some of them dynamically without stopping the deposition system (voltage, flux of solution, distance from target) possibly leading to different geometrical features of the ejected drops [60].

EHDJ has been investigated with good results to print scaffolds for biological applications, for example Kim et al. [47] successfully printed a 2D layer of collagen on an agarose coated glass while Gupta et al. [38] were able to print biodegradable and non biodegradable nanocomposite scaffolds into predesigned structures with a thickness limited to five layers of material. There is also a raising interest in the EHDJ process to electro spray viable undamaged mammalian cells, for example Mongkoldhumrongkul et al. [61] proved that the EHDJ process have no significant impact on gene expression and as a consequence on general cell function while Clarke et al. [20] demonstrated the ability to electro spray multicellular zebra fish embryos without harmful effects.

EHDJ is a process that can also be exploited for encapsulation of living cells using an alginate solution [100], commonly used for encapsulation of living cells [64] since it's permissive to nutrients diffusion and undergoes a sol-gel transition under conditions compatible with cell survival. Multivalent cations (for example Calcium or Barium ions [72, 29]) bind the

guluronic blocks of the alginate chains, creating ionic interchain bridges which cause the gelification of aqueous alginate solutions [80, 53]. Alginate can also be chemically modified to tune its degradation kinetics [106] or can be chemically treated to dissolve and to release the cells entrapped [87].

Combining together EHDJ, a computer aided positioning system, an alginate solution containing cells and a proper deposition substrate we believe it's possible to join the two phases of scaffold fabrication and cell seeding by assembling in one single step a scaffold permissive to nutrients diffusion already containing living cells.

In this work we proved the possibility to use computer controlled EHDJ printing techniques to obtain depositions of cell laden hydrogels studying the main process parameters and evaluating the effect of the process itself to cell viability. As a substrate we used gelatin, a thermoresponsive polymer that undergoes a reversible sol-gel transition under 34-36°C and being liquid at physiological conditions[49] can be easily removed from the printed sample. Using this hydrogel enriched with calcium ions as biopaper it was possible to crosslink the alginate bioink upon contact on the substrate without the need of further processing.

4.2. Materials

Alginic acid sodium salt from brown algae (alginate), calcium chloride dihydrate, low gelling agarose and gelatin from porcine skin were purchased from Sigma-Aldrich (USA). Calcein AM, Propidium Iodide (PI), Phosphate buffer saline without calcium and magnesium (PBS), Dulbecco's modified eagle medium (DMEM) were purchased from Invitrogen (USA). The positioning system of the printer is a Janome JR2000N desktop robot

(Japan), the deposition system is made of a generator (ES30, Gamma High Voltage Research Inc, USA), a pump (NE-300, New Era Pump Systems, USA), a polytetrafluoroethylene tube and a gauge 33 stainless steel needle (outer diameter: 0.210 mm, inner diameter:0.108 mm Hamilton, Bonaduz/Switzerland). Mouse fibroblasts 3T3 cells line were purchased from the Istituto Profilattico Sperimentale, Brescia, Italy.

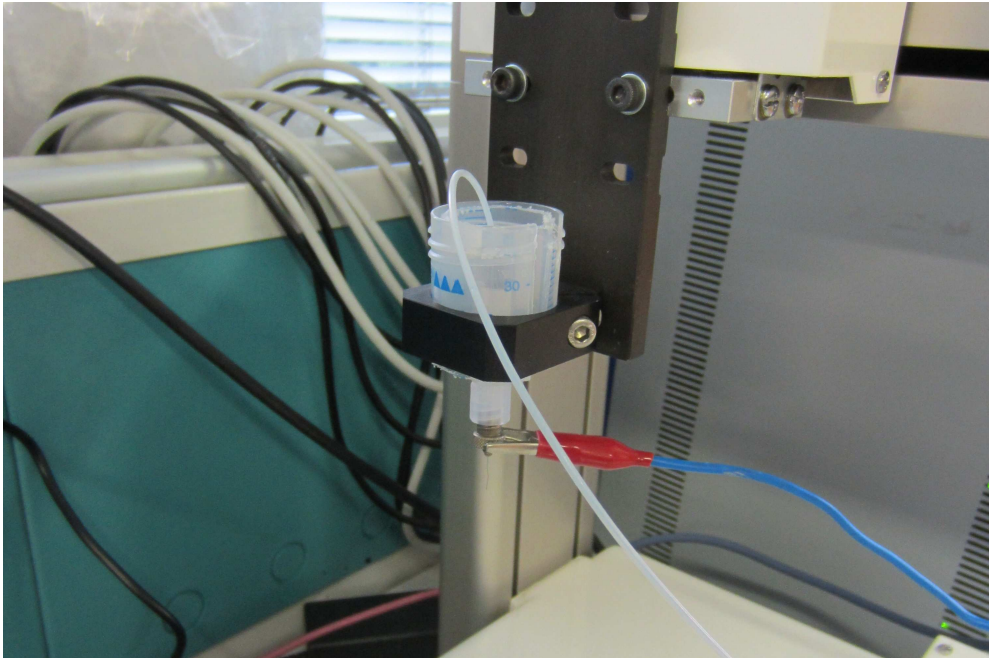


Figure 4.1.: EHDJ deposition system

4.3. Methods

4.3.1. Preparation and sterilization of alginate, agarose and gelatin

Alginate powder was dissolved in PBS for 8 hours at room temperature under mild stirring to obtain a 2 % alginate solution (2g/100ml). Under a biological sterile hood the solution was loaded in a syringe and capped with a 0.22 μm Luer lock filter, at the other end of the filter a vial was attached and sealed with parafilm. The syringe was placed on an electrical pump set at 0.01 ml/min and filtered overnight. The sterile solution obtained in the vial was immediately used after filtration. The agarose powder was dissolved under mild stirring in PBS for 3 hours at 60°C to obtain a 2 % agarose solution (2g/100ml). Similarly to the alginate, the agarose solution was filtered but this time the filtration process took place in a oven set at 45°C. For the gelatin coating a 400 mM calcium chloride solution was prepared by dissolving the salt in PBS, gelatin powder was added and dissolved under mild stirring condition at 40°C for 3 hours to obtain a 10% gelatin solution (10g/100ml). The filtration process of gelatin was the same of agarose with the oven set at 40°C. After filtration the solution in the vial was poured in a 94 mm Petri dish under a biological hood at room temperature, the Petri coated with gelatin was left under the hood for 3 hours to allow the sol-gel transition, 20ml of solution were used for each Petri dish.

4.3.2. Preparation of alginate containing cells

The cell culture was performed using standard protocols, in brief about one million of 3T3 mouse fibroblasts cells were defrosted and seeded in

a 25cm² flask using DMEM containing 2mM Glutamine and 10% Fetal Bovine Serum (Gibco) as culture medium. After 24 h cells were washed in PBS to remove residues of DMSO left from the freezing solution. At sub confluence (80%) cells were detached from the flask with 0,05 % Trypsin/EDTA (Euroclone) and reseeded in a 175 cm² flask. At confluence cells were detached and moved to a 15 ml vial. Cells inside the vial were stirred at 1000 rounds/min for 10 minutes and the supernatant was removed. In order to remove any residue of medium containing cations that could crosslink the alginate solution, cells on the bottom of the vial were resuspended in PBS and stirred again. Cells were dispersed by vibration inside the buffer and an aliquot of the solution was taken to count the cells using a Cellometer Auto T4 and Trypan Blue 0,4% (Invitrogen) as contrast agent. Cells were stirred again, and after removing the supernatant the alginate solution was added to obtain an alginate solution containing 5 millions cells for milliliter. Medium, PBS, Trypsin/EDTA and the alginate solution used were prewarmed at 37°C.

4.3.3. Printing

The printer (see Fig. Figure [Fig. 4.2](#) on page [95](#) A) was carefully cleaned with ethanol and placed under a biological hood. It consist of a positioning and deposition system which are decoupled and can be run independently, in this article we will refer to the printer as the whole apparatus. The positioning system can be programmed by a computer or by a console connected to the printer with three degrees of freedom. It consists of a metallic plate moving linearly (x) on the base of the printer and a plastic holder above it moving in y and z. A metallic plate connected to the ground of the generator was placed on a polymeric insulator lying on the printer to avoid conductive contact between the two metallic

objects. The Petri dish coated with the gelatin hydrogel containing ions was placed on the plate. The dropping system consist of a needle with a custom fit that was placed in the plastic holder of the printer above the plate and connected to a polytetrafluoroethylene tube with a Luer lock, The tip of the needle was connected to the positive cathode of the generator. The other side of the polytetrafluoroethylene tube was connected to a 3 ml syringe loaded with alginate solution and placed on a pump set to a fixed flux. A calibration was performed for each Petri dish, in particular the z axis of the printer was set as zero when the needle touched the gelatin coating. To perform the experiments the pump was started and when the solution reached the tip of the needle the generator was turned on and the printing program was initialized. In order to remove the samples from the coating the Petri dish was placed in an incubator to obtain a gel-sol transition of the gelatin, this way the alginate deposition could be easily removed from the gelatin solution using tweezers.

4.3.4. Agarose mold and alginate dissolution

Some of the alginate depositions containing cells were entrapped in a agarose mold for post processing. First some agarose was poured to coat the bottom of the bottom of a 24 wells plate and left at room temperature to undergo the sol-gel transition. Once the coating was obtained the alginate deposition was placed on the hydrogel and more liquid agarose was poured in the wells. The samples were left at room temperature until the second layer of agarose became an hydrogel. Samples were removed with tweezers, placed in a 6 well plate containing DMEM and moved in an incubator.

To dissolve the alginate, first the supernatant was removed and the sam-

ples were washed with PBS at 37°C, a Trypsin/Hepes solution was added and the samples were moved to an incubator for twenty minutes. Samples in the agarose mold were cut with a scalpel to give cells a way out from the hydrogel and observe the reattachment on the tissue culture plate.

4.3.5. Confocal microscopy

A live/dead assay with Calcein AM and Propidium Iodide was performed on printed hydrogel samples using standard protocols. In brief the samples were moved with tweezers to a new plate containing medium with a 10% v/v Calcein-AM solution, then the well plate was placed in a dark incubator for 30 minutes. At the end of the incubation time the samples were moved to a new well plate and washed three times before adding a 2% v/v Propidium iodide solution. The samples were left for 3 minutes protected from light at room temperature and washed again. All solutions used were at 37°C. Observations with the confocal microscope (Nikon A1, Japan) were performed in wet state, a separate image was taken for each setup.

4.4. Results

4.4.1. Description of printing process

The printing process can be tuned either to obtain single dot or continuous line deposition. Fig. [Fig. 4.2 B](#) shows two different kinds of parallel depositions obtained with one single run of the printer, the first is a continuous deposition while the second is a series of aligned dots parallel

to the first. This sample was obtained by programming the printer to perform a 100 mm deposition of alginate on a straight line along y then changing the x coordinate and moving back in a parallel path along y increasing the speed of the needle and the flux of solution but keeping the distance from target and applied voltage constant. The first deposition clearly shows separate beads formed by the EHDJ process laying on the gelatin coating, while the straight line results from the coalescence of closed packed dots, as evidenced in the optical microscope image in [Fig. 4.2 D](#) where the boundaries between the beads can be recognized.

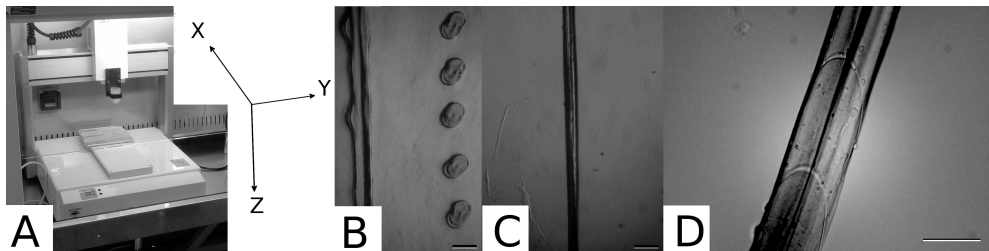


Figure 4.2.: Deposition of alginate A) the printer B) two different kinds of deposition by changing the speed of the needle C) thickness of the continuous line deposition D) beads that “fuse” together to create a continuous line

In the optical microscope image on [Fig. 4.2](#) it's possible to observe perfectly aligned and almost equally spaced dots, by decreasing the speed of the needle the inter space become lower until the beads collide forming a continuous deposition.

The beads undergo a fast sol-gel transition upon contact to the gelatin hydrogel containing calcium cations so that an hydrogel immediately forms sticking to the coating and maintaining its position. In a EHDJ process the drops eject from the needle at high speed and this aspect can be observed on the printed samples. In fact as a result from the

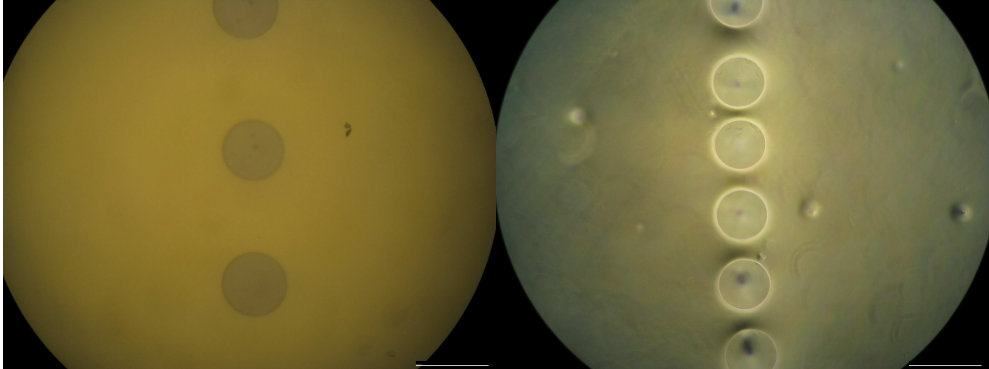


Figure 4.3.: Beads closer together by decreasing the speed of the needle.
Bar is $500 \mu m$

impact the beads tend to squeeze on the coating losing the spherical shape . It's likely that the sol gel transition starts from the initial contact point between the gelatin and the alginate then, given the speed of the beads and the beads squeezing on the surface, this contact area becomes bigger increasing the amount of solution in contact with the cations. Subsequently the cations diffuse in the alginate leading to a complete sol-gel transition of the whole bead.

Fig. 4.4 shows an horizontal and vertical deposition of alginate crossing each other. The two depositions joins in the point of contact and the joint has enough mechanical properties so that in can be lifted from the liquid gelatin.

The ability of alginate to diffuse divalent cations allows the fabrication of thicker printed samples by a layer by layer deposition. The thicker the deposition is the more time is needed to obtain a sol-gel transition of the last deposited layers. For this reasons a pause could be necessary after each layer in the case the diffusion speed is not sufficient to fully gelify the alginate. This is particularly evident for small samples where

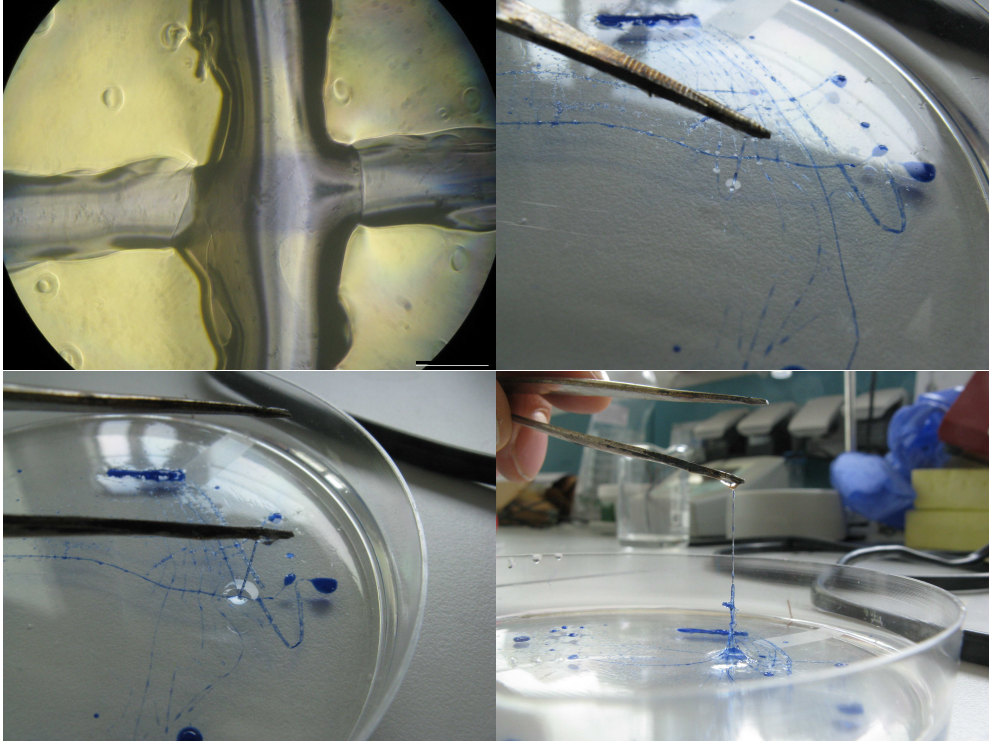


Figure 4.4.: Cross shaped alginate deposition with enough mechanical properties to be handled. Bar is 500 μm

this pause is necessary to avoid the deposition of alginate solution on top of a layer of alginate that is still partially liquid. If the sample is big enough and, as such, the printer takes more time to complete each layer this pause is not necessary (ex [Fig. 4.5](#)).

Given the deposition process used and the experimental setup it's not possible to control the start of the drop formation. Once the generator is turned on a short time is needed to establish a jet of drops, so it's not possible to predict when the first drop will be ejected from the needle. For this reason it was convenient to plan a deposition that include a sacrificial

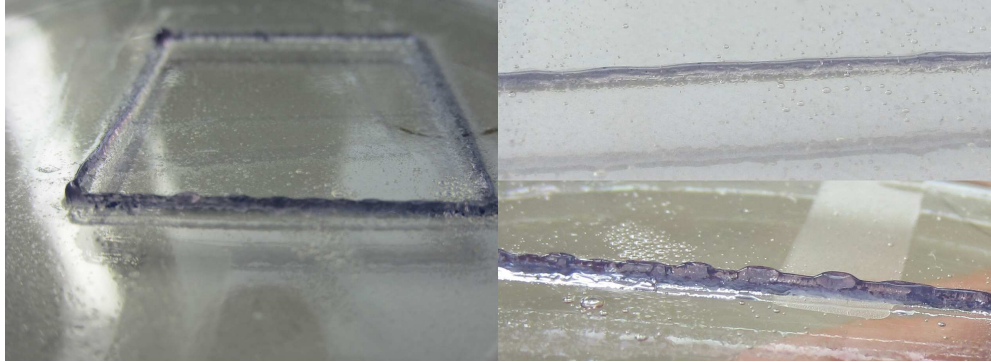


Figure 4.5.: Square shaped continuous deposition, border 5 cm. On the right magnifications that show the evolution of the deposition increasing the number of layers.

part that can be easily removed at the end of the printing process. Fig [Fig. 4.6](#) A shows parts of the procedure to obtain a small multilayered sample, for example if a cylindrical structure with a diameter of 3 mm (average diameter) must be printed, it was found convenient to move the needle slowly in a “standby area” (zone between points 1 and 2) to allow enough time for the sol-gel transition of the previously deposited layers, then to rapidly accelerate in a fast approaching zone (between points 2 and 3) to limit material deposition and facilitate the removal from the final construct. Once in the deposition zone (circular ring after point 3) speed is set for optimal deposition. Full 3D fabrication can be obtained by the overlapping of layers, repeating the procedure progressively increasing z position of the needle.

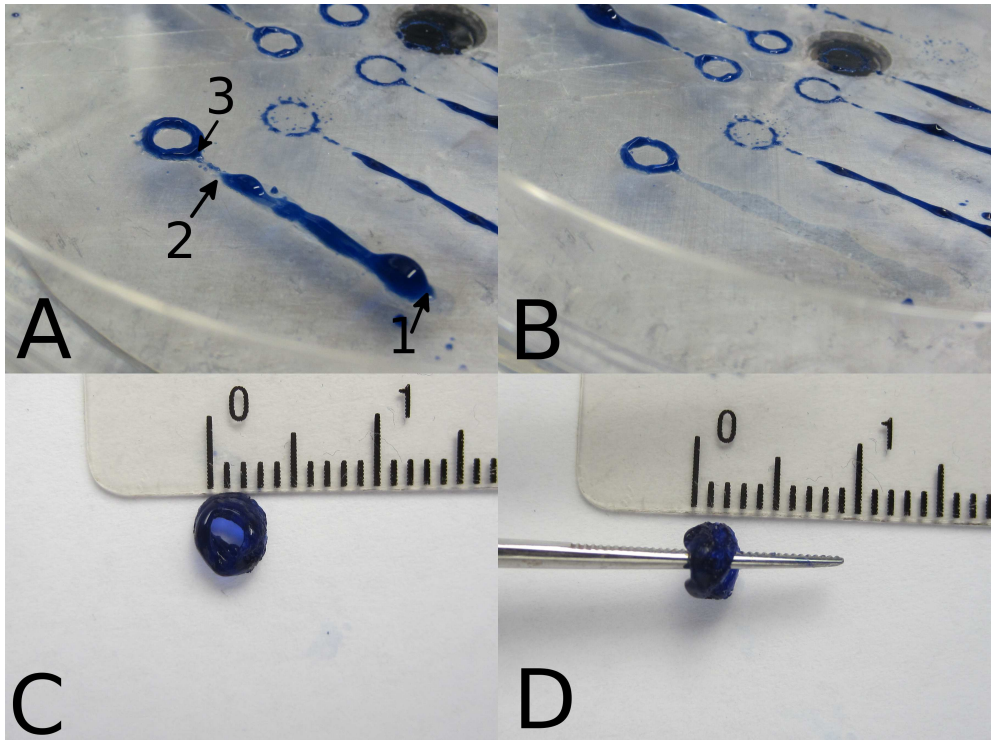


Figure 4.6.: Printing a “small thick sample”, A) initial deposition design with sacrificial part B) sample with sacrificial part removed C and D) sample after few layers of deposition.

4.4.2. Process parameters

The EHDJ printing process is influenced by easy to control parameters such as: the flux of solution flowing through the needle, the potential applied, the speed of the needle in the x and y plane and the distance from target (the length between the tip of the needle and the top of the gelatin coating underneath it). Since the speed of the needle was found to have a strong influence on the characteristics of the printed samples, we tested all the aforementioned parameters versus speed, ranging from 1 to

6 mm/s. As a starting set up we printed samples at 14KV, 0.01ml/min at a distance of 5 mm varying one single parameter for each experiment.

4.4.3. Flux of solution vs speed

Increasing the flux of solution from 0.005 to 0.01 and 0.02ml/min more deposition were continuous and thicker. At 0.005 ml/min the tendency was to obtain dotted depositions, partially bridged together at low speeds while at 0.02 ml/min the tendency was opposite and more continuous deposition could be obtained with only one dotted printed line at the highest speed tested (6 mm/s). At 0.01 ml/min the depositions were continuous at low speeds becoming aligned dots at higher speeds. All the tested samples didn't present any deviations from a straight line. For each set of samples it's possible to observe an inverse relation between speed of needle and diameter of the deposition, with smaller deposition obtained at higher speeds. Deposition are generally thicker at higher fluxes. For example it's possible to observe dots showing a diameter of about 250 at 0.005 ml/min and 6 mm/s speed rising up to almost 500 μm with solution flow set at 0.02 ml/min.

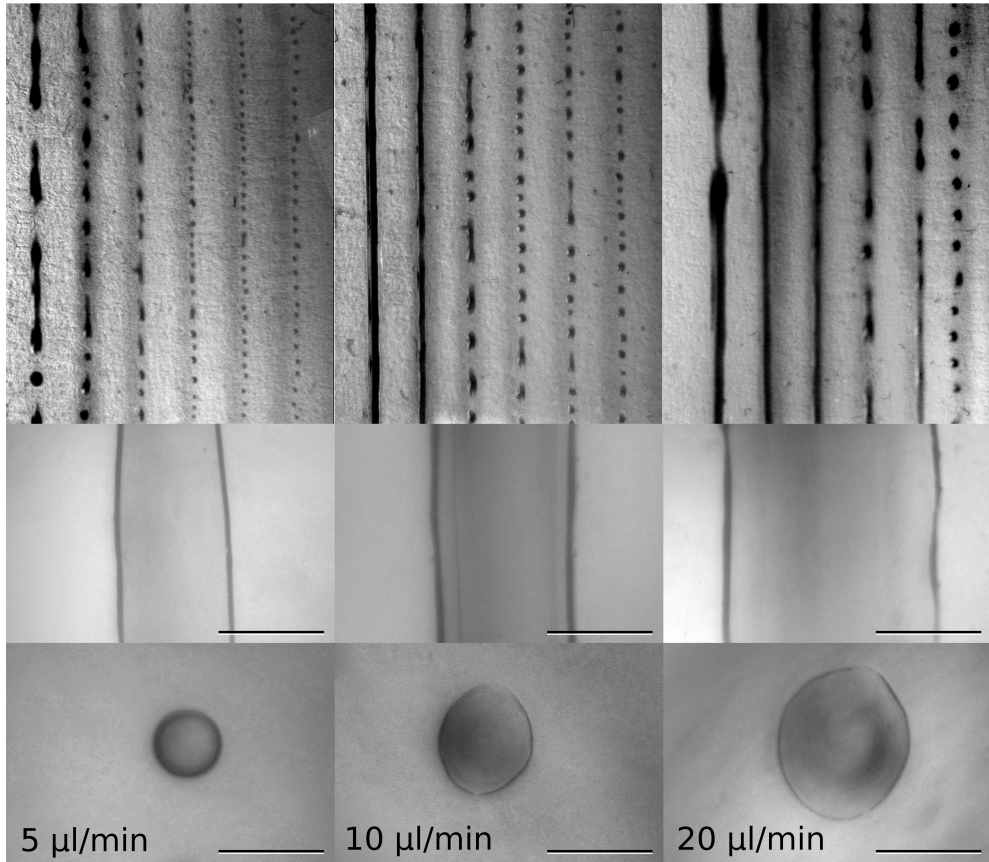


Figure 4.7.: From left to right depositions at 0.005ml/min, 0.01ml/min, 0.02ml/min. Top row shows the geometrical feature of the depositions varying the needle speed from 1 to 6 mm/s. Middle row shows depositions obtained at 1 mm/s while last row shows depositions at 6 mm/s. Scale bar is 500 μm

4.4.4. Voltage vs speed

The tested voltages ranged between 12 to 20 KV with increments of 2 KV. At 12KV a proper jet of drops could not be established as shown in

Fig. **Fig. 4.8:** single beads are deposited by gravitational dripping and they are closer to each other at lower speed. From 14 KV up the jet of drops could be established. By further increasing the voltage a certain degree of disorder appears on the printed samples. At 20KV the voltage is too high to obtain an ordered deposition, all the lines are misaligned and irregular.

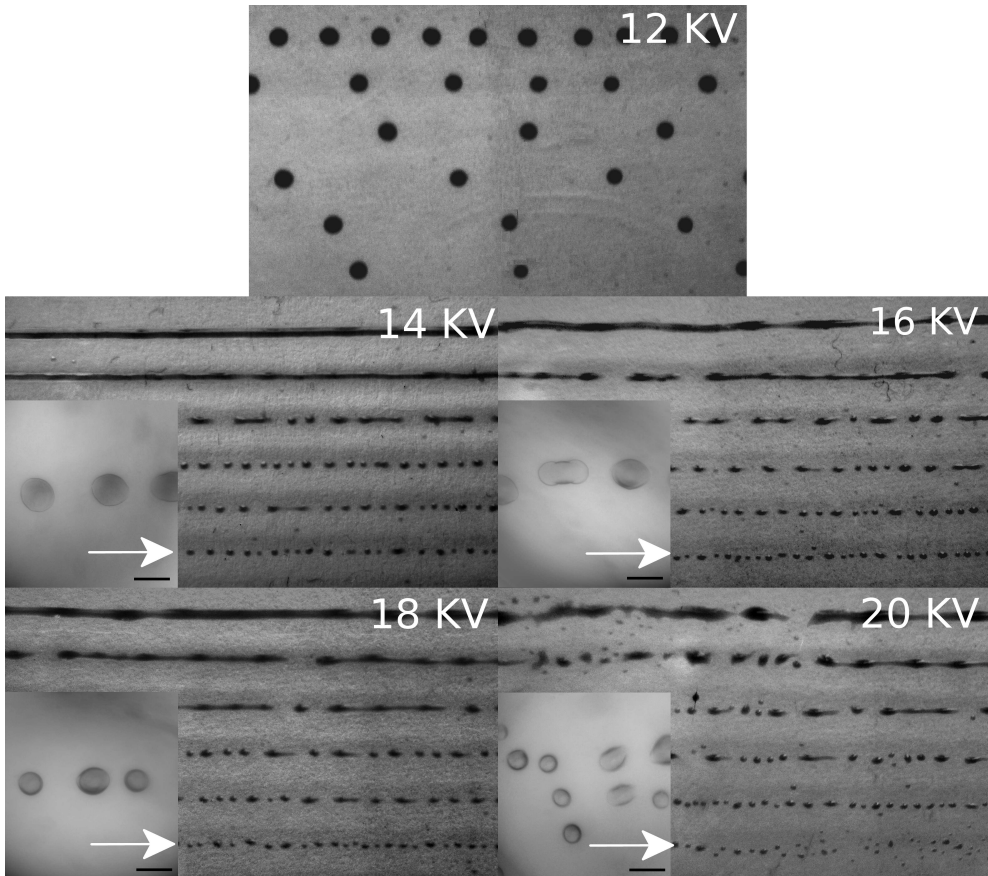


Figure 4.8.: Geometrical feature at different voltages of the depositions varying the speed of the needle from 1 to 6 mm/s, the magnifications show the depositions obtained at 6 mm/s. Bar is 500 μm

4.4.5. Distance from target vs speed

The tested distances from target ranged between 4 and 7 mm. At 4 and 5 mm results are quite similar, there are two continuous lines in each sample at 1 and 2mm/s, all 12 depositions (either continuous or dotted lines) are uniform and straight. By increasing the distance from target over 5mm the beads ejected from the needle tend to aggregate in specific spots leading to deposition lines with a diameter that changes along the deposition path. At 7 mm it's possible to observe deviations from a straight line. For distances under 4 mm the tip of the needle is too close to the gelatin target and there are electrical discharges between the two objects inhibiting the jet formation.

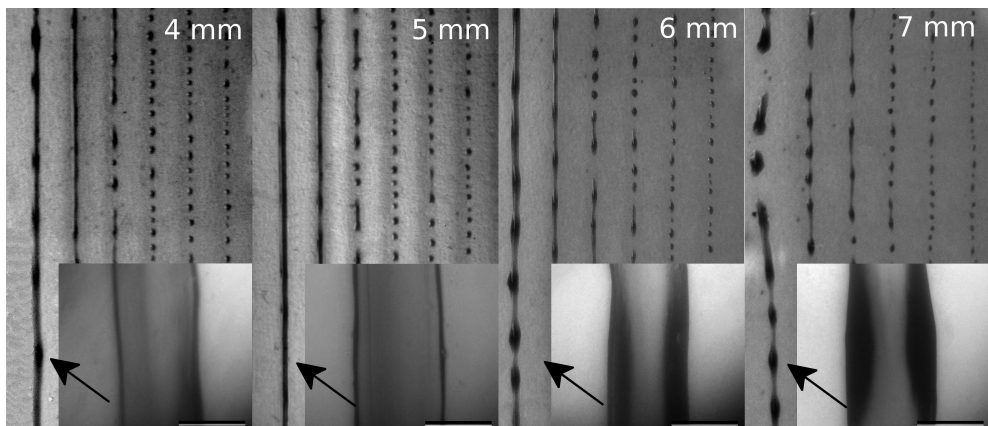


Figure 4.9.: From left to right depositions at a distance of 4, 5, 6, 7 mm showing the geometrical feature of the depositions varying the needle speed from 1 to 6 mm/s (left to right). Magnifications show the depositions obtained at 1 mm/s. Bar is 500 μm

4.4.6. Printed samples with cells

In order to assess the possibility to use EHDJ printing to deposit alginate hydrogel scaffolds containing living mammalian cells we chose the most uniform and ordered deposition among the ones obtained in the previous tests, in particular we observed samples printed at 14KV, 0.01 ml/min, 4 mm/s at a distance of 5mm starting with an alginate solution containing 5×10^6 cells /ml. Samples observed at the confocal microscope result from 5 layers deposition. We preferred to observe samples made of more than one layer to asses if this technique is usable for printing 3D living constructs. All the observed samples were printed on a single gelatin coated Petri dish from the same solution of alginate containing cells.

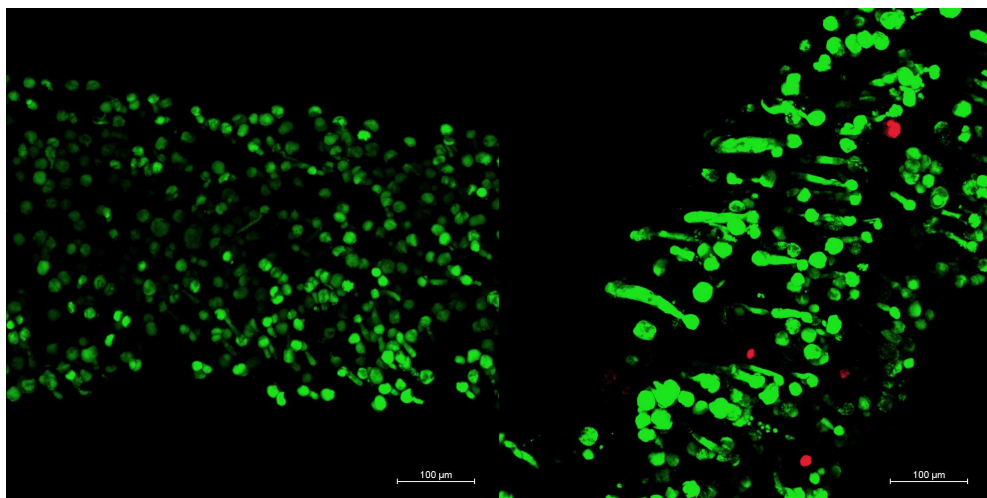


Figure 4.10.: Alginate deposition after 1 day (left) and 7 days of culture (right)

Samples were cultured for 1 and 7 days before observing them with the confocal microscope, in both cases they showed to maintain entrapped cells viable and evenly distributed (Fig. 4.11). It seems that there is no

substantial differences between samples at day 1 and sample at 7 days in terms of number of cells.

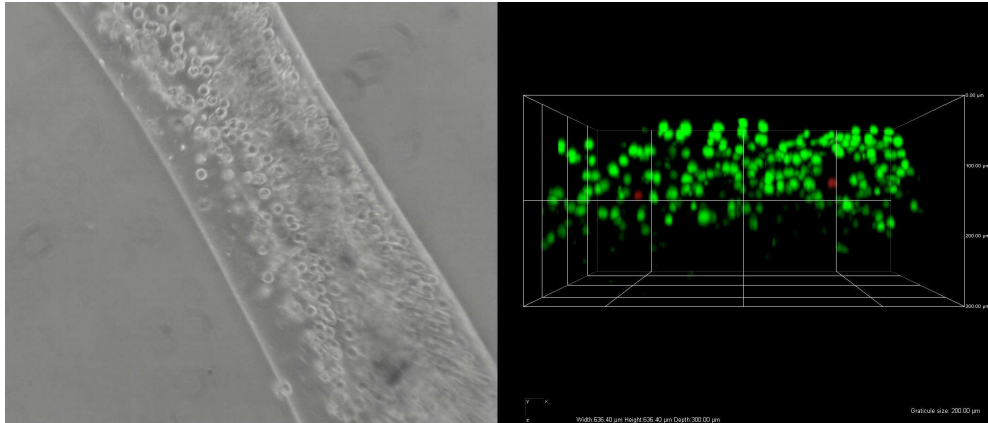


Figure 4.11.: Alginate EHDJ deposition after 7 days: on the left picture at optical microscope, on the right a 3D image obtain with the confocal microscope

Some samples were molded in agarose and underwent the dissolving procedure of alginate at day 6. After being cultured for 1 day they were observed with confocal and optical microscope. As shown in Fig Fig. 4.12 the treatment determines a change in cells distribution inside the sample: cells rather than being evenly distributed in 3 dimensions tend to form a two dimensional coating in the agarose. Cells released from the matrix were able to move outside the cut mold and reattach on the tissue culture plate.

4.5. Discussion

The flux of solution plays a crucial role. An high flux of solution is necessary to obtain an high throughput but this leads to thicker depositions

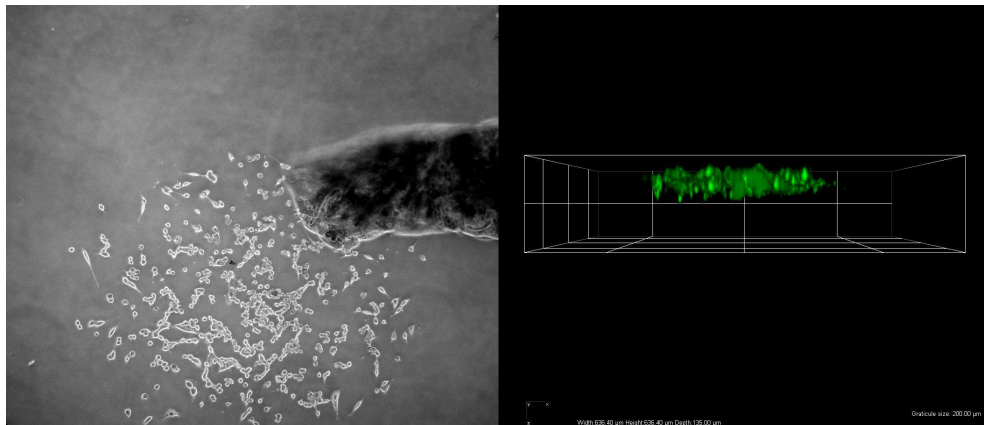


Figure 4.12.: Alginate EHDJ deposition after treatment: on the left picture at optical microscope, on the right a 3D image obtain with the confocal microscope

and consequently to a lower resolution bioprinter. On the other side it's possible to partially mitigate this phenomenon by increasing the speed of the needle. The increase of flux and needle speed leads to some complications in the process: higher flux means higher pressure in the deposition system which could be harmful to cells considering that they have to flow through an orifice slightly bigger than $100\ \mu\text{m}$.

Considering the voltage the best set up is the one that creates a jet of beads at the minimum voltage which is the condition to obtain the the most ordered depositions. In fact, increasing the voltage, the depositions are less uniform and particularly at 20KV it's possible to observe also the presence of very small beads. Reasonably the high voltage that generates the initial jet creates droplets with a high charge to mass ratio that overcome the Rayleigh limit rising a secondary disintegration. The secondary disintegration is very difficult to control determining the conditions for a disordered deposition. It should be noted that with our set

up higher voltages are needed to obtain a jetting conditions compared to the typical results found in literature concerning cell encapsulation (6 - 7 KV)[57] where the beads are ejected directly in a calcium chloride bath. We believe that the presence of the gelatin coating between the cathode and the anode mitigates the effect of the applied voltage. In fact if the generator is turned on at 14 KV when the needle is far from the gelatin the jetting condition is initiated and then it stops if the needle is moved closer to the gelatin to start again if the gelatin is removed.

It's worth of note that for each distance from the target it was possible to find the best voltage to obtain an ordered deposition. Shorter distances are generally preferred since the droplets, once ejected, are subject to perturbations that influence their trajectory. However if the distance is too short electric discharge could occur at the needle tip before overcoming the Rayleigh limit which determines the jetting condition. For our setup the best distance possible were 4 and 5 mm. On this matter it's worth of note that most of commercial bioprinters previously presented need a strict calibration of the z axis in order to cleanly deposit successive layers of material and a precise z mapping of the sample if it doesn't have a planar shape. By having a range of possible suitable distance for our printer this strict approach is not needed.

We didn't test other parameters characterizing the process like polymer concentration, density of cells and diameter of needle since their effect on the EHDJ process were already characterized (data not shown). In brief the best concentration of alginate was found to be 2% since higher concentrations are too viscous while lower concentration are more likely to create secondary disruption of the beads and as such irregular depositions. The density of cells in the starting solution has an influence in the EHDJ process, for example higher cell densities ($10 - 20 \times 10^6$ cells/ml)

needs a higher voltage to establish a jet of drops. However once the jet of drops is established there are no substantial differences on the diameter of the ejected beads. Finally, the diameter of the needle was chosen because it was the best compromise between viscosity and printer spot size since higher diameter allow higher flux of solution but increase the spot size of the printer creating bigger beads.

	Spot size (μm)	Max print speed (ml/s)	Max cell throughput(cells/s)
Our printer	250-1000	0.02 ml/s	1600 (6000*)
Laser Guided Direct Write	30	9×10^{-8} ml/s	0.04
Modified Laser Induced Forward Transfer	30-100	10^2 drops/s	10^4
Inkjet - Thermal	>300	5×10^5 drops/s	850
Inkjet - Piezo	Not reported	1×10^4 drops/s	2
Syringe Extrusion	>300	Continuous	Not reported

	Loaded volume (ml)	Cell viability (%)
Our printer	3* (50*)	>95
Laser Guided Direct Write	Not reported	Not reported
Modified Laser Induced Forward Transfer	20×10^{-3}	>95
Inkjet - Thermal	0.3 - 0.5	75 - 90
Inkjet - Piezo	0.3 - 0.5	-
Syringe Extrusion	0.6	>90

Table 4.1.: Feature of the printer system reported (gray background) compared to other printers found in scientific literature (white background). * Tested but not reported[77]

In [Tab. 4.1](#) we reported some features of the printer used in these experiments and compared to other printing system found in scientific literature. This table doesn't consider the ability to print directly 3D structures that in some cases is missing. As an example in the Modified Laser Induced Forward Transfer manually added basement membranes are needed to obtain a multilayered structure. Our printer has a spot

size similar to the inkjet and syringe extrusion printers and the maximum cell throughput is among the highest of the reported printers. Moreover it has a loaded volume dependent on reservoir used on the pump that can mount up to 50 ml syringes. This high load volume, not available in all other systems, allows uninterrupted printing for extended periods of time. Another aspect not present in all other printers is that the part of deposition system on top of the biopaper has a small size being constituted of only a needle, a cable and tube. This aspect increase the versatility of the system, for example more EHDJ heads could be used in parallel with different set ups. Furthermore potentially the system can be adapted to deposit other materials than alginate given some basic requirements like material compatibility with cells in the sol and gel states and the compatibility of the sol-gel transition with cell survival.

4.6. Conclusions

The electro hydro dynamic process can be exploited to create a jet of alginate beads that can be precisely deposited on a target surface, for this reason it's potentially a good candidate to be used as the deposition system of a bioprinter. If the target surface is a hydrogel containing divalent cations the alginate crosslink upon contact without the need of further processing. The printing process is compatible with cell survival and allows the deposition of a three dimensional alginate scaffold containing living cells. The deposition system used has a small size and now that the influence of the parameters of the process are known we believe is possible to mount more EHDJ heads calibrated to deposit beads on the same spot, achieving the possibility to use different solutions at the same time.

4.7. Acknowledgment

This research was done thanks to Biotools srl (Trento - Italy) that lent the Janome JR2300N desktop robot.

5. Conclusions

In this research work we faced the challenge to design and realize a printer for living constructs. The research activity has been focused on the main critical variables conditioning the process: by one side the development of optimal methods for cell encapsulation to produce cell laden building blocks, and by the other the setting up and tuning of a proper methodology for the controlled and effective placement of the living blocks. By combining the two processes of encapsulation and scaffold production and by using a specific substrate for the printed samples it was possible to obtain a direct printing of computer designed 3D hydrogel scaffolds containing living mammalian cells.

Initially we manufactured samples with a printer similar to commercially available bioprinters but with a new approach aimed at obtaining directly 3D structures by a direct injection in an hydrogel. The hydrogel acted as a sacrificial support and had the functional role to crosslink the construct. Later we designed a more advanced and novel contactless bioprinter that exploit a deposition technique typically employed for the encapsulation of cells, the electro hydro dynamic process. The base building blocks of this printer are cell laden micrometric beads and scaffolds are produced with a bottom-up approach by assembling the blocks piece by piece to obtain more complex structures.

The electro hydro dynamic process parameters were carefully charac-

terized to obtain spherical mono sized beads and as such optimize the spot size of the printer. Biological tests were performed to assess the condition of different kind of entrapped cells inside the beads and once released from the hydrogel. The beads showed viable cells in a quiescent state which were able to regain their viability after dissolving the entrapping matrix.

The information obtained were transferred directly to the bioprinter and the printing parameters were investigated to obtain controlled and ordered depositions. 3D structures are obtained by the deposition of more layers of material that crosslink upon contact on the target substrate without needing any further postprocessing.

The bioprinter has some features that are not available in other system. It's contactless, avoiding the need of a strict calibration and a possible contamination of the sample by the deposition system. The part of the deposition system over the sample it's small sized, being constituted only of a needle, a tube and a cable without adversely effecting the high load capacity of feeding solution to allow uninterrupted printing for long periods of time .

Applying computer aided manufacturing to build functional tissue is a promising approach, but still far from being fully successful. However the possibility to place small drops of alginate containing living cells at predefined positions can be exploited for many application. A potential and promising application could be building a device for the release of therapeutic molecules , such as insulin, by carefully designing the positioning of highly cell loaded alginate beads leaving channels for the nutrient supplies and removal of waste.

Acknowledgments

The chapter entitled :”Electro hydro dynamic encapsulation: more biological evaluations “ has been done in cooperation with Miss. Volha Liaudanskaya being part of her doctorate thesis. Miss. Silvia Lucchi took part on some on those experiments for her bachelor diploma.

The dekstop robot and the ecoPen has been lent by Biotools srl.

A. Appendix

A.1. Technical data (from the manufacturers)

A.1.1. Eco-PEN300

Business Unit Components & Devices

preeflow[®] *eco-PEN300*
by ViscoTec

Fig.: Side view

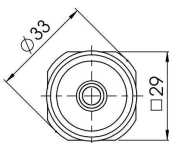
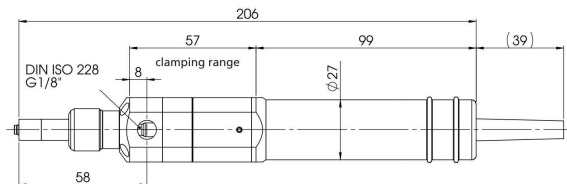
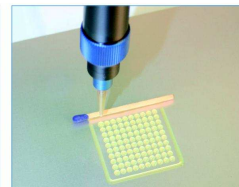


Fig.: Front view



TECHNICAL DATA

Dimensions:	Length 206 mm, \square 29 x 29 mm, \varnothing 33 mm
Weight:	approx. 380 gram
Material infeed:	1/8" cylindrical Whitworth pipe thread DIN/ISO 228
Material outfeed:	Luer lock with O ring, patented
Min. operating pressure:	0 bar, non-self-levelling-fluid
Max. operating pressure:	0 to 6 bar input pressure, self-levelling-fluid
Max. dosing pressure:	16 to 20 bar
Intrinsic tightness ^[1] :	approx. 2 bar (reference medium approx. 1000mPas at 20°C)
Parts in contact with the media:	HD-POM / stainless steel
Seals:	High-molecular PE, VisChem
Static seals:	Viton O ring (medium) NBR (dust)
Motor:	18 - 24 V DC, incremental encoder, planetary gears
Operating conditions:	+10°C to +40°C, air pressure 1 bar
Medium temperature:	+10°C to +40°C
Storage environment:	dry & dust-free, -10°C to +40°C
Approx. dosing volume per revolution:	0.012 millilitres per revolution
Accuracy of dosing ^[2] :	\pm 1%
Repeat accuracy:	> 99%
Min. dosing quantity:	0.001 millilitres
Volume flow ^[3] :	0.12 – 1.48 millilitres per minute



^[1] Max. dosing pressure and intrinsic tightness will decrease in direct proportion to a decrease in viscosity and increase in direct proportion to an increase in viscosity. Consultation with the manufacturer recommended.

^[2] Volumetric dosing as absolute deviation in relation to one dispenser revolution. Depends on the viscosity of the dosing medium.

A.1.2. Jenome JR2300N

Specifications



JR2303N

Model number		JR2300 N
Range of operation	X axis	300 mm
	Y axis	320 mm
	Z axis	100 mm
Speed	PTR(X,Y)	8~800mm/sec
	PTR(Z)	3.2~320mm/sec
	CP(X,Y,Z)	0.1~800mm/sec
Repeatability accuracy		±0.01mm
Resolution	X,Y axis	0.01mm
	Z axis	0.01mm
Portable weight	Work	11 kg
	Tool	6 kg
Teaching method		Remote teaching, MDI
Drive method		5-phase stepping motor
Control method		PTP, CP method
Number of controllable axes		2 axis
		3 axis
		4 axis (360°)
External interface		RS232-C 2ch
External input/output		IN: 16, OUT: 16 (24 I/O option)
PLC function		50 programs, 100 steps/1 program
Data memory capacity		6,000 points or 100 program
Program system		Memory card
CPU		32bit
dimension	Wide	560mm
	Depth	529mm
	Height	649(799 tall)/mm
Weight		35kg
Power source		Dual voltage 100-200V
Consumption current		200VA
Working ambient temperature		0 - 40°C
Relative humidity		20 - 95% no condensation

A.1.3. nScript Bioassembly tool

Micro Dispense Pump 3D Direct Printing Tabletop Series Technical Specifications



Computer and Software

- Cutting-edge software enables ultra-precise 3D printing on conformal surfaces.
- Create and organize printing jobs for high throughput manufacturing with our customizable, user-friendly software.
- Pentium™ 4 with CD-ROM Drive; 17" LCD Monitor and Video Monitor
- Ethernet Network Port and RS232

Input / Output

- Digital I/O: 24 inputs, 24 outputs
- Analog I/O: 3 inputs (12 bits), 3 outputs (16-bit)

Micro Dispense Pump Options

- SmartPump™ 100: 100 pico-liter control
 - Dynamic flow control allows for adjustment as material properties change over time
 - Precise starting and stopping without tailing; tight volumetric control
- Positive Displacement Pump - nano-liter control and cluster placement
- Air Pressure Pump - nano-liter control and high volume placement
- Micro Mixer Pump - Real time 3 part mixing

Frame and Base

- Machine Frame: Sicon supplied
- Motion Base: Aluminum base, risers, and bridge

Installation Requirements

- Air Supply: 80 PSI to 120 PSI
- Power: 120 volts at 30 amps



A.1.4. Envisiontec 3D-Bioplotter™

3D-Bioplotter™

Technical Data
March 2011

3D-Bioplotter™ (4th generation)

The 3D-Bioplotter™ System is a suitable Rapid Prototyping tool for processing a great variety of biomaterials within the process of Computer Aided Tissue Engineering from 3D CAD models and patient's CT data to the physical 3D scaffold with a designed and defined outer form and an open inner structure.

Description

Tissue Engineering and Controlled Drug Release require 3D scaffolds with well defined external and internal structures. The 3D-Bioplotter™ has the capacity of fabricating scaffolds using the widest range of materials of any singular Rapid Prototyping machine, from soft hydrogels over polymer melts up to hard ceramics and metals. The 3D-Bioplotter™ is specially designed for work in sterile environments in a laminar flowbox, a requirement of Biofabrication, for example when using alginate cell suspensions for scaffold construction. In contrast to other Rapid Prototyping techniques the new 3D-Bioplotter™ uses a very simple and straightforward technology, invented and developed at the Materials Research Centre in Germany.

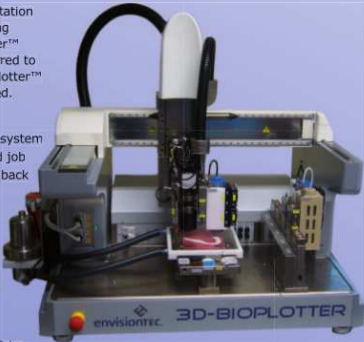
System	3D-Bioplotter™
Axis Resolution (XYZ)	0,001mm
Speed	0,1 - 150mm/s
Build Volume	150 x 150 x 140mm
Needle Sensor Resolution (Z)	0,001mm
Camera Resolution (XY)	0,009mm per Pixel
Minimum Strand Diameter	0,100mm (Material dependent)

System Data Handling

The 3D-Bioplotter™ is delivered together with a PC workstation which operates and monitors the system. After transferring the 3D CAD data to the PC it is processed by the Bioplotter™ Software Package. The preprocessed data is then transferred to the 3D-Bioplotter™ using a network connection. The Bioplotter™ software monitors the working process until it is completed.

System Properties

- 3-Axis positioning system with automatic tool changing system
- 5 different cartridges can be used during the same build job
- Strand diameter control via high resolution camera feedback
- Primary filter and sterile filter are included
- High temperature dispensing head (up to 250 °C)
- Low temperature dispensing head (~2°C to 70 °C)
- Easy to use and easy to clean cartridge system
- User friendly and intuitive CAD CAM software package
- Multi exchangeable base plate fixtures with heating and cooling capabilities (~0°C to 65°C)



Specifications

- Overall size (L W H): 976 x 623 x 773mm, Weight: ~ 80 kg
- The system needs 6 – 8 bar air pressure, approx. 30 l/min
- Power 100 – 240V AC, 10A, F 50/60Hz

Patents pending

envisionTEC GmbH Brüsseler Straße 51 • 45968 Gladbeck • Germany
Phone +49 2043 98 75-0 • Fax +49 2043 98 75-99

USA Distributor 1100 Hilton Road • Ferndale, MI 48220 • USA
Phone +1-248-582-0038 • Fax +1-248-582-0039

www.envisiontec.com info@envisiontec.com



Computer Aided Modeling Devices®

A.1.5. Syseng Bioscaffolder

SYS^oENG Dipl.-Ing. Hendrik John

Engineering Service

Development / Engineering of process chains for CAD and direct manufacturing of

- customised 3D tissue scaffolds for R&D in Tissue Engineering
- patient specific implants for clinical applications

based on medical imaging, 3D-CAD/CAM and Rapid Manufacturing Technologies.

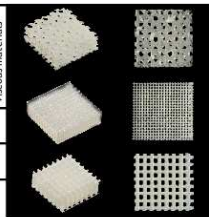
System "BioScaffolder"

System-Solution for manufacturing of customised 3D tissue scaffolds / patient specific implants with defined external shape and internal architecture (three dimensional distribution of inter-connective porosity and material) from multiple biomaterials based on 3D-dispensing.



www.syseng.de

Dispense Head	Dispensing Principle	Fluid	Gel	Paste	Melt	Slurry	low to medium viscous materials	medium to high viscous materials
Low Temperature: • Room Temp. • 2 °C - 50 °C (temp. controlled)	Pressure - Time Vol. controlled via linear drive	•	•	•			•	•
High Temperature: • Room Temp. - 250 °C (temp. controlled)	Auger Screw Pump		•	•	•			•



System

- Desktop, overall dimensions: Depth 680mm, Width 800mm, Height 500mm, weight: ca. 50kg
- 3 Axis (XYZ) gantry version, 4th axis for linear driven dispense heads
- Additional rotational axis (optional)
- 5 phase high resolution stepper motors (resolution ca. 5µm/step)
- Overall repeatability: ± 25µm (mechanical system)
- Working range XYZ: 200mm x 150mm x 90mm
- Low & high temperature dispense heads with 3 different dispense principles
- Automatic tool-changing system for up to 5 dispense heads
- Needle Sensor (optical), repeatability: ± 5µm (same needle type), ± 25µm (different needle types)
- Base Plate with vacuum plate, heating: Room Temp. - 100 °C and cooling: 2 °C - 50 °C (optional)
- System Control via Industrial-PC with Control Board
- 2 ½ D CAD-CAM Software with 3D-Data Import: 3D-DXF, STL, multiple STL's

©2008 SYS-ENG Dipl.-Ing.-Hendrik John

A.1.6. Standard formulation (salts)

A.1.6.1. DMEM

Component	Concentrate mg/L
CaCl ₂ · 2H ₂ O	264.92
Ferric Nitrate (Fe(NO ₃) ₃ ·9H ₂ O)	0.10
Potassium Chloride (KCl)	400.00
MgSO ₄ · 7H ₂ O	200.00
Sodium Chloride (NaCl)	6400.00
Sodium Bicarbonate (NaHCO ₃)	3700.00
Sodium Phosphate (NaH ₂ PO ₄ ·H ₂ O)	125.00

A.1.6.2. Phosphate buffer saline w/o Ca and Mg

Component	Concentrate mg/L
Potassium Chloride (KCl)	200.00
Sodium Chloride (NaCl)	8000.00
Potassium Phosphate Monobasic (KH ₂ PO ₄)	200.00
Sodium Phosphate Dibasic (Na ₂ HPO ₄)	2170.00

Bibliography

- [1] Abraham, S.: 1996, Novel technology for the preparation of sterile alginate-poly-l-lysine microcapsules in a bioreactor, ... *and technology* .
URL: <http://informahealthcare.com/doi/abs/10.3109/10837459609031419>
- [2] Allan-Wojtas, P., Truelstrup Hansen, L. and Paulson, A.: 2008, Microstructural studies of probiotic bacteria-loaded alginate microcapsules using standard electron microscopy techniques and anhydrous fixation, *LWT - Food Science and Technology* **41**(1), 101–108.
URL: <http://dx.doi.org/10.1016/j.lwt.2007.02.003>
- [3] Arica, M., Kaçar, Y. and Genç, O.: 2001, Entrapment of white-rot fungus *Trametes versicolor* in Ca-alginate beads: preparation and biosorption kinetic analysis for cadmium removal from an aqueous, *Bioresource technology* .
URL: <http://www.sciencedirect.com/science/article/pii/S0960852401000840>
- [4] Arumuganathar, S., Irvine, S., McEwan, J. R. and Jayasinghe, S. N.: 2007, Pressure-assisted cell spinning: a direct protocol for spinning biologically viable cell-bearing fibres and scaffolds, *Biomedical Materials* **2**(4), 211–219.
URL: <http://iopscience.iop.org/1748-605X/2/4/002/>
- [5] Augst, A. D., Kong, H. J. and Mooney, D. J.: 2006, Alginate Hydrogels as Biomaterials, *Macromolecular Bioscience* **6**(8), 623–633.

- URL:** <http://dx.doi.org/10.1002/mabi.200600069>
<http://www3.interscience.wiley.com/cgi-bin/fulltext?ID=112734164&PLACEBO=IE.pdf&mode=pdf>
- [6] Barber, R. D., Harmer, D. W., Coleman, R. A. and Clark, B. J.: 2005, GAPDH as a housekeeping gene: analysis of GAPDH mRNA expression in a panel of 72 human tissues., *Physiological genomics* **21**(3), 389–95.
URL: <http://physiolgenomics.physiology.org/content/21/3/389>
- [7] Barron, J., Wu, P., Ladouceur, H. and Ringeisen, B.: 2004, Biological Laser Printing: A Novel Technique for Creating Heterogeneous 3-dimensional Cell Patterns, *Biomedical Microdevices* **6**(2), 139–147.
URL: <http://www.springerlink.com/content/t628236vuw7v7735/>
- [8] Bhadriraju, K. and Chen, C. S.: 2002, Engineering cellular microenvironments to improve cell-based drug testing, *Drug Discovery Today* **7**(11), 612–620.
URL: [http://dx.doi.org/10.1016/S1359-6446\(02\)02273-0](http://dx.doi.org/10.1016/S1359-6446(02)02273-0)
- [9] Bhushan, I. and Parshad, R.: 2008, Immobilization of Lipase by Entrapment in Ca-alginate Beads, *Journal of Bioactive and Compatible Polymers* **23**(6), 552–562.
- [10] Bishop, S. M., Walker, M., Rogers, A. A. and Chen, W. Y.: 2003, Importance of moisture balance at the wound-dressing interface., *Journal of wound care* **12**(4), 125–128.
URL: <http://www.scopus.com/inward/record.url?eid=2-s2.0-0037809477&partnerID=40&md5=1c5687cac5eb3c5ce346201bd5324619>
- [11] Bock, N., Dargaville, T. and Woodruff, M.: 2012, Electrospraying of polymers with therapeutic molecules: State of the art, *Progress in Polymer Science* **37**(11), 1510–1551.

- [12] Braun, F. and Behrend, M.: 2007, *Side Effects of Drugs Annual Volume 29*, Vol. 29 of *Side Effects of Drugs Annual*, Elsevier.
- [13] Buck, C. and Horwitz, A.: 1987, Cell surface receptors for extracellular matrix molecules, *Annual review of cell biology* .
URL: <http://www.annualreviews.org/doi/abs/10.1146/annurev.cb.03.110187.0>
- [14] Canny, J.: 1986, A Computational Approach to Edge Detection, *IEEE Transactions on Pattern Analysis and Machine Intelligence PAMI-8*(6), 679–698.
- [15] Chan, L., Lee, H. and Heng, P.: 2006, Mechanisms of external and internal gelation and their impact on the functions of alginate as a coat and delivery system, *Carbohydrate polymers* .
URL: <http://www.sciencedirect.com/science/article/pii/S0144861705003218>
- [16] Chang, P.: 1999, The in vivo delivery of heterologous proteins by microencapsulated recombinant cells, *Trends in Biotechnology* **17**(2), 78–83.
- [17] Chapman, V.: 1952, Seaweeds and their uses, *Soil Science* .
URL: http://journals.lww.com/soilsci/Abstract/1952/12000/Seaweeds_and_5
- [18] Chuah, M., Hale, D. and West, A.: 2011, Interaction of olfactory ensheathing cells with other cell types< i> in vitro</i> and after transplantation: Glial scars and inflammation, *Experimental neurology* .
URL: <http://www.sciencedirect.com/science/article/pii/S0014488610002943>
- [19] Chuah, M. and West, A.: 2002, Cellular and molecular biology of ensheathing cells, *Microscopy research and technique* .
URL: <http://onlinelibrary.wiley.com/doi/10.1002/jemt.10151/abstract>
- [20] Clarke, J. D. W. and Jayasinghe, S. N.: 2008, Bio-electrosprayed multicellular zebrafish embryos are viable and develop normally.,

- Biomedical materials (Bristol, England)* **3**(1), 011001.
URL: <http://www.ncbi.nlm.nih.gov/pubmed/18458487>
- [21] Cloupeau, M. and Prunet-Foch, B.: 1994, Electrohydrodynamic spraying functioning modes: a critical review, *Journal of Aerosol Science* .
URL: <http://www.sciencedirect.com/science/article/pii/0021850294901996>
- [22] Craig, E. A. and Gross, C. A.: 1991, Is hsp70 the cellular thermometer?, *Trends in Biochemical Sciences* **16**(4), 135–140.
URL: <http://europepmc.org/abstract/MED/1877088/reload=0>
- [23] Cui, X. and Boland, T.: 2009, Human microvasculature fabrication using thermal inkjet printing technology., *Biomaterials* **30**(31), 6221–7.
URL: <http://dx.doi.org/10.1016/j.biomaterials.2009.07.056>
- [24] de Vos, P., Faas, M. M., Strand, B. and Calafiore, R.: 2006, Alginate-based microcapsules for immunoisolation of pancreatic islets., *Biomaterials* **27**(32), 5603–17.
- [25] DeRamos, C., Irwin, A., Nauss, J. and Stout, B.: 1997, ¹³C NMR and molecular modeling studies of alginic acid binding with alkaline earth and lanthanide metal ions, *Inorganica chimica acta* .
URL: <http://www.sciencedirect.com/science/article/pii/S0020169396054187>
- [26] Dimitrov, D. S.: 2012, Therapeutic proteins., *Methods in molecular biology (Clifton, N.J.)* **899**, 1–26.
URL: <http://www.ncbi.nlm.nih.gov/pubmed/22735943>
- [27] Ding, L., Lee, T. and Wang, C.-H.: 2005, Fabrication of monodispersed Taxol-loaded particles using electrohydrodynamic atomization., *Journal of controlled release : official journal of the Controlled Release Society* **102**(2), 395–413.

- [28] Doucette, R.: 2004, Glial influences on axonal growth in the primary olfactory system, *Glia* .
URL: <http://onlinelibrary.wiley.com/doi/10.1002/glia.440030602/abstract>
- [29] Duvivier-Kali, V. F., Omer, A., Parent, R. J., O'Neil, J. J. and Weir, G. C.: 2001, Complete Protection of Islets Against Allojection and Autoimmunity by a Simple Barium-Alginate Membrane, *Diabetes* **50**(8), 1698–1705.
URL: <http://diabetes.diabetesjournals.org/content/50/8/1698.short>
- [30] Elbert, D. L.: 2011, Bottom-up tissue engineering., *Current opinion in biotechnology* **22**(5), 674–80.
URL: <http://dx.doi.org/10.1016/j.copbio.2011.04.001>
- [31] Elcin, Y.: 1995, Encapsulation of urease enzyme in xanthan-alginate spheres, *Biomaterials* .
URL: <http://www.sciencedirect.com/science/article/pii/0142961295935807>
- [32] Espevik, T., Otterlei, M., Skjak-Braek, G., Ryan, L., Wright, S. D. and Sundan, A.: 1993, The involvement of CD14 in stimulation of cytokine production by uronic acid polymers, *European Journal of Immunology* **23**(1), 255–261.
URL: <http://www.scopus.com/inward/record.url?eid=2-s2.0-0027533285&partnerID=40&md5=6b4a92832026123dc0c8f3ae6fd6d48b>
- [33] Francisco, H., Yellen, B. B., Halverson, D. S., Friedman, G. and Gallo, G.: 2007, Regulation of axon guidance and extension by three-dimensional constraints., *Biomaterials* **28**(23), 3398–407.
URL: <http://dx.doi.org/10.1016/j.biomaterials.2007.04.015>
- [34] Goh, C. H., Heng, P. W. S. and Chan, L. W.: 2012, Alginates as a useful natural polymer for microencapsulation and therapeutic applications, *Carbohydrate Polymers* **88**(1), 1–12.
- [35] Gombotz, W. and Wee, S.: 2012, Protein release from alginate

- matrices, *Advanced drug delivery reviews* .
URL: <http://www.sciencedirect.com/science/article/pii/S0169409X12002670>
- [36] Gomez, C., Rinaudo, M. and Villar, M.: 2007, Oxidation of sodium alginate and characterization of the oxidized derivatives, *Carbohydrate Polymers* **67**(3), 296–304.
- [37] Groves, R. W., Allen, M. H., Ross, E. L., Barker, J. and MacDonald, D. M.: 1995, Tumour necrosis factor alpha is pro-inflammatory in normal human skin and modulates cutaneous adhesion molecule expression, *British Journal of Dermatology* **132**(3), 345–352.
URL: <http://www.scopus.com/inward/record.url?eid=2-s2.0-0028901436&partnerID=40&md5=789acf4be3dd6533b3119d77fe141495>
- [38] Gupta, A., Seifalian, A. M., Ahmad, Z., Edirisinghe, M. J. and Winslet, M. C.: 2007, Novel Electrohydrodynamic Printing of Nanocomposite Biopolymer Scaffolds, *Journal of Bioactive and Compatible Polymers* **22**(3), 265–280.
- [39] Hari, P. R., Chandy, T. and Sharma, C. P.: 1996, Chitosan/calcium-alginate beads for oral delivery of insulin, *Journal of Applied Polymer Science* **59**(11), 1795–1801.
URL: [http://dx.doi.org/10.1002/\(SICI\)1097-4628\(19960314\)59:11<1795::AID-APP16>3.0.CO;2-T](http://dx.doi.org/10.1002/(SICI)1097-4628(19960314)59:11<1795::AID-APP16>3.0.CO;2-T)
<http://www3.interscience.wiley.com/cgi-bin/fulltext?ID=60804&PLACEBO=IE.pdf&mode=pdf>
- [40] Hayati, I., Bailey, A. and Tadros, T.: 1987, Investigations into the mechanisms of electrohydrodynamic spraying of liquids: I. Effect of electric field and the environment on pendant drops and factors affecting the, *Journal of colloid and interface science* .
URL: <http://www.sciencedirect.com/science/article/pii/0021979787901858>
- [41] Hori, Y., Winans, A. M. and Irvine, D. J.: 2009, Modular injectable

- matrices based on alginate solution/microsphere mixtures that gel in situ and co-deliver immunomodulatory factors., *Acta biomaterialia* **5**(4), 969–82.
- [42] Hunt, N. C., Shelton, R. M., Henderson, D. J. and Grover, L. M.: 2013, Calcium-alginate hydrogel-encapsulated fibroblasts provide sustained release of vascular endothelial growth factor., *Tissue engineering. Part A* **19**(7-8), 905–14.
URL: <http://online.liebertpub.com/doi/abs/10.1089/ten.tea.2012.0197?journal>
- [43] Jain, R. K., Au, P., Tam, J., Duda, D. G. and Fukumura, D.: 2005, Engineering vascularized tissue., *Nature biotechnology* **23**(7), 821–3.
URL: <http://dx.doi.org/10.1038/nbt0705-821>
- [44] Kapur, J., Sahoo, P. and Wong, A.: 1985, A new method for gray-level picture thresholding using the entropy of the histogram, *Computer vision, graphics, and image processing* **29**(3), 273–285.
- [45] Khademhosseini, A. and Langer, R.: 2007, Microengineered hydrogels for tissue engineering, *Biomaterials* **28**(34), 5087–5092.
URL: <http://www.sciencedirect.com/science/article/B6TWB-4PFDPK4-1/2/b858c812c86ca392931f2cedbfd1b611>
http://www.sciencedirect.com/science?_ob=ArticleURL&_udi=B6TWB-4PFDPK4-1&_user=1613343&_coverDate=12%2F31%2F2007&_alid=14118
http://www.sciencedirect.com/science?_ob=MImg&_imagekey=B6TWB-4PFDPK4-1-5&_cdi=5558&_user=1613343&_pii=S01429612
- [46] Kievit, F. M., Florczyk, S. J., Leung, M. C., Veisoh, O., Park, J. O., Disis, M. L. and Zhang, M.: 2010, Chitosan-alginate 3D scaffolds as a mimic of the glioma tumor microenvironment., *Biomaterials* **31**(22), 5903–10.
- [47] Kim, H.-S., Lee, D.-Y., Park, J.-H., Kim, J.-H., Hwang, J.-H. and Jung, H.-I.: 2007, Optimization of Electrohydrodynamic Writing

- Technique To Print Collagen, *Experimental Techniques* **31**(4), 15–19.
URL: <http://doi.wiley.com/10.1111/j.1747-1567.2007.00154.x>
- [48] Klöck, G., Pfeffermann, A., Ryser, C., Gröhn, P., Kuttler, B., Hahn, H.-J. and Zimmermann, U.: 1997, Biocompatibility of mannuronic acid-rich alginates, *Biomaterials* **18**(10), 707–713.
- [49] Klouda, L. and Mikos, A. G.: 2008, Thermo-responsive hydrogels in biomedical applications., *European journal of pharmaceuticals and biopharmaceutics : official journal of Arbeitsgemeinschaft für Pharmazeutische Verfahrenstechnik e. V* **68**(1), 34–45.
URL: <http://dx.doi.org/10.1016/j.ejpb.2007.02.025>
- [50] Kong, H.: 2003, Designing alginate hydrogels to maintain viability of immobilized cells, *Biomaterials* **24**(22), 4023–4029.
URL: [http://dx.doi.org/10.1016/S0142-9612\(03\)00295-3](http://dx.doi.org/10.1016/S0142-9612(03)00295-3)
- [51] Kong, H. J., Kaigler, D., Kim, K. and Mooney, D. J.: 2004, Controlling rigidity and degradation of alginate hydrogels via molecular weight distribution., *Biomacromolecules* **5**(5), 1720–7.
URL: <http://dx.doi.org/10.1021/bm049879r>
- [52] Lamprecht, M., Sabatini, D. and Carpenter, A.: 2007, CellProfiler: free, versatile software for automated biological image analysis, *BioTechniques* **42**(1), 71–75.
- [53] Lee, K. Y. and Mooney, D. J.: 2012, Alginate: Properties and biomedical applications, *Progress in Polymer Science* **37**(1), 106–126.
- [54] Li, B., Trail, N. A. and Roy, T. D.: 2007, International Manufacturing Science And Engineering Conference, *A robust true direct-print technology for tissue engineering*, pp. 1–6.

- [55] Li, J. P., de Wijn, J. R., Van Blitterswijk, C. A. and de Groot, K.: 2006, Porous Ti6Al4V scaffold directly fabricating by rapid prototyping: preparation and in vitro experiment., *Biomaterials* **27**(8), 1223–35.
URL: <http://dx.doi.org/10.1016/j.biomaterials.2005.08.033>
- [56] Luna, S. M., Gomes, M. E., Mano, J. F. and Reis, R. L.: 2010, Development of a Novel Cell Encapsulation System Based on Natural Origin Polymers for Tissue Engineering Applications, *Journal of Bioactive and Compatible Polymers* **25**(4), 341–359.
- [57] Manojlovic, V., Djonlagic, J., Obradovic, B., Nedovic, V. and Bugarski, B.: 2006, Investigations of cell immobilization in alginate: rheological and electrostatic extrusion studies, *Journal of Chemical Technology & Biotechnology* **81**(4), 505–510.
URL: <http://onlinelibrary.wiley.com/doi/10.1002/jctb.1465/full>
- [58] Mellor, N., Chowdhury, S., Selden, C. and Hodgson, H.: 2001, Human hepatocytes encapsulated in alginate maintain differentiated function and capacity for DNA synthesis.
URL: <http://discovery.ucl.ac.uk/1325504/>
- [59] Mironov, V., Visconti, R. P., Kasyanov, V., Forgacs, G., Drake, C. J. and Markwald, R. R.: 2009, Organ printing: tissue spheroids as building blocks., *Biomaterials* **30**(12), 2164–74.
URL: <http://www.ncbi.nlm.nih.gov/pubmed/19176247>
- [60] Moghadam, H., Samimi, M., Samimi, A. and Khorram, M.: 2010, Electro spray modeling of highly viscous and non-Newtonian liquids, *Journal of Applied Polymer Science* **118**(3), 1288–1296.
- [61] Mongkoldhumrongkul, N., Best, S., Aarons, E. and Jayasinghe, S. N.: 2009, Bio-electrospraying whole human blood : analysing cellular viability at a molecular level, (June), 562–566.

-
- [62] Moroni, L., Wijn, J. D. and Blitterswijk, C. V.: 2006, 3D fiber-deposited scaffolds for tissue engineering: Influence of pores geometry and architecture on dynamic mechanical properties, *Biomaterials* .
URL: <http://www.sciencedirect.com/science/article/pii/S0142961205006320>
- [63] Murua, A., Orive, G., Hernández, R. M. and Pedraz, J. L.: 2009, Xenogeneic transplantation of erythropoietin-secreting cells immobilized in microcapsules using transient immunosuppression., *Journal of controlled release : official journal of the Controlled Release Society* **137**(3), 174–8.
- [64] Murua, A., Portero, A., Orive, G., Hernández, R. M., de Castro, M. and Pedraz, J. L.: 2008, Cell microencapsulation technology: Towards clinical application, *Journal of controlled release : official journal of the Controlled Release Society* **132**(2), 76–83.
- [65] Noble, M., Fok-Seang, J. and Cohen, J.: 1984, Glia are a unique substrate for the in vitro growth of central nervous system neurons, *The Journal of neuroscience* .
URL: <http://www.jneurosci.org/content/4/7/1892.short>
- [66] Orive, G., Tam, S. K., Pedraz, J. L. and Hallé, J.-P.: 2006, Biocompatibility of alginate-poly-L-lysine microcapsules for cell therapy., *Biomaterials* **27**(20), 3691–700.
URL: <http://www.ncbi.nlm.nih.gov/pubmed/16574222>
- [67] Otsu, N.: 1979, Threshold selection method from gray-level histograms., *IEEE Trans Syst Man Cybern* **SMC-9**(1), 62–66.
- [68] Otterlei, M., Ostgaard, K., Skjak-Braek, G., Smidsrod, O., Soon-Shiong, P. and Espevik, T.: 1991, Induction of cytokine production from human monocytes stimulated with alginate, *Journal of Immunotherapy* **10**(4), 286–291.

- URL:** <http://www.scopus.com/inward/record.url?eid=2-s2.0-0025830568&partnerID=40&md5=a8e4cb1a3acac78ca2f9a7c31fe219aa>
- [69] Paine, M., Alexander, M. and Stark, J.: 2007, Nozzle and liquid effects on the spray modes in nanoelectrospray, *Journal of colloid and interface*
URL: <http://www.sciencedirect.com/science/article/pii/S0021979706008393>
- [70] Pareta, R. and Brindley, A.: 2005, Electrohydrodynamic atomization of protein (bovine serum albumin), *Journal of Materials*
URL: <http://www.springerlink.com/index/V3L53822GJ18854R.pdf>
- [71] Park, J.-U., Hardy, M., Kang, S. J., Barton, K., Adair, K., Mukhopadhyay, D. K., Lee, C. Y., Strano, M. S., Alleyne, A. G., Georgiadis, J. G., Ferreira, P. M. and Rogers, J. a.: 2007, High-resolution electrohydrodynamic jet printing., *Nature materials* **6**(10), 782–9.
- [72] Peirone, M., Ross, C. J., Hortelano, G., Brash, J. L. and Chang, P. L.: 1998, Encapsulation of various recombinant mammalian cell types in different alginate microcapsules., *Journal of biomedical materials research* **42**(4), 587–96.
URL: <http://www.ncbi.nlm.nih.gov/pubmed/9827683>
- [73] Phadke, M., Krynetskaia, N., Mishra, A. and Krynetskiy, E.: 2011, Accelerated cellular senescence phenotype of GAPDH-depleted human lung carcinoma cells., *Biochemical and biophysical research communications* **411**(2), 409–15.
URL: <http://dx.doi.org/10.1016/j.bbrc.2011.06.165>
- [74] Prewitt, J.: 1970, Object enhancement and extraction, *Picture processing and psychopictorics* **75**, n/a.
- [75] Ridler, T. W. and Calvard, S.: 1978, Picture thresholding using an

- iterative selection method., *IEEE Transactions on Systems, Man and Cybernetics* **SMC-8**(8), 630–632.
- [76] Ringeisen, B. R., Kim, H., Barron, J. A., Krizman, D. B., Chrisey, D. B., Jackman, S., Auyeung, R. Y. C. and Spargo, B. J.: 2004, Laser printing of pluripotent embryonal carcinoma cells., *Tissue engineering* **10**(3-4), 483–91.
URL: <http://online.liebertpub.com/doi/abs/10.1089/107632704323061843>
- [77] Ringeisen, B. R., Othon, C. M., Barron, J. a., Young, D. and Spargo, B. J.: 2006, Jet-based methods to print living cells., *Biotechnology journal* **1**(9), 930–48.
URL: <http://www.ncbi.nlm.nih.gov/pubmed/16895314>
- [78] Rokstad, A. M., Brekke, O.-L., Steinkjer, B. r., Ryan, L., Koláríková, G., Strand, B. L., Skjå k Bræ k, G., Lacík, I., Espevik, T. and Mollnes, T. E.: 2011, Alginate microbeads are complement compatible, in contrast to polycation containing microcapsules, as revealed in a human whole blood model., *Acta biomaterialia* **7**(6), 2566–78.
- [79] Rosenfeld, A.: 1981, The Max Roberts Operator is a Hueckel-Type Edge Detector, *IEEE Transactions on Pattern Analysis and Machine Intelligence* **PAMI-3**(1), 101–103.
- [80] Rowley, J. a., Madlambayan, G. and Mooney, D. J.: 1999, Alginate hydrogels as synthetic extracellular matrix materials., *Biomaterials* **20**(1), 45–53.
- [81] Sakai, S., Ito, S. and Kawakami, K.: 2010, Calcium alginate microcapsules with spherical liquid cores templated by gelatin microparticles for mass production of multicellular spheroids., *Acta biomaterialia* **6**(8), 3132–7.
- [82] Sakai, S., Mu, C., Kawabata, K., Hashimoto, I. and Kawakami, K.:

- 2006, Biocompatibility of subsieve-size capsules versus conventional-size microcapsules., *Journal of biomedical materials research. Part A* **78**(2), 394–8.
- [83] Segal, H. C., Hunt, B. J. and Gilding, K.: 1998, The effects of alginate and non-alginate wound dressings on blood coagulation and platelet activation, *Journal of Biomaterials Applications* **12**(3), 249–257.
URL: <http://www.scopus.com/inward/record.url?eid=2-s2.0-0031594444&partnerID=40&md5=645c9269d9a2bbac6c87d208c85ede43>
- [84] Shapiro, L. and Cohen, S.: 1997, Novel alginate sponges for cell culture and transplantation, *Biomaterials* .
URL: <http://www.sciencedirect.com/science/article/pii/S0142961296001810>
- [85] Sieminski, A. and Gooch, K.: 2000, Biomaterial-microvasculature interactions, *Biomaterials* .
URL: <http://www.sciencedirect.com/science/article/pii/S0142961200001496>
- [86] Sirover, M. A.: 1997, Role of the glycolytic protein, glyceraldehyde-3-phosphate dehydrogenase, in normal cell function and in cell pathology., *Journal of cellular biochemistry* **66**(2), 133–40.
URL: <http://www.ncbi.nlm.nih.gov/pubmed/9213215>
- [87] Siti-Ismail, N., Bishop, A. E., Polak, J. M. and Mantalaris, A.: 2008, The benefit of human embryonic stem cell encapsulation for prolonged feeder-free maintenance., *Biomaterials* **29**(29), 3946–52.
- [88] Smidsrod, O.: 1990, Alginate as immobilization matrix for cells, *Trends in biotechnology* .
URL: <http://www.sciencedirect.com/science/article/pii/0167779990901390>
- [89] Sobel, I.: 1970, *Camera models and machine perception*, PhD thesis.
- [90] Sutherland, I.: 1991, Alginates, *Biomaterials; Novel Materials from*

Biological Sources .

URL: <http://scholar.google.com/scholar?q=Sutherland,+Biomaterials:+Novel>

- [91] Tam, S. K., Bilodeau, S., Dusseault, J., Langlois, G., Hallé, J.-P. and Yahia, L. H.: 2011, Biocompatibility and physicochemical characteristics of alginate-polycation microcapsules., *Acta biomaterialia* **7**(4), 1683–92.
- [92] Tan, T.-W., Hu, B., Jin, X.-H. and Zhang, M.: 2003, Release Behavior of Ketoprofen from Chitosan/Alginate Microcapsules, *Journal of Bioactive and Compatible Polymers* **18**(3), 207–218.
- [93] Tang, M., Chen, W., Weir, M. D., Thein-Han, W. and Xu, H. H. K.: 2012, Human embryonic stem cell encapsulation in alginate microbeads in macroporous calcium phosphate cement for bone tissue engineering., *Acta biomaterialia* **8**(9), 3436–45.
- [94] Taylor, A. L., Watson, C. J. E. and Bradley, J. A.: 2005, Immunosuppressive agents in solid organ transplantation: Mechanisms of action and therapeutic efficacy., *Critical reviews in oncology/hematology* **56**(1), 23–46.
- [95] Taylor, G.: 1964, Disintegration of water drops in electric field, *Proceedings of the royal society of London* **280**(1380), 383–397.
- [96] Uludag, H., De Vos, P. and Tresco, P. a.: 2000, Technology of mammalian cell encapsulation., *Advanced drug delivery reviews* **42**(1-2), 29–64.
- [97] Valenti, M. T., Bertoldo, F., Dalle Carbonare, L., Azzarello, G., Zenari, S., Zanatta, M., Balducci, E., Vinante, O. and Lo Cascio, V.: 2006, The effect of bisphosphonates on gene expression: GAPDH as a housekeeping or a new target gene?, *BMC cancer* **6**, 49.

URL: </pmc/articles/PMC1473200/?report=abstract>

- [98] Waring, M. J. and Parsons, D.: 2001, Physico-chemical characterisation of carboxymethylated spun cellulose fibres, *Biomaterials* **22**(9), 903–912.
URL: <http://www.scopus.com/inward/record.url?eid=2-s2.0-0035342611&partnerID=40&md5=d1cd85510d2d4f466b1d3820d9338cbe>
- [99] Xie, J., Ng, W., Lee, L. and Wang, C.: 2008, Encapsulation of protein drugs in biodegradable microparticles by co-axial electrospray, *Journal of colloid and interface science* .
URL: <http://www.sciencedirect.com/science/article/pii/S002197970701435X>
- [100] Xie, J. and Wang, C.-H.: 2007, Electrospray in the dripping mode for cell microencapsulation., *Journal of colloid and interface science* **312**(2), 247–55.
- [101] Xu, Q., Schett, G., Li, C., Hu, Y. and Wick, G.: 2000, Mechanical Stress-Induced Heat Shock Protein 70 Expression in Vascular Smooth Muscle Cells Is Regulated by Rac and Ras Small G Proteins but Not Mitogen-Activated Protein Kinases, *Circulation Research* **86**(11), 1122–1128.
URL: <http://circres.ahajournals.org/content/86/11/1122.short>
- [102] Xu, T., Jin, J., Gregory, C., Hickman, J. J. J. J. and Boland, T.: 2005, Inkjet printing of viable mammalian cells., *Biomaterials* **26**(1), 93–9.
URL: <http://dx.doi.org/10.1016/j.biomaterials.2004.04.011>
- [103] Xu, Y. and Hanna, M. A.: 2008, Electrosprayed bovine serum albumin-loaded tripolyphosphate cross-linked chitosan capsules: Synthesis and characterization, *Journal of Microencapsulation* **24**(2), 143–151.
- [104] Xu, Y., Skotak, M. and Hanna, M.: 2006, Electrospray encapsulation of water-soluble protein with polylactide. I. Effects of for-

-
- mutations and process on morphology and particle size, *Journal of Microencapsulation* **23**(1), 69–78.
- [105] Yamada, K.: 1983, Cell surface interactions with extracellular materials, *Annual review of biochemistry* .
URL: <http://www.annualreviews.org/doi/abs/10.1146/annurev.bi.52.070183.0>
- [106] Yang, J.-S., Xie, Y.-J. and He, W.: 2010, Research progress on chemical modification of alginate: A review, *Carbohydrate Polymers* **84**(1), 33–39.
- [107] Yao, R., Zhang, R., Luan, J. and Lin, F.: 2012, Alginate and alginate/gelatin microspheres for human adipose-derived stem cell encapsulation and differentiation, *Biofabrication* **4**(2), 025007.
URL: <http://stacks.iop.org/1758-5090/4/i=2/a=025007?key=crossref.42ccd0>
- [108] Zhong, H. and Simons, J. W.: 1999, Direct comparison of GAPDH, beta-actin, cyclophilin, and 28S rRNA as internal standards for quantifying RNA levels under hypoxia., *Biochemical and biophysical research communications* **259**(3), 523–6.
URL: <http://dx.doi.org/10.1006/bbrc.1999.0815>

Nomenclature

DMEM	Dulbecco's modified eagle medium
ECM	Extra celullar matrix
EHD	Electro Hydro Dynamic
PBS	Phosphate buffer saline
SEM	Scannin Electron Microscopy